# SYNTHESIS AND CHARACTERIZATION OF MANGANESE (IV) OXIDE NANOWIRE VIA HYDROTHERMAL METHOD

SUBASHINI A/P SUPRAMANIAM

DISSERTATION SUBMITTED IN PARTIAL FULLFILMENT OF THE REQUIREMENTS FOR THE DEGREE OF MASTER OF ENGINEERING

FACULTY OF ENGINEERING
UNIVERSITY OF MALAYA
KUALA LUMPUR

2013

**UNIVERSITY OF MALAYA**

**ORIGINAL LITERARY WORK DECLARATION**

**Name of Candidate:** SUBASHINI A/P SUPRAMANIAM

**Registration/Matric No:** KGC 060007

**Name of Degree:** MASTER OF ENGINEERING

**Title of Dissertation ("this Work"):**

SYNTHESIS AND CHARACTERIZATION OF MANGANESE (IV) OXIDE NANOWIRE VIA HYDROTHERMAL METHOD

**Field of Study:** NANOMATERIALS

I do solemnly and sincerely declare that:
(1) I am the sole author / writer of this work;
(2) This Work is original;
(3) Any use of any work in which copyright exists was done by way of fair dealing and for permitted purposes and any excerpt or extract from, or reference to or reproduction of any copyright work has been disclosed expressly and sufficiently and the title of the Work and its authorship have been acknowledged in this Work;
(4) I do not have any actual knowledge nor do I ought reasonably to know that the making of this work constitutes an infringement of any copyright work;
(5) I hereby assign all and every rights in the copyright to this Work to the University of Malaya ("UM"), who henceforth shall be owner of the copyright in this Work and that any reproduction or use in any form or by any means whatsoever is prohibited without the written consent of the UM having been first had and obtained;
(6) I am fully aware that if in the course of making this Work I have infringed any copyright whether intentionally or otherwise, I may be subject to legal action or any other action as may be determined by UM.

**Candidate's Signature:** **Date:**

Subscribed and solemnly declared before,

**Witness's Signature:** **Date:**

**Name:**

**Designation:**

# ABSTRACT

In this study, single crystalline nanowires of manganese (IV) oxide have been successfully synthesized via soft chemical process through a facile hydrothermal method. Characterization analysis has been carried out for manganese (IV) oxide as-received, as-synthesized, as well as calcinated at 400, 500 and 600 ℃. Various characterization techniques have been used such as structural analysis using X-Ray Diffractometer (XRD), surface analysis using Field Emission Scanning Electron Microscope (FE-SEM), chemical composition analysis using Energy Dispersive X-Ray Spectroscopy (EDX), morphology and physical size analysis using Transmission Electron Microscope (TEM), and thermal analysis using Thermogravimetry (TGA). Through these studies, X-ray diffraction revealed that phase transitions occurred for manganese oxide nanowires at calcination temperature 500 ℃. The crystallite sizes of manganese oxide nanowires reduces as the calcination temperature increases. FE-SEM analysis shows larger production of manganese oxide nanowires obtained through hydrothermal method and forming into clusters as the calcination temperature increases. EDX test confirmed the presence of manganese and oxygen as dominant elements in the compound. The chemical compositions remain unchanged even after applying higher temperature. An increase in temperature affected the particle size is shown in TEM images. The particle size is reduced as the calcination temperature is increased. This indicates the diameter of the nanowires gets smaller as the heating temperature gets higher forming thinner and longer nanowires. TGA results identified the changes in weight as well as determine the thermal stability as the calcination temperature increases. The decomposition temperature for $MnO_2$ nanowires to reach thermal stability is starting at 600 ℃.

# ABSTRAK

Dalam penyelidikan ini, mangan (IV) oksida disintesis menggunakan satu kaedah kimia yang mudah iaitu melalui kaedah hidroterma. Analisis atas sifat-sifatnya dijalankan untuk mangan (IV) oksida asli, telah disintesis dan dipanaskan pada suhu 400, 500 dan 600 ℃ masing-masing. Pelbagai teknik digunakan seperti Belauan Sinar-X (XRD) untuk analisis struktur, Mikroskop Electron Pembebasan Imbasan Tinggi (FE-SEM) untuk analisis permukaan, Spectroskopi Tenaga Dispersi Sinar-X (EDX) untuk analisis komposisi kimia, Mikroskop Elektron Pancaran (TEM) untuk analisis saiz dan bentuk zarah, dan Gravimetri Terma (TGA) untuk analisis terma. Melalui kajian yang dijalankan, XRD menunjukkan bahawa mangan oksida bersaiz nano mengalami pertukaran fasa pada suhu 500 ℃. Saiz kristal mangan oksida bersaiz nano semakin mengecil apabila suhu pemanasan semakin meningkat. Analisis FE-SEM menunjukkan mangan oksida bersaiz nano dapat dihasilkan dalam quantiti yang banyak melalui kaedah hidroterma dan bentuknya semakin dekat dan terikat apabila suhu pemanasan dinaikkan. Ujian EDX membuktikan kehadiran Mn & O sebagai elemen dominan dalam komponen $MnO_2$. Komposisi kimia $MnO_2$ tidak terjejas walaupun di bawah suhu tinggi. Peningkatan dalam suhu mempengaruhi saiz partikel seperti yang ditunjukkan dalam imej TEM. Ini menunjukkan diameter mangan oksida bersaiz nano semakin mengecil apabila suhu semakin meningkat menghasilkan mangan oksida bersaiz nano yang kurus and panjang. TGA identifi perubahan jisim mangan oksida dan mengkaji kestabilan terma terhadap peningkatan suhu pemanasan. $MnO_2$ bersaiz nano mencapai kestabilan terma bermula pada suhu 600 ℃.

## ACKNOWLEDGEMENT

From the bottom of my heart, I would like to express my never ending thank you to my 1st Supervisor Prof.Dr.Mohd.Rafie Johan. Eventhough I was from Manufacturing Engineering department, he doesn't hesitate to accept me and support me throughout my thesis with his great patience and knowledge. At the same time, I would like to shower my sincere gratitude to my 2nd Supervisor, Dr.Hamdi Mohd, who is very dynamic, supportive, humble and very helpful in many ways. Without both of my supervisors' good guidance, this research would have not been completed. Furthermore, I would like to thank the laboratory technicians for their great assistance during the laboratory testing. I would also like to express my gratitude to the Masters students from Advance lab as their help has supported me a lot in completing my research.

Nothing in this world is precious than our parents. Millions of thank you and love I shall honor to my parents, Mr&Mrs.Pon.Supramaniam-Devi who has become the main encouraging person for me to take up Masters Degree. This Masters Degree is a gift from me to my parents. Thank you to my beloved husband, Mr.Vicneswaran Arumugam who is also a Masters student in M.Eng, who has been a great supporter to me throughout completing my postgraduate studies. Special thanks to my lovely son, Thevesh who has actually motivated me to the maximum to complete this research without any delay.

Finally thank you to everyone who has involved directly and indirectly in this research completion.

# TABLE OF CONTENTS

**CHAPTER TWO LITERATURE REVIEW**

## LIST OF FIGURES

# LIST OF TABLES

## LIST OF SYMBOLS AND ABBREVIATIONS

| | |
|---|---|
| α | - alpha |
| β | - beta |
| γ | - gamma |
| δ | - delta |
| Å | - Angstrom |
| θ | - angle of the peak |
| λ | - X-ray wavelength |
| t | - Scherrer thickness which determine the crystallite size |
| $\beta_1$ | - FWHM in radians |
| μ | - micron |
| 1-D | - One dimensional |
| 3-D | - Three dimensional |
| Al | - Aluminium atom |
| CMOS | - Complimentary Metal Oxide Semiconductor |
| EDX | - Energy Dispersive X-ray Spectroscopy |
| FE-SEM | - Field Emission Scanning Electron Microscope |
| FWHM | -Full Width Height Maximum |
| $H_2O$ | - Water |
| IS | - Impedance Spectroscopy |
| JCPDS | - Joint Committee on Powder Diffraction Standards |
| $Li/MnO_2$ | - Lithium Manganese (IV) Oxide |
| LCD | - Liquid Crystal Display |
| Mn | - Manganese atom |
| $MnO_2$ | - Manganese (IV) Oxide |

| | |
|---|---|
| $MnO_6$ | - Manganese Hexoxide |
| $MnSO_4$ | - Manganese Sulfat |
| $Mn_2O_3$ | - Manganese (III) Oxide |
| $Mn_3O_4$ | - Manganese (II,III) Oxide |
| $KMnO_4$ | - Potassium permanganate |
| O | - Oxygen atom |
| Si | - Silicon atom |
| SEM | - Scanning Electron Microscope |
| TEM | - Transmission Electron Microscopy |
| TGA | - Thermogravimetry |
| UV-VIS | - Ultraviolet-visible Spectrophotometer |
| XRD | - X-ray Diffractometer |

# CHAPTER ONE

# INTRODUCTION

## 1.1 Background

For past decades, intensive and broad studies on nanoscience and nanotechnology were initialized all over the world (Laherto, 2010). One-dimensional (1-D) nanoscale materials particularly the nanowires provide good models to investigate many interesting properties on size confinement and dimensionality. An important aspect of nanowires relates to the assembly of individual atoms into such unique 1-D nanostructures in a controlled fashion. The physical properties of nanomaterials are novel and completely different from those in bulk materials. Nanowires are likely to play a vital role as interconnects and active components in nanoscale devices. The new discovered properties of nanomaterials not only reflected in electronics field but also exhibited in optics and magnetism. Among the 1-D nanoscale materials, $MnO_2$ nanowires are of particular interest due to its potential applications in catalysts, ion-sieves and especially as electrode materials in Li/$MnO_2$ batteries(Wei, 2005).

Essentially, Manganese (IV) oxide is one of the most stable with excellent physical and chemical properties. As well known, $MnO_2$ exists in many polymorphic forms in nature, such as the α-, β-, γ-, δ- types. The crystal structures are commonly believed to be responsible for their properties and the controlled synthesis of $MnO_2$ has always been the focus of material researchers. Much effort has been made to synthesize crystalline $MnO_2$ with a low-dimensional nanostructure, because dimensionality is a crucial factor in determining the properties of nanowires (Luo, 2008).

The synthesis of nanowires with controlled composition, size, purity and crystallinity, requires a proper understanding of the nucleation and growth processes at

the nanometer regime. 1-D nanostructures have been fabricated using nanolithographic techniques but it is not very cost effective and rapid for the purpose of making large quantities of 1-D nanostructures based on a broad range of materials (Rao, 2004). Chemical methods such as hydrothermal synthesis tend to be superior and provide an alternative strategy for generating 1-D nanostructures (Xia, 2003). The possible advantages of hydrothermal method compared to other types of crystal growth include the ability to generate crystalline phases which are stable at the melting point. Also, materials which have a high vapour pressure near their melting points can also be grown by the hydrothermal method. The method is also particularly suitable for the growth of large good-quality crystals while maintaining good control over their composition even at higher temperature.

## 1.2 Research Objectives

The objectives of this research are:

1. To produce single-crystalline nanowires by synthesizing manganese oxide by a simple method via chemical route called hydrothermal treatment. .
2. To investigate the effect of various calcination temperature towards manganese oxide nanowires.
3. To characterize the properties of the manganese oxide nanowires using analytical methods such as XRD, FESEM, EDX, TEM, and TGA.

## 1.3 Scope of Research

A study is conducted to synthesis $MnO_2$ by chemical reaction route via hydrothermal method and continued with calcination by heating in the furnace at temperature 400, 500 and 600℃. This is followed by characterization study to determine the properties of the manganese oxide nanowires using various analytical methods such as XRD, FESEM, EDX, TEM, and TGA.

## 1.4 Importance of the Research

Nanowire has been a well known contributor to nanotechnology industry. Nanotechnology is very diverse, ranging from novel extensions of conventional device physics, to completely new way based on molecular self-assembly till developing new materials with nanoscaled dimensions, even to speculation on whether we can directly control on the atomic scale. Generally nanotechnology deals with structures of the size 100 nanometers or smaller, and involves developing materials or devices within that size. (Huang, 2009).

Of all the $MnO_2$ structures, $\gamma$-$MnO_2$ is the best known as an electrode material in the battery industry. Nanowire devices show more outstanding performance as they are made smaller. This clearly shows the reason, not merely to publicity but to consider developing nanowire devices for electronic applications with the hope that their performance can prove the best achievement in industry. Specific applications for nanowire transistors in future include their use in building high-performance logic circuits as well as in electronics applications on unconventional substrates, such as plastics, where such high-performance devices have not been possible.

## 1.5 Organization of Thesis

### 1.5.1 Chapter One

Chapter One gives a general introduction as well as the aim of this study. It described the research objectives, scope of the research and the importance of the research.

### 1.5.2 Chapter Two

Chapter Two touches on the literature review which gives a detail review of the previous researches done on the area of study and fundamentals on current research.

### 1.5.3 Chapter Three

Chapter Three gives a complete report on the methodology of the research and characterization techniques, equipments and materials used to carry out the analysis.

### 1.5.4 Chapter Four

Chapter Four presents the results of the analysis and the discussion on the results obtained.

### 1.5.5 Chapter Five

Chapter Five gives the conclusion based on the outcome gained and some recommendations for future studies.

# CHAPTER TWO

# LITERATURE REVIEW

## 2.1 Manganese (IV) Oxide ($MnO_2$)

In recent years, intense research interests has been devoted to manganese oxide as it is inexpensive, its raw materials are abundant in nature, environmentally friendly and also widely used in batteries (Devaraj, 2007). Manganese (IV) oxide or also called as manganese dioxide is the inorganic compound with a molecular formula $MnO_2$. It appeared as blackish powder as shown in Fig 2.1. It is odorless and occurs naturally as the mineral pyrolusite, which is the main ore of manganese and a component of manganese nodules. It has specific gravity of 5.0m/$s^2$ and melting point of 1539 ℃. $MnO_2$ is insoluble in water and inert to most acids except when heated. The density of $MnO_2$ is 5.026g/cm3 and molecular weight is 86.94g/mol (Chandra, 1999).

Figure 2.1: Sample of Manganese (IV) oxide (Internet reference, 15/01/2012)

Manganese (IV) oxide is one of the most stable manganese oxides with excellent physical and chemical properties under ambient condition. The molecular bonding of $MnO_2$ with layered and tunneled frameworks consisting of edge-shared $MnO_6$ octahedral units is shown in Figure 2.2 (Passerini, 1988).

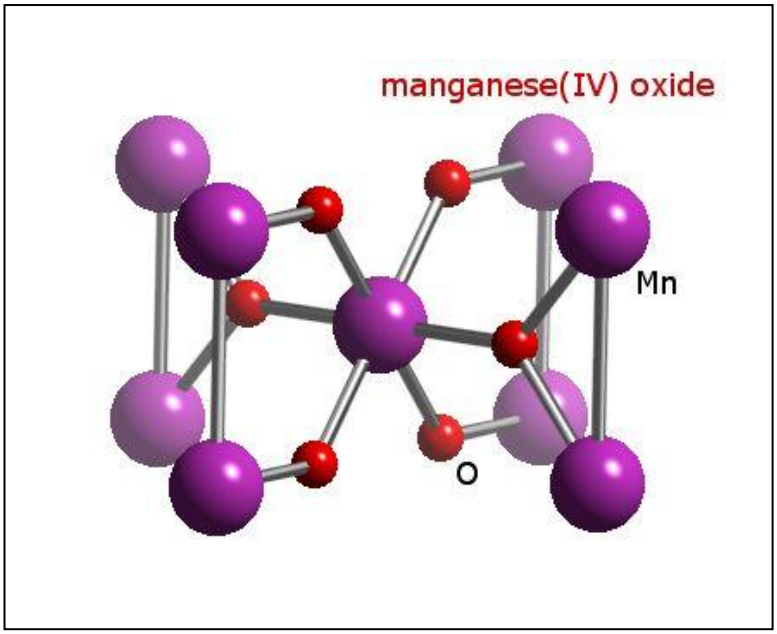


Figure 2.2: Geometry of Manganese (IV) 0xide (Passerini, 1988).

Pyrolusite as shown in Fig 2.3 is the chief source of manganese and all its compounds, when derived from ores. Pyrolusite has some interesting habits despite its common occurrence as dull, grimy, black masses and earthy forms. Pyrolusite is widely used as a chemical oxidant in organic synthesis. Possibly it is most popular form is its dendritic habit that forms wonderfully detailed, fern-like patterns on the surfaces of rocks and sandstone. These dendrites are so astonishing that they have often been mistaken for fossil plants (Potter, 1979). Often specimens of pyrolusite are very hard to differentiate from other manganese oxides. As a consequence of its rich distribution, pyrolusite is the default name for black, hair-like manganese crystals or powdery black alteration products of manganese minerals in general.

Figure 2.3: Pyrolusite (Internet reference, 26/01/2012)

Manganese oxide can form many kinds of polymorphs, such as α-., β-, γ- and δ-type, offering distinctive properties and wide applications as catalysts, ion-sieves, and especially as electrode materials in Li/$MnO_2$ is the best known as an electrode material by the battery industry. The structure of γ-$MnO_2$ is considered to be a random intergrowth of 1 x 1 tunnels of pyrolusite and 2 x 1 tunnels of ramsdellite, which are constructed of $MnO_6$ octahedral units of edge or corner sharping. γ-$MnO_2$ materials can be usually prepared by electrochemical oxidation of acidic $MnSO_4$ solutions, as well as by chemical methods, however, these powdered particles prepared in usual methods are in irregular shapes (Yuan, 2003).

## 2.2 Product and Application of Manganese (IV) Oxide

The predominant application of $MnO_2$ is as a component of dry cell batteries such as the alkaline battery and the zinc carbon battery. $MnO_2$ is widely used as high energy and power density electrodes in lithium manganese dioxide batteries. Approximately 500,000 tonnes are consumed for this application annually (Internet Reference, 15/01/2012). Other industrial applications include the use of $MnO_2$ as an inorganic pigment in ceramics and in glass making.

### 2.2.1 Miniature Alkaline $MnO_2$ Battery

The miniature manganese (IV) oxide primary battery is designed to provide an economical power source for device applications. It is used as substitutes in calculators, automatic exposure control cameras, watches and a variety of small toys. It has good rate sensitivity equivalent to silver oxide, good low temperature characteristics, good resistance to shock, vibration, and acceleration. A cutaway of miniature manganese oxide battery is illustrated in Figure 2.4 below (Alkaline, 2012).

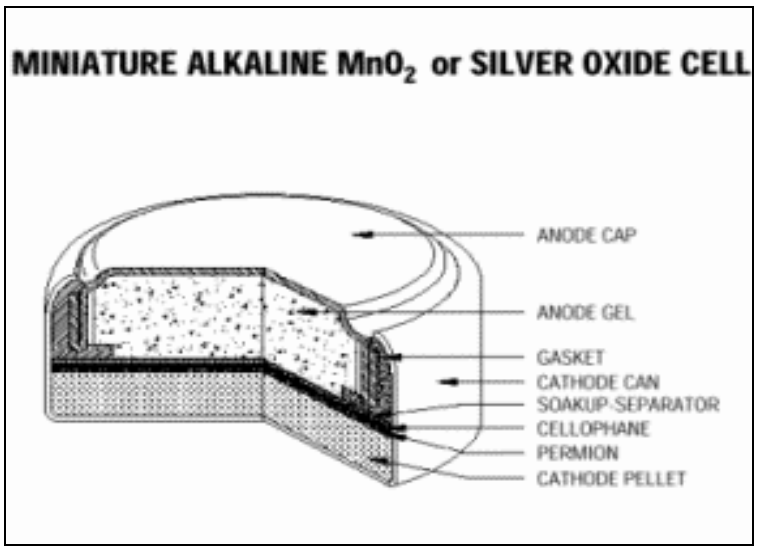


Figure 2.4: Miniature Alkaline $MnO_2$ Battery (Alkaline, 2012)

Miniature $MnO_2$ batteries consist of a $MnO_2$ cathode, a zinc anode of high surface area, and a highly alkaline electrolyte consisting of potassium hydroxide. The open circuit voltage of miniature manganese dioxide batteries is approximately 1.6 volts. The operating voltage at typical current drains varies with the depth of discharge of the battery as shown in Figure 2.5 (Alkaline, 2012).

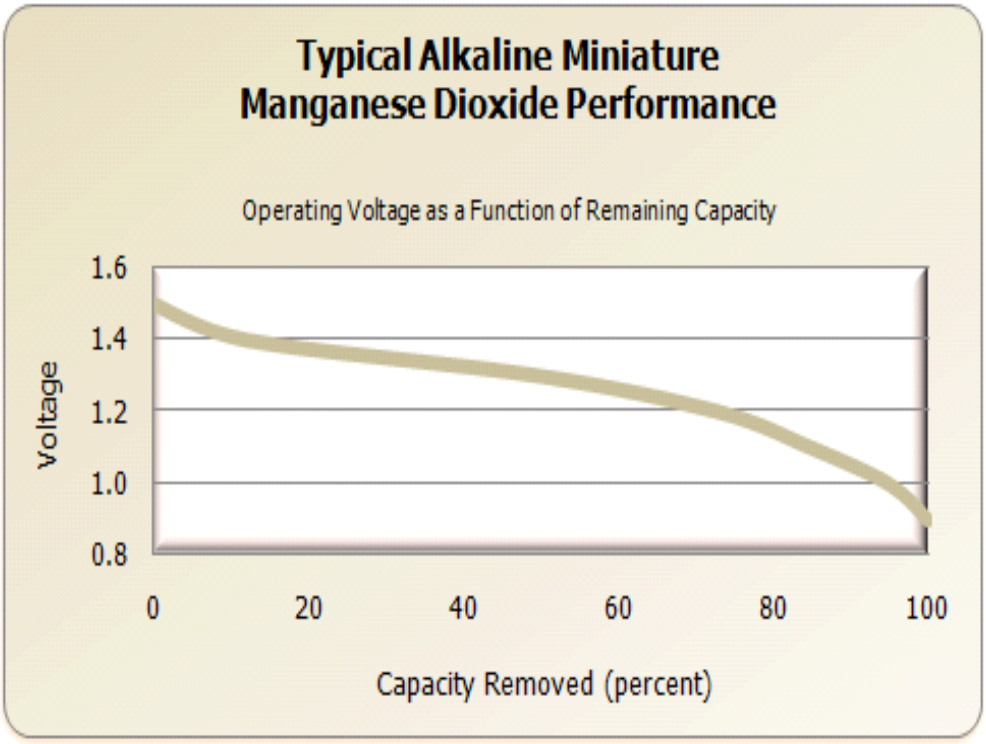


Figure 2.5: $MnO_2$ Battery Operating Voltage (Alkaline, 2012)

### 2.2.2 Zinc Carbon Battery

A zinc–carbon battery is an electrochemical cell that is packaged in a zinc case that serves as negative electrode and carbon rod as positive electrode. The positive terminal is a carbon rod surrounded by a mixture of manganese (IV) oxide and carbon powder. The electrolyte used is a paste of zinc chloride and ammonium chloride dissolved in water. The ratio of manganese (IV) oxide and carbon powder in the cathode paste affects the characteristics of the cell whereby more carbon powder lowers the

internal resistance, but more manganese (IV) oxide improves the capacity and increase the electrical conductivity (Linden, 2002). A cross section zinc-carbon battery is demonstrated in Figure 2.6 below.

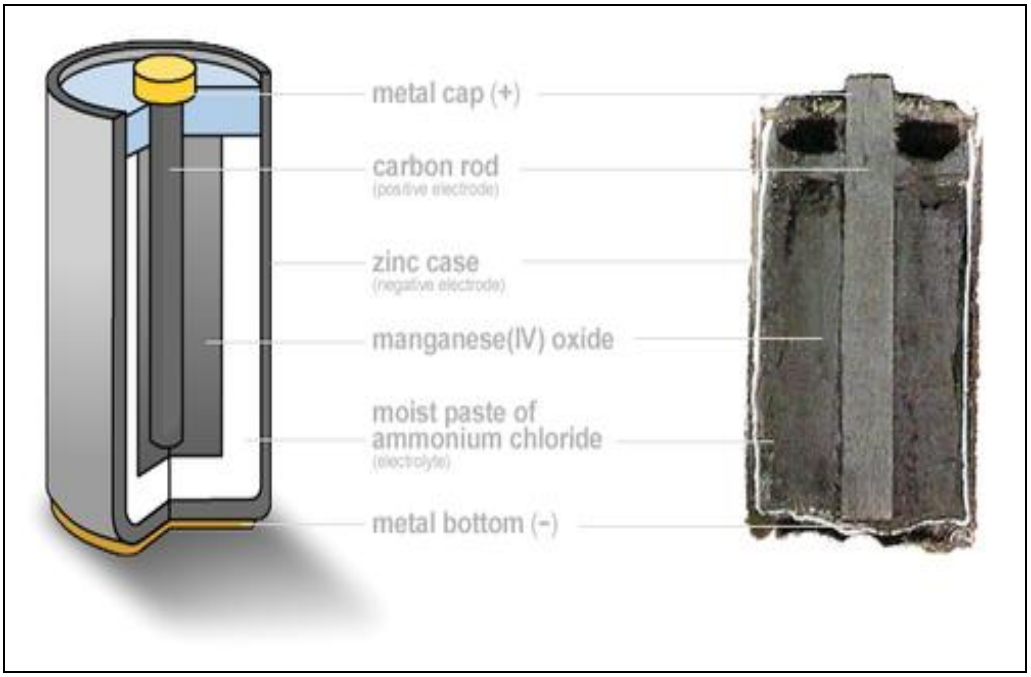


Figure 2.6: Cross section of a zinc-carbon battery (Internet reference, 08/02/2012)

Its nominal voltage is 1.5V. Zinc–carbon battery is preferable due to inexpensive, standardized product and it can be applied to low current product. Zinc-carbon batteries are widely used in different household applications like clock, remote controls, radios, recorders, electric watches, cameras, torches, toy, flashlight and heater (Khan, 2012).

### 2.2.3 Lithium Manganese (IV) Oxide battery (Li-$MnO_2$ Battery)

Lithium manganese batteries are found in a variety of shapes, with the most common being the button cells and the cylindrical batteries as shown in Figure 2.7. Lithium batteries are used in cardiac pacemakers in CMOS (complimentary metal-

oxide-semiconductor) memory storage, powering LCD's in watches, calculators and in other military and medical applications

The major advantages of lithium manganese batteries over alkaline batteries are their high energy and power density, good storage life and good discharge performance. It has high-reliability and it is lightweight battery with an operating voltage of 3V which is twice the voltage of other button cell batteries. It has the ability to operate over a wide range of temperature range from low to high. Because of lithium manganese oxide's stability, these batteries can be stored for several years. Operating temperatures have little effect on operating characteristics because the cell is so efficient (Park, 2003).

Figure 2.7**:** Li-$MnO_2$ Batteries

### 2.2.4 Black Glass Bottle

$MnO_2$ is used as pigment in the colouring of ceramics and glass making industry. It is pigment in clay and it produces colours such as yellow, brown, purple or black colors. Most pigments used in manufacturing are dry colourants represented as a fine powder. This powder is added to a relatively neutral or colourless material that acts as a binder. $MnO_2$ is colourant used in making black glass bottle as shown in Figure 2.8

Figure 2.8: Black glass bottle

Black colors are obtained by adding a mixture of iron oxide and manganese (IV) oxide as shown in material combination under oxidation condition as below:

$$MnO_2+Fe_2O_3+NiO+CoO+CuO \longrightarrow \text{black color} \qquad (1.1)$$

## 2.3 Nanowires

Nanowire is a nanostructure, with the diameter of the order of a nanometer ($10^{-9}$ meters). On the other hand, nanowires can also be defined as structures that owns a lateral size constrained to tens of nanometers or less and an unconstrained longitudinal size.At these scales, such wires are also known as quantum wires as quantum mechanical effects are important here. There are many different types of nanowires including metallic, semiconducting and insulating. Molecular nanowires are composed of repeating molecular units either organic or inorganic. The nanowires could be used to link tiny components into extremely small circuits, in the near future. By using nanotechnology, such components could be created out of chemical compounds.

Nanowires have an amazing length-to-width ratio. Nanowires can be incredibly thin. It is possible to create a nanowire with the diameter of just one nanometer, though engineers and scientists tend to work with nanowires that are between 30 and 60 nanometers wide. As such, they are often referred to as one-dimensional (1-D) materials.

Nanowires have many interesting properties that are not seen in bulk or 3-D materials. This is because electrons in nanowires are quantum confined laterally and occupy energy levels that are different from the traditional continum of energy levels or bands found in bulk materials. The increased surface area, very high density of electronic states , enhanced binding energy and the increased surface scattering for electrons and photons are just some of the ways in which nanowires vary from their corresponding bulk materials (Dresselhaus, 2003)

One- dimensional nanostructure (nanowires, nanorods, nanotubes) are expected to exhibit some superior physical and electrochemical properties which have generated intense research interests over the past recent years due to their novel properties (Ren, 2009).

From an applications viewpoint, nanowires have the advantage that some of the materials parameters that are crucial for certain properties can be independently controlled in nanowires, but not in their bulk material. By exploiting the singular aspects of the 1-D electronic density of states, certain properties can be enhanced non-linearly in small diameter nanowires. Furthermore, nanowires have been shown to provide a promising framework for applying the bottom-up approach for the design of nanostructures for nanoscience investigations and for potential nanotechnology applications (Dresselhaus, 2003).

Driven by these new research and development opportunities, the smaller and smaller length scales now being used in the semiconductor, electronics and magnetics industries, and the remarkable development of the biotechnology industry where the achievement is also at the nanoscale. The nanowire research field has developed in high speed in the last few years. As a result, an analysis of the current status of nanowire research shows a significant wide attention and huge interest is being implemented on nanowire research and development at the present time. It is the aim of this analysis to focus on nanowire properties that differ from those of their parent crystalline bulk materials, with aiming towards potential applications that might gained from the unique properties of nanowires and from future discoveries in this field (Dresselhaus, 2003).

## 2.4 Manganese (IV) Oxide Nanowires

One-dimensional Manganese (IV) Oxide nanowires, have attracted considerable interest in recent years due to their novel electronic, optical, mechanical and magnetic properties (Zhang, 2008). There has been an increasing interest in developing materials based on manganese oxides, owing to their wide structural diversity combined with unique chemical and physical properties and their numerous applications as catalysts and in ion-sieves, rechargeable batteries and supercapacitors. Manganese dioxides have many polymorphic forms, such as α-, β-, γ-, and δ-types, which differ in the way in which the basic octahedral $MnO_6$ units are linked together. Interestingly, the various polymorphs generally have different properties (Zhang, 2008).

A single crystal ultra-long manganese oxide nanowire has diameter about 10-40nm and lengths up to several tens of micrometers. Owing to their properties, they have high potential applications in catalysis, ion-sieves, and especially as electrode materials in lithium batteries(Wei, 2005). Particularly, manganese oxides are considered to be a most attractive candidate as cathodic materials for the next generation of lithium ion because of its abundant natural resources, low-cost and environmental friendliness (Yang, 2008).

$MnO_2$ nanowires have high electrode surface area for rechargeable energy storage applications. It also has excellent mechanical strength**.** $MnO_2$ nanowires have good better electrical conductivity and gives excellent supercapacitor performances (Li, 2012).

## 2.5 Synthesis of Manganese (IV) Oxide Nanowires

Various approaches have been used to synthesis manganese (IV) oxide, such as via microemulsion, solid reaction, and hydrothermal methods (Pang, 2012). Such manganese dioxide nanostructures are of considerable importance in technological applications. It has been intensively investigated as promising electrode materials in primary and secondary batteries and as electrochemical capacitors due to their excellent electrochemical properties, low-cost, environmental safe and easy in preparation. (Subramaniam, 2005).

### 2.5.1 Synthesis of $MnO_2$ nanowires via Microemulsion Method

Reactions carried out in microemulsion media produce nanoparticles. Microemulsion method is used to synthesis nanoscale particles of $MnO_2$ for electrochemical supercapacitor properties studies (Devaraj, 2007).

The reactants are confined in a micro-nano droplets of water dispersed in an organic medium and the emulsion is stabilized by a suitable surface active agent. As the reaction zone is confined to the size of the water droplet, the growth of solid particles of the product is limited to nanometer scale. Microemulsion is a suitable route for synthesis of nanoparticles of several metals or metal oxides. The $MnO_2$ particle is calcined at several temperatures to produce nanowires of 5nm diameter of varying dimensions. It remains in α-structure with nanoscale particles in the temperature range from 70–400 ℃. At 500 ℃, α-$MnO_2$ exhibits chemical transformation becomes $Mn_2O_3$. At 900 ℃, the sample transforms into $Mn_3O_4$. The morphology is highly influenced by the annealing temperature. On annealing at different temperatures, a mixture of nanowires and nanoparticles was noticed (Devaraj, 2007).

### 2.5.2 Synthesis of $MnO_2$ nanowires via Solid Reaction Method

A simple method based on a conventional solid-state process is proposed for synthesis of manganese oxide nanowires (Eftekhari, 2005).

Solid-state synthesis is different from hydrothermal synthesis, in which the nanowires are dispersed in a fluid medium. As diffusion of Na ions through the $MnO_2$ structure leads to the formation of a nanostructured material, the application of a high temperature may coordinate the diffusion direction. It can be considered as an alternative to conventional template-based methods. This is solid-state synthesis which is the most common method for preparation of cathode materials such as manganese oxide for lithium batteries. This method provides an opportunity for bunching the nanowires synthesized, since the nanowires form in one direction. Thus, aligned bunches >100 $\mu$m long and about 50$\mu$m in diameter consisting of individual nanowires diameters ranging between 50 and 200 nm can be prepared simply. Nanowires generated, they are aligned unidirectionally. The close packing of nanowires in a bunch, which is an important feature of this method, causes difficulty in distinguishing individual nanowires. For instance, by viewing at the image of an entire bunch it may be conclude that they are microwires. However, a closer look reveals the existence of nanowires. Therefore it needs extensive crystallographic investigation to find out the crystal structural of the sample (Eftekhari, 2005).

### 2.5.3 Synthesis of $MnO_2$ nanowire via Sonochemical Method

Sonochemical technique was used to prepare nanostructured amorphous $MnO_2$ by reduction of potassium permanganate with manganese (II) acetate and adjusting the pH of the solution with ammonia hydroxide (Nam, 2010).

$MnO_2$ was synthesized by sonochemical methods wherein potassium permanganate and manganese (II) acetate are mixed. Nanostructured $MnO_2$ had the flower-like shapes and nanowires by changing the pH in the aqueous solution. A specific capacitance of 300 $Fg^{-1}$ for a nanowire structure was obtained using relatively high loading weight. The preparation involves reduction of potassium permanganate with manganese acetate in a mole ratio of 2:3. Manganese acetate and of potassium permanganate is dissolved in distilled water of different volume. The as-prepared potassium permanganate solution is then added drop-wise into the manganese acetate solution using a syringe pump and ammonium hydroxide was added in the same manner under ultrasound irradiation for 30 minutes. The resulting brown precipitate was separated by decantation and washed several times with distilled water. It was subsequently dried at 40 ℃ under vacuum for 12 h. Samples were prepared with and without ultrasonic treatment at different pH ranging from 3 to 10. $MnO_2$ nanowires showed the maximum specific capacitance of 300 $Fg^{-1}$ at a scan rate of 5 mV $s^{-1}$ in 1.0 M $Na_2SO_4$ solution and the minimum charge transfer resistance of 0.4 Ω. This could be explained by the long chained nanowires that were thought to be providing pathways and facilitate diffusion of protons in the electrolyte, thus resulting in enhanced accessibility of ionic species to the active materials (Nam, 2010).

### 2.5.4 Synthesis of $MnO_2$ nanowire via Hydrothermal Method

The hydrothermal method is a powerful synthesis approach for synthesizing various forms of manganese oxides (Pang, 2012). Various types of inorganic nanowires have been synthesized with the aid of templates or catalysts. Templates are being used to confine the growth of crystals, while catalysts may act as energetically favorable sites for the adsorption of reactant molecules. However, the introduction of templates or catalysts to a reaction system is often accompanied by drawbacks such as the need to prepare or select appropriate templates or catalysts. Besides, the impurities in the final product may be difficult to removed, thereby making the overall synthesis process more complicates and costly (Pang, 2012). Recently, some researchers had used Pluronic P123 as structure directing agent to synthesize $MnO_2$ nanowires at room temperature. However, this copolymer is very expensive and it is tedious to remove the copolymer from the end product after synthesis. Finally, $MnO_2$ nanowires were prepared by hydrothermal treatment of $MnO_2$ nanoparticles in water or ammonia solution at temperature 120–160 ℃.

A hydrothermal method is a free-template method without the use of any templates or catalysts which is more favorable for the preparation of low-dimensional nonstructural. This method is superior to traditional methods since no specific and expensive equipment is required for synthesizing the nanostructured materials at lower temperatures. Manganese (IV) oxide nanowires can be synthesized via soft chemical process through a hydrothermal method using distilled water which is found to be a favorable solvent in hydrothermal reactions.

## 2.6 Characterization Study of $MnO_2$ Nanowire Synthesized via Hydrothermal Method

### 2.6.1 Water as a solution

After hydrothermal treatment of $MnO_2$ granular crystals in water at temperature 130℃ for 24hours, the crystallite size in the resultant product is reduced. However the crystalline phase is the same with the original pure material. Further heating of the resultant product to higher temperature leads to further reduction of the crystallite size and occurrence of phase transformation as shown in Figure 2.9, the XRD pattern obtained for $MnO_2$ samples.

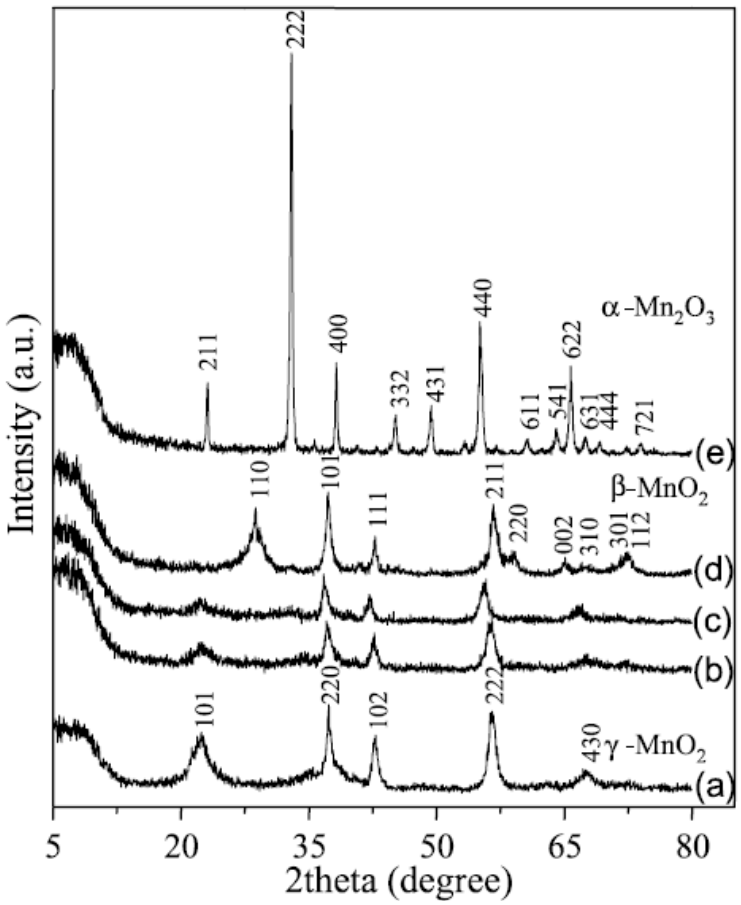


Figure 2.9: XRD pattern a) for raw material $MnO_2$; (b-c) after synthesized by hydrothermal method; (d,e)after calcination at 500 and 600℃ respectively (Yuan, 2003)

$MnO_2$ nanowires aligned well to present a form of coaxial nanopores or coiled together as shown in Figure 2.10 obtained from SEM. The diameters are found to be from 5-50nm and lengths up to several tens micrometers.

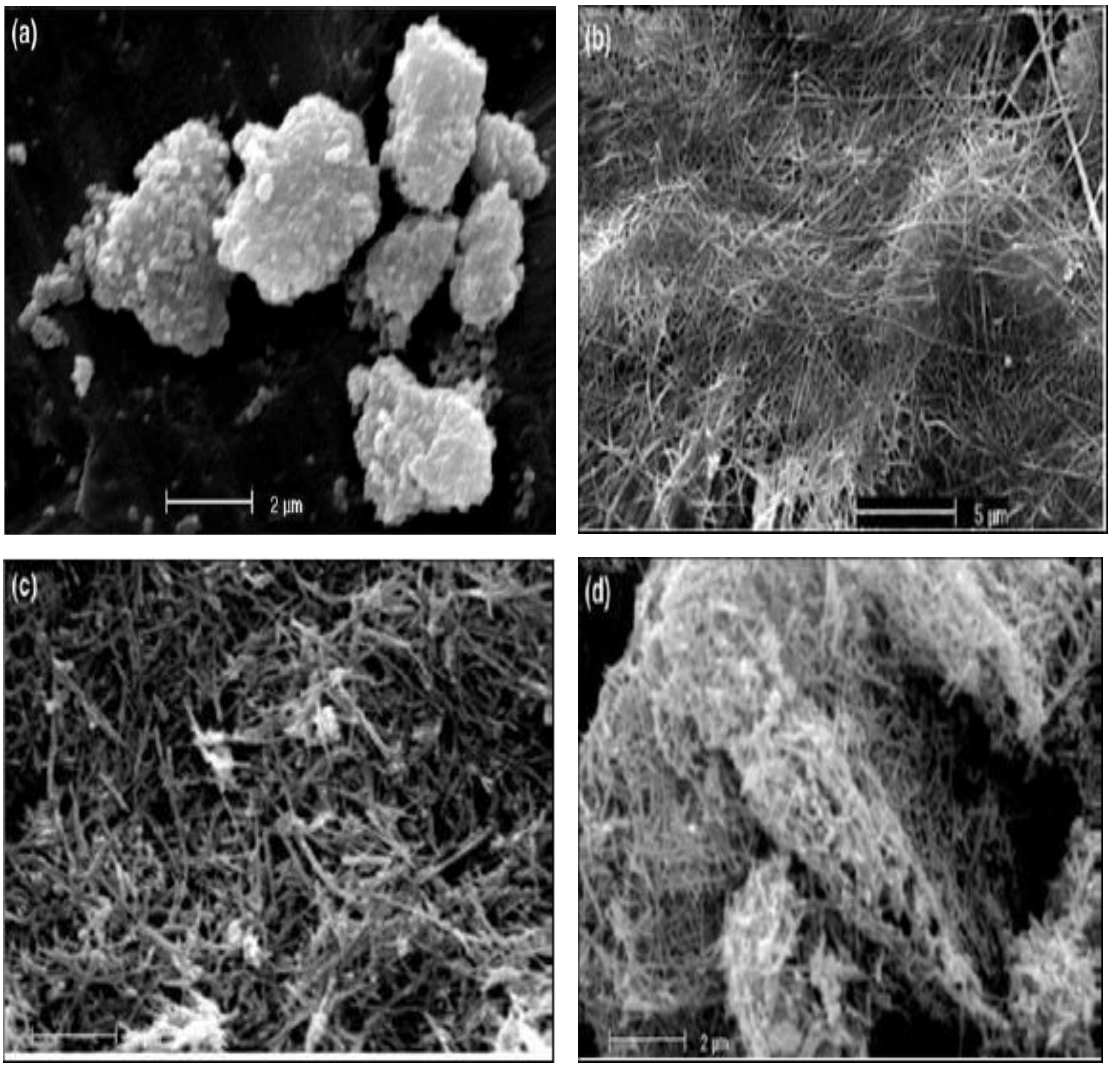


Figure 2.10: SEM images of $MnO_2$ (a) raw material; (b) after synthesized; (c) after calcination at 500 ℃; (d) after calcination at 600 ℃ (Yuan, 2003)

$MnO_2$ nanowires are formed in large quantity and disclosed a well-organized nanostructure of these wires. TEM results shows one single nanowire has a circular cross-section perpendicular to its axis as shown in Figure 2.11.

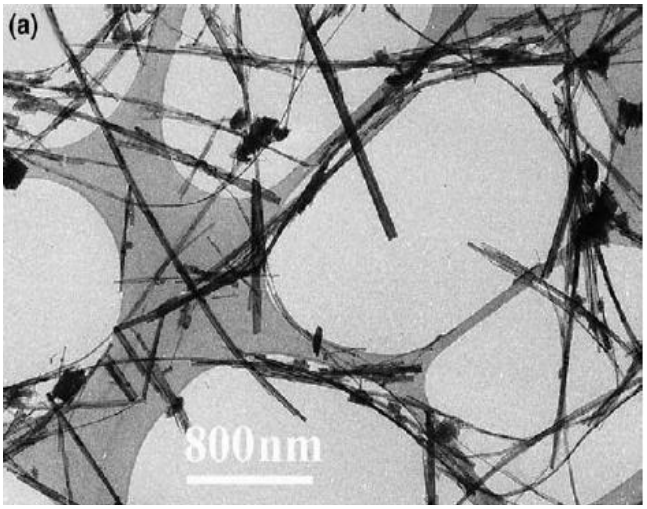


Figure 2.11: TEM image (Yuan, 2003)

Composition analysis reveals the presence of Mn and O as the dominant elements in the compound as shown in Figure 2.12.

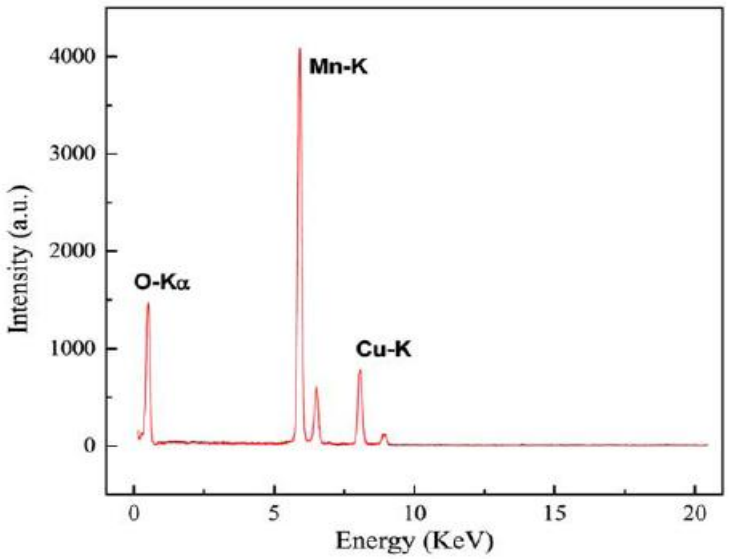


Figure 2.12: EDX image (Yuan, 2003)

TGA analysis reveals the presence of structural water and oxidation during the phase transformation as shown in Figure 2.13. The progressive weight loss at 20-250 ℃ is due to the removal of physically adsorbed water in the sample. The slight weight loss at temperature 300-450 ℃ is due to release of much more tightly bound water and transformation to β-MnO2. The sharp weight loss at temperature 500 ℃ is due to oxygen release for the transformation to α-$Mn_2O_3$ (Yuan, 2003).

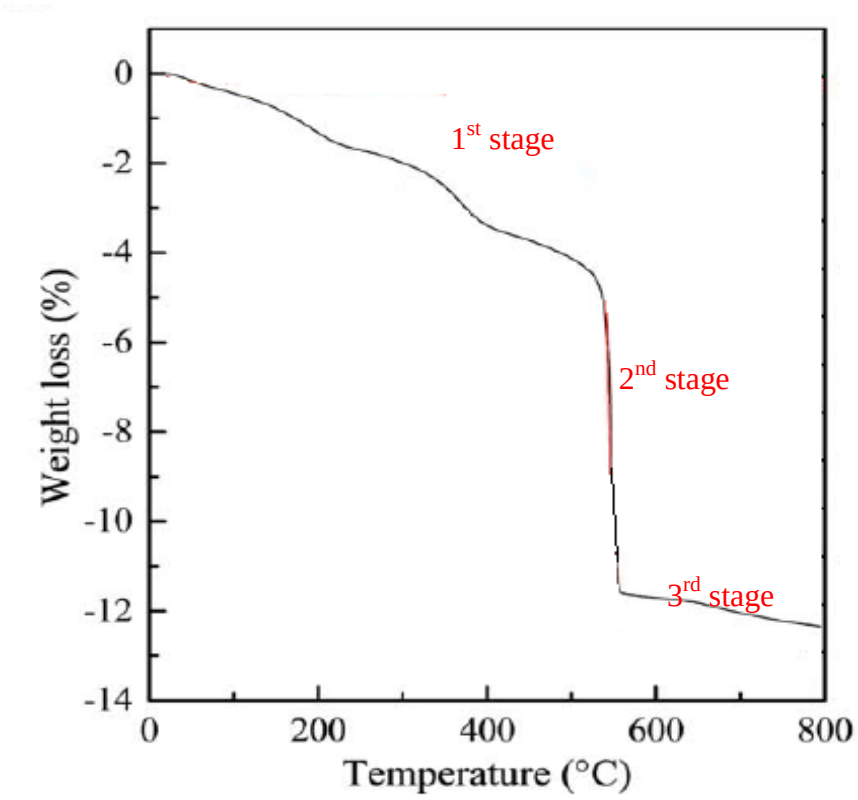


Figure 2.13: TGA curve (Yuan, 2003)

### 2.6.2 $MnSO_4$ and $KMnO_4$ as solution (temperature 25 ℃ and 80 ℃)

$MnO_2$ nanoparticles were synthesized by mixing aqueous solutions of $KMnO_4$ and $MnSO_4$ at ambient temperature being aged for 24hours for 25 ℃ and 80 ℃. $MnO_2$ nanostructures went through rapid transformation from $\delta$-$MnO_2$ to $\alpha$-$MnO_2$ phase as shown in Figure 2.14. Crystalline phase of the $MnO_2$ nanostructures were varied by the hydrothermal aging duration and temperature.

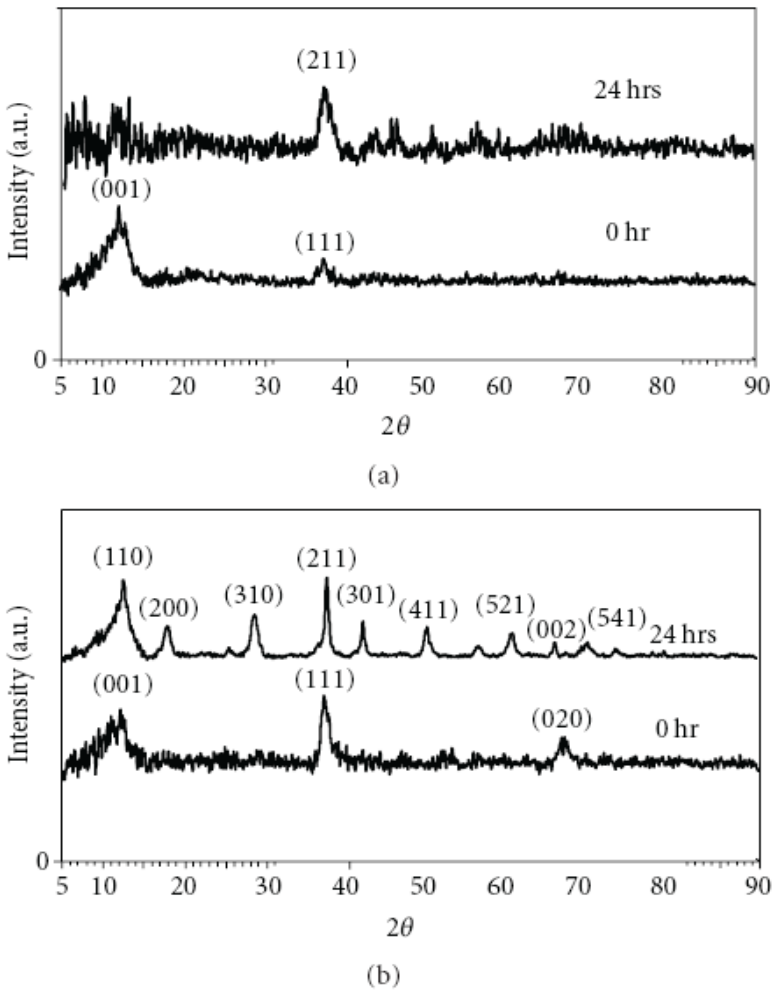


Figure 2.14: XRD patterns of MnO2 synthesized at (a) 25 ℃ and (b) 80 ℃ for 0 and after 24 hrs (Pang, 2012)

$MnO_2$ nanoparticles showed high tendency to aggregate and formed spherical agglomerates of various sizes. The aging temperature was found to play a crucial role in accelerating the rate of evolution of $MnO_2$ nanostructures from spherical agglomerates to aggregates of well-defined nanostructures as shown in Figure 2.15.

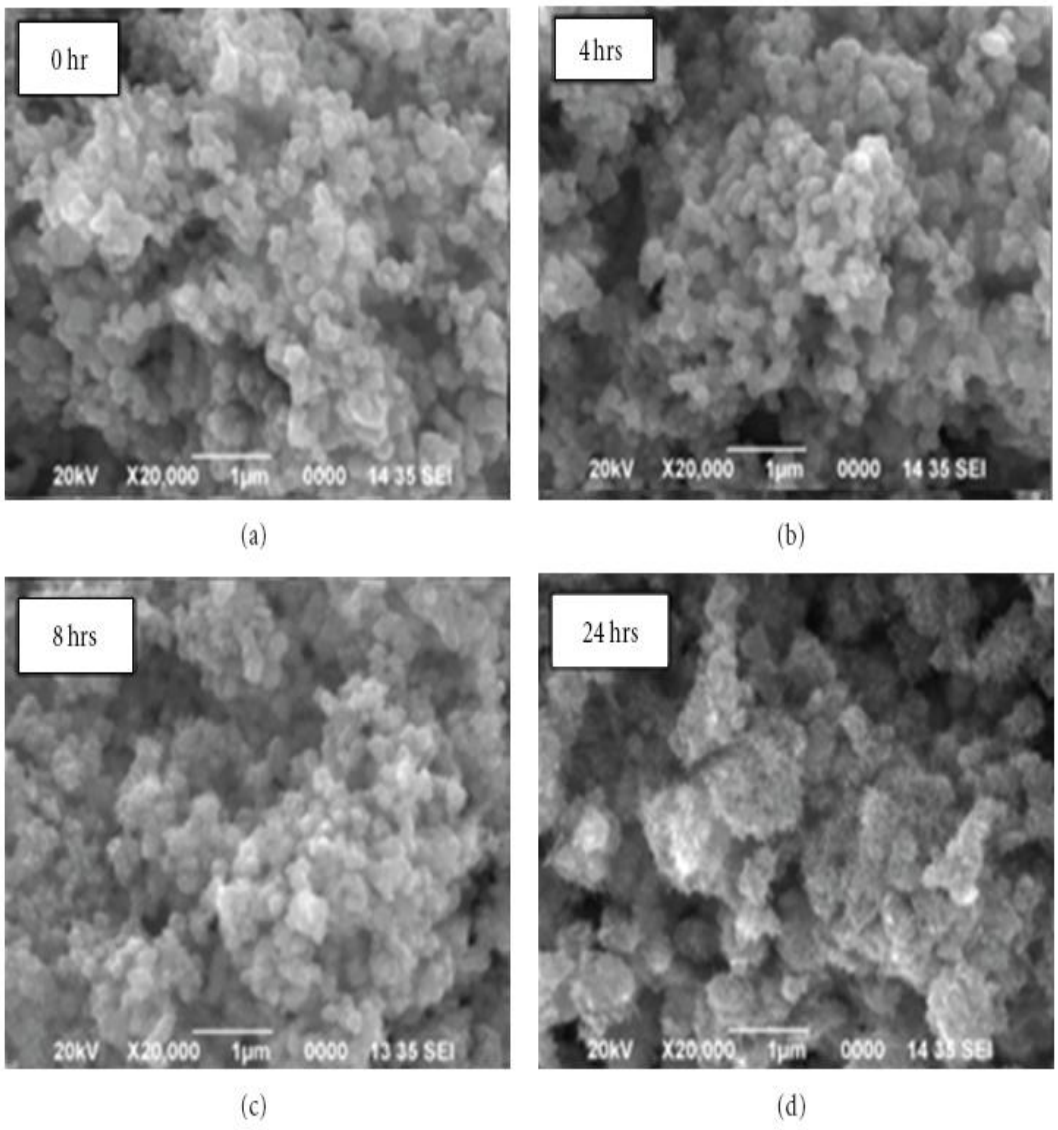


Figure 2.15: SEM micrographs of $MnO_2$ samples synthesized at various aging durations at 25 ℃ (Pang, 2012)

A higher aging temperature appeared to favor the growth of one-dimensional (1D) $MnO_2$ nanostructures which could be attributed to the rapid rate of decomposition of $MnSO_4$ to form $MnO_2$ at elevated temperatures. These nanorod-like nanostructures continued to grow in length due to their anisotropic nature and eventually led to the high formation of nanowires as shown in Figure 2.16. Henceforth, hydrothermal synthesis conditions could be controlled and optimized for the synthesis of $MnO_2$ nanostructures of desired morphology and crystalline phase.

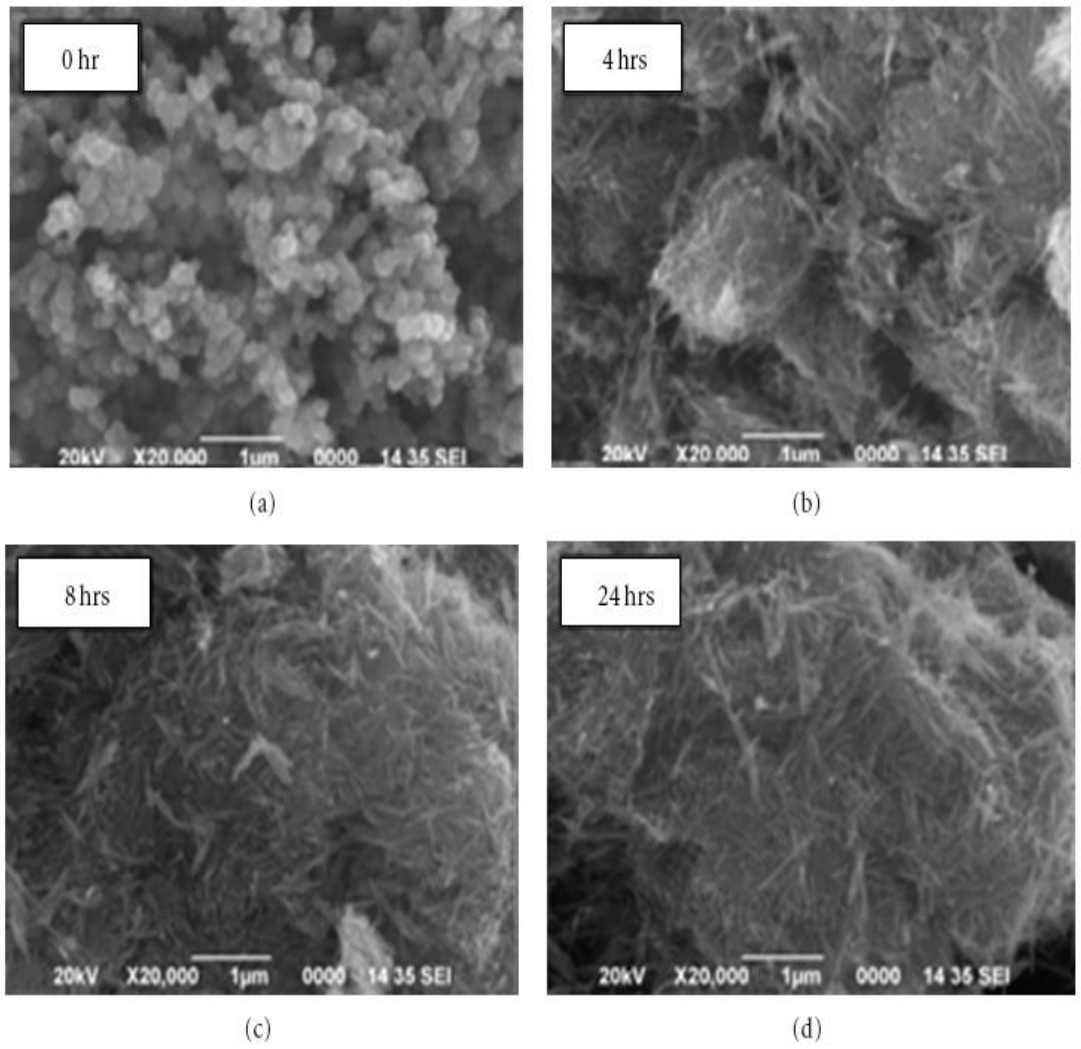


Figure 2.16: SEM micrographs of $MnO_2$ samples synthesized at various aging durations at 80 ℃ (Pang, 2012)

The evolution of nanorod-like nanostructures was observed to have initiated from the surfaces of $MnO_2$ nanoparticles after being aged for 4 hours at 25◦C. More distinctive and defined nanorod-like nanostructures had evolved from spherical $MnO_2$ nanoparticles after being aged for 8 hours. Long and well-defined nanorods were observed to have developed on $MnO_2$ nanoparticles forming nanostructures after being aged for 24 hours at 25 ℃ as shown in Figure 2.17.

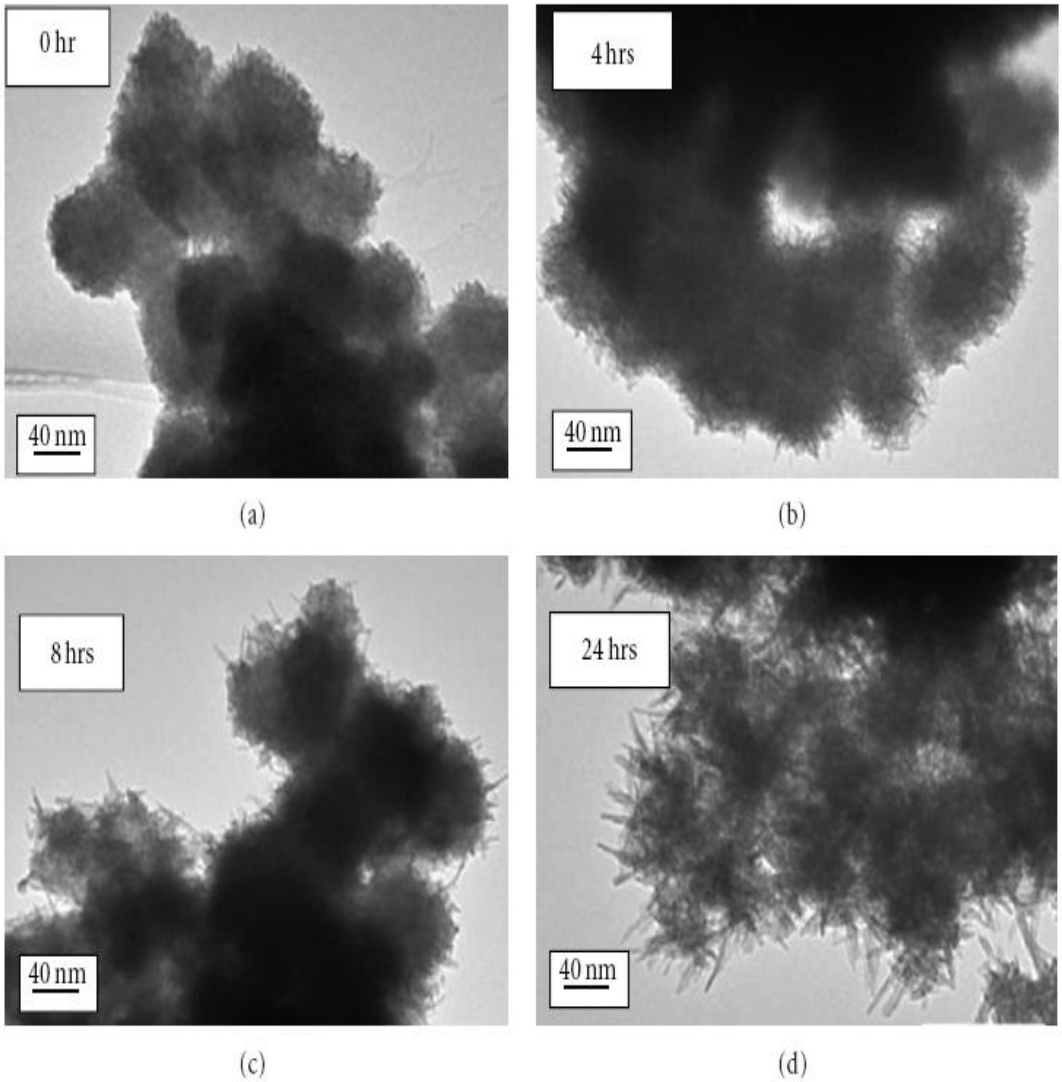


Figure 2.17: TEM micrographs of $MnO_2$ samples synthesized at various aging durations at 25 ℃ (Pang, 2012)

All $MnO_2$ nanoparticles were completely transformed into well-developed nanowires after being aged for 8 hours. No notable morphological changes of nanorods were observed after prolonged aging duration for up to 24 hours at 80 ℃ as shown in Figure 2.18. The diameter and length of well-defined $MnO_2$ nanorods ranged from 20 to 30nm and 300 to 400 nm, respectively.

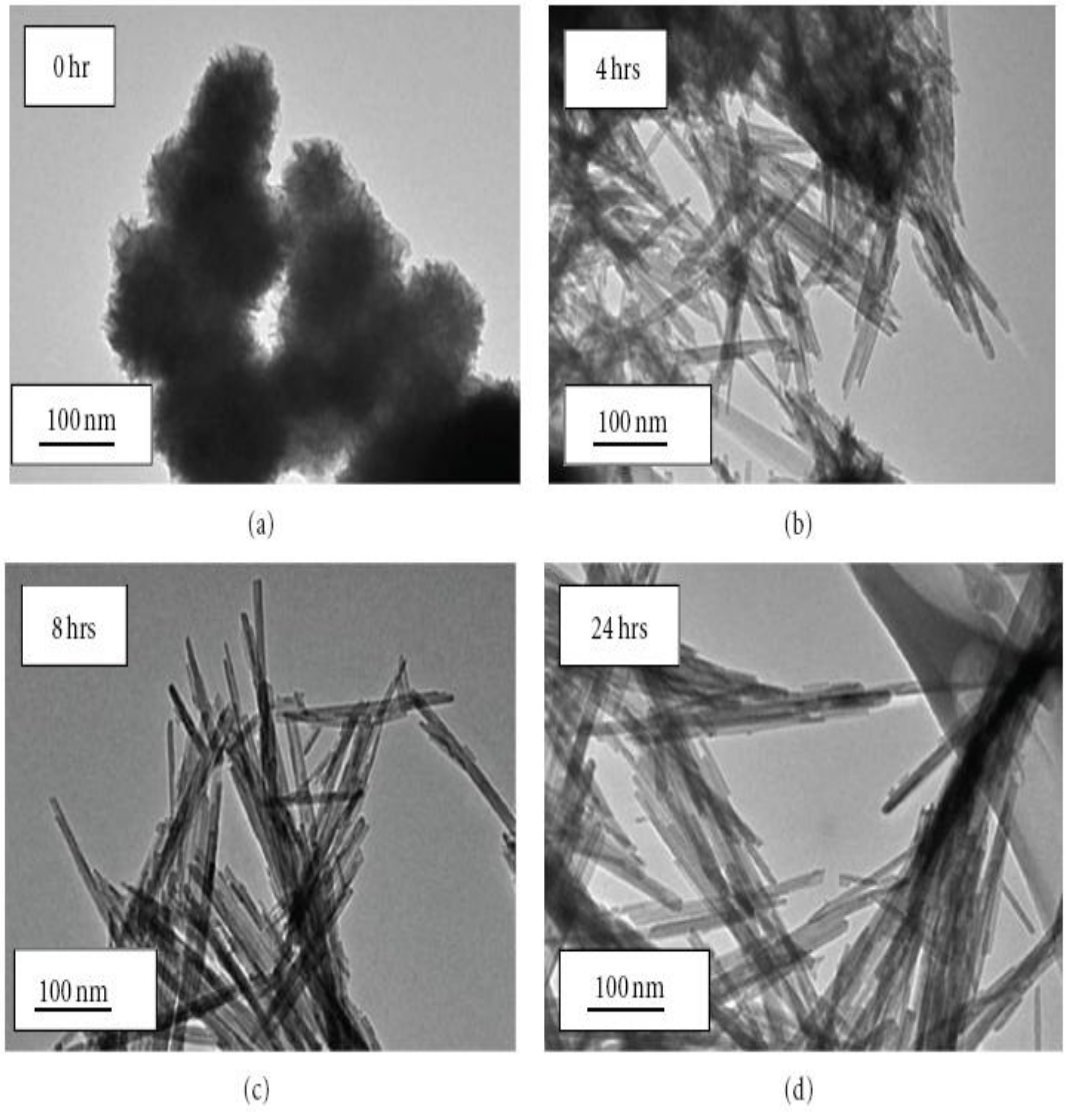


Figure 2.18: TEM micrographs of $MnO_2$ samples synthesized at various aging durations at 80 ℃ (Pang, 2012)

### 2.6.3 $MnSO_4$ and $KMnO_4$ as solution (temperature 160 ℃)

Figure 2.19 shows that polymorphic form of $MnO_2$ can be selectively controlled by varying the hydrothermal dwell time. The resulting products after hydrothermal treatment for 8hours and 72hours appeared as pure tetragonal phase of α-$MnO_2$ and β-$MnO_2$ respectively with the lattice constant confirmed by referring to the JC-PDS as reference (Zhang, 2008).

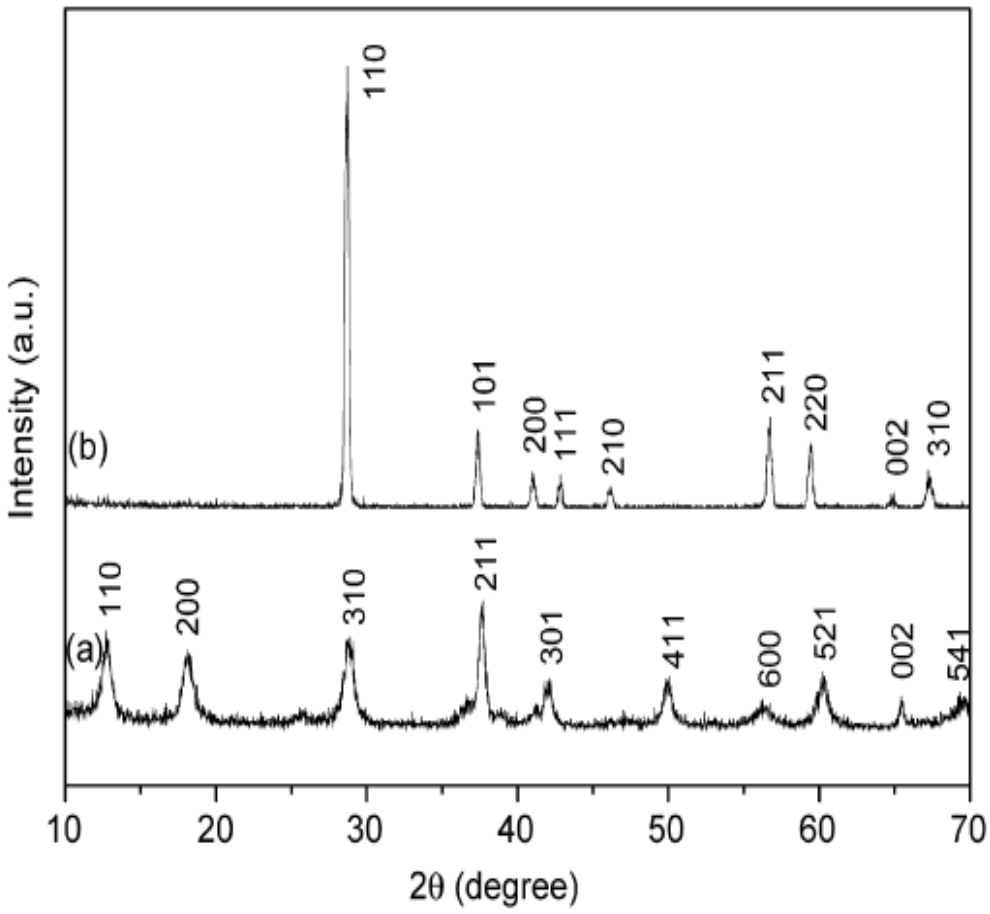


Figure 2.19: X-Ray diffraction of the products after different hydrothermal reaction times at 160 ℃ a) 8hrs and b)72hrs (Zhang, 2008)

Figure 2.20 a-b shows the SEM image for as prepared α-$MnO_2$. The products consist of nanowires with diameters about 30-40nm and length ranging between 1 and 4μm (Zhang, 2008). The presence of clear lattice fringes in the HRTEM image in Figure 2.20c confirms the single-crystalline nature of the α-$MnO_2$ nanowire, although some crystal defects can be observed on the surface of the nanowire. The β-$MnO_2$ products exhibits a prismatic morphology with pyramidal ends with bigger diameters and length compared to α-$MnO_2$ nanowire.

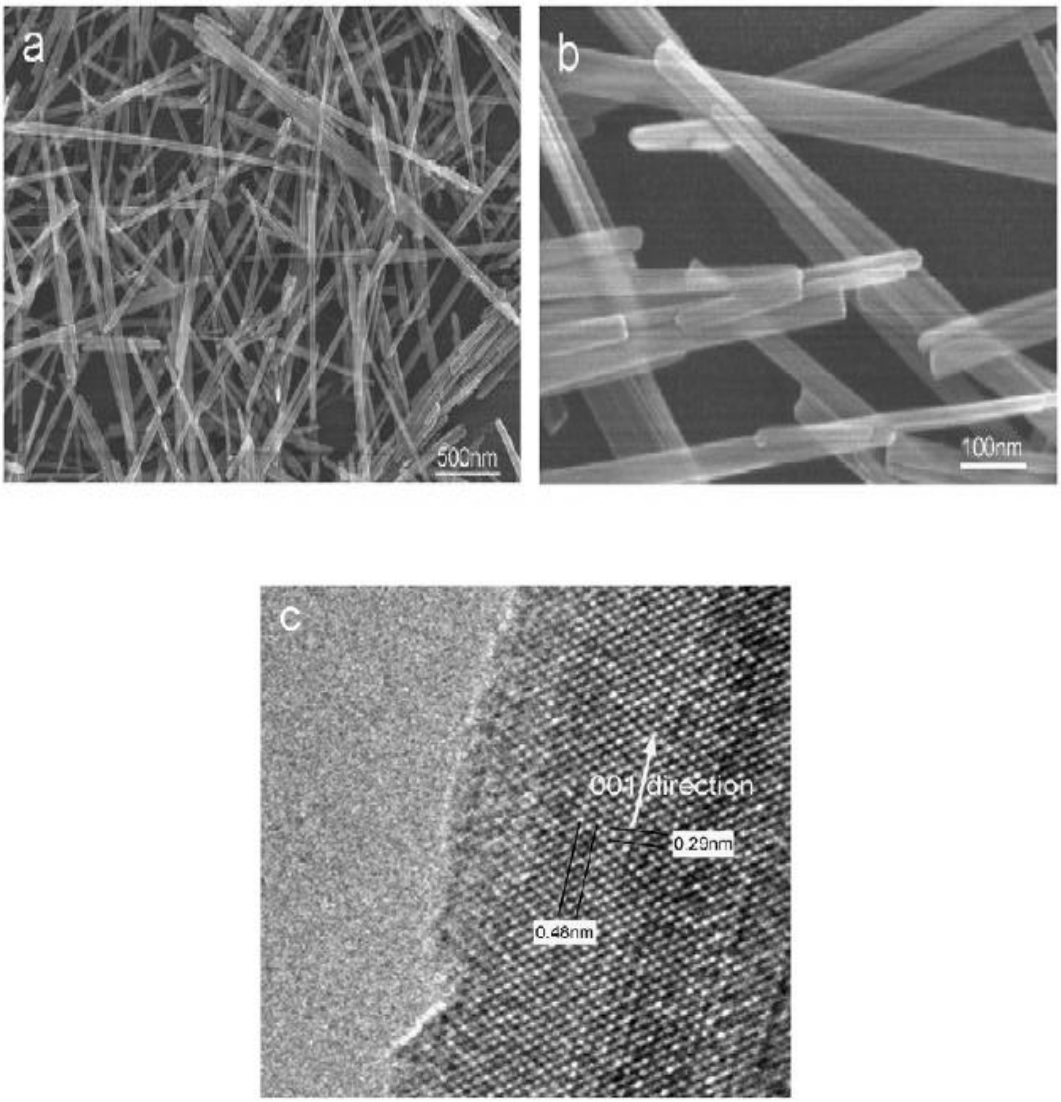

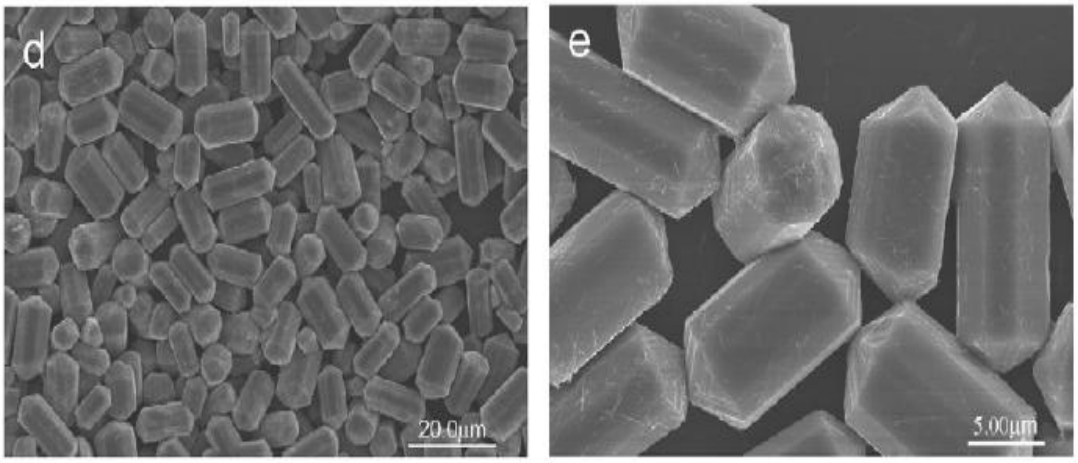


Figure 2.20: SEM images of the α-$MnO_2$ nanowires at (a) low-magnification (b) high-magnification (c) HRTEM image of the α-$MnO_2$ nanowire; SEM image of the β-$MnO_2$ nanorods at (d) low-magnification (e) high-magnification (Zhang, 2008).

Figure 2.21a-c shows SEM images of α-$MnO_2$ nanowires self-assembled into bundles and, subsequently converted to β-$MnO_2$ nanorods after hydrothermal reaction $\geq$48hrs.

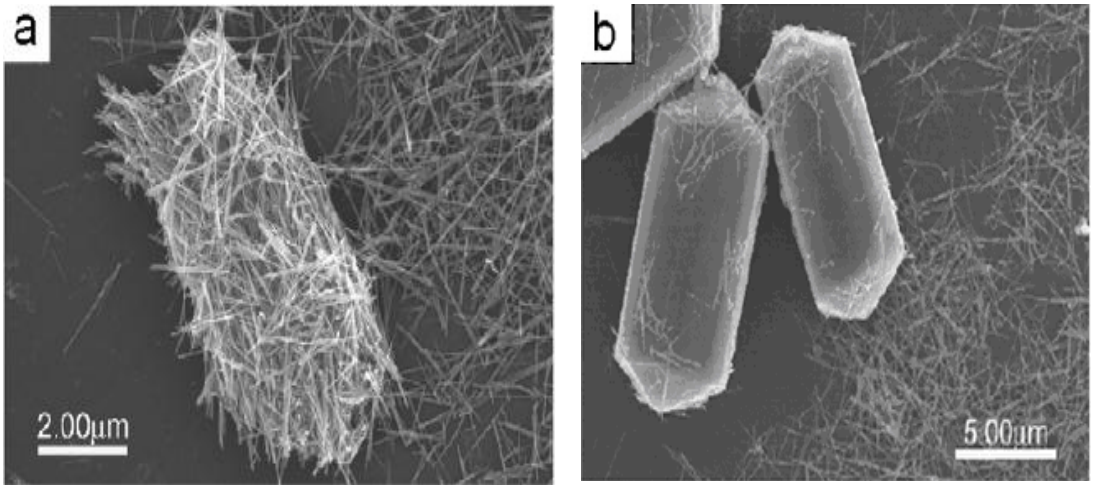


Figure 2.21: SEM images of $MnO_2$ synthesized with hydrothermal reaction time at 160 ℃ at (a) 36hours (b) 48hours (Zhang, 2008)

The α-$MnO_2$ showed four stages of weight losses between 30 and 900 ℃ as shown in Figure 2.22. Above 650 ℃, the product started to lose lattice oxygen from the framework structure and decomposed to an $Mn_3O_4$ phase. On the basis of the TG curve, it can be concluded that the limit of the thermal stability of a-$MnO_2$ is about 500 ℃ in an inert atmosphere. In contrast, β-$MnO_2$ showed only three stages of weight losses. The limit of the thermal stability of β-$MnO_2$ is about 550 ℃ in an inert atmosphere, which is a bit higher than α-$MnO_2$.

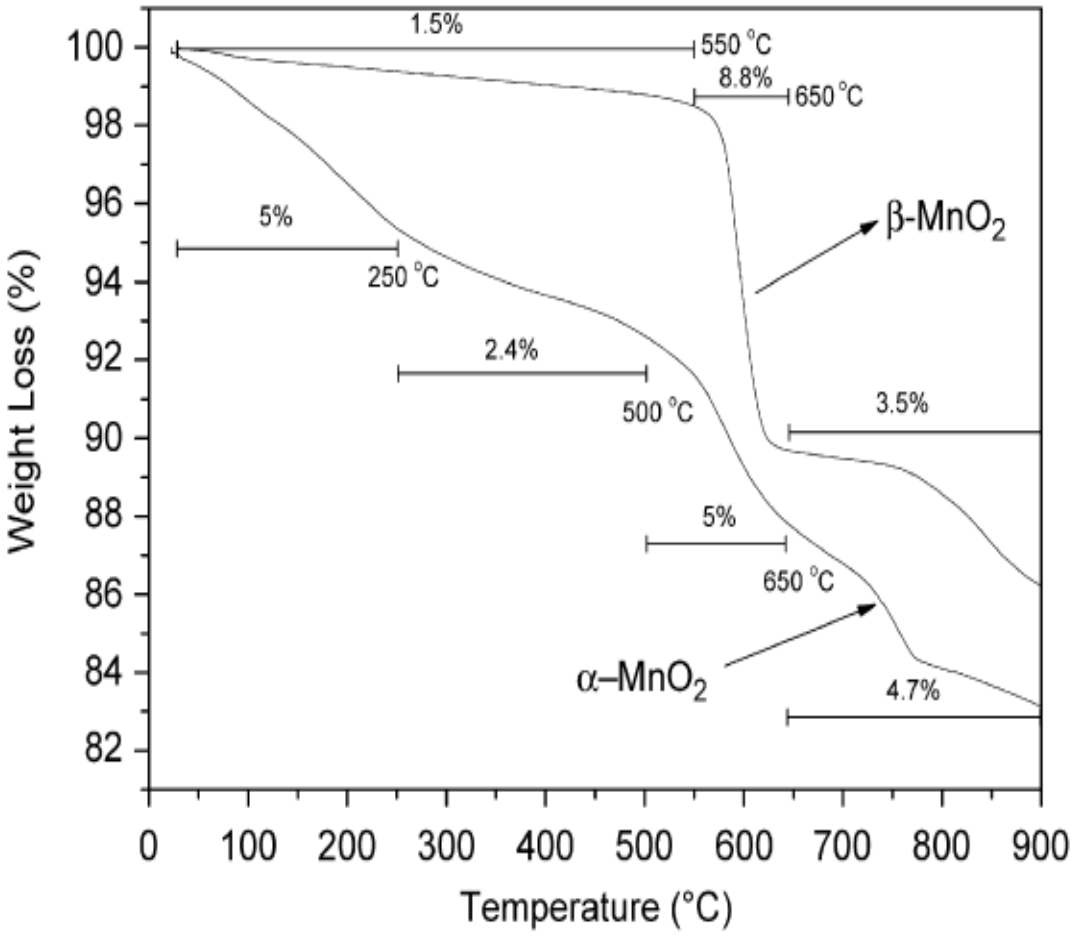


Figure 2.22: TGA curve for α-$MnO_2$ and β-$MnO_2$ (Zhang, 2008)

## 2.7 Material Characterizations

Various characterization techniques were carried out to study the properties of materials. Various characterization equipments were used for this purpose.

### 2.7.1 X-Ray Powder Diffraction (XRD) for Structural analysis

X-ray powder diffraction (XRD) is an important analytical technique used for phase identification of a crystalline material and provide information on unit cell dimensions.

### 2.7.2 Field Emission Scanning Electron Microscope (FE-SEM) for Surface analysis

Field emission scanning electron microscope, FE-SEM is a type of electromicroscope used for visualize detail images of the sample surface by scanning it with a high-energy beam electrons.

### 2.7.3 Energy-dispersive X-ray spectroscopy (EDX) for Elemental Composition analysis

Energy-dispersive X-ray spectroscopy (EDX) is an analytical technique used for the elemental composition analysis of a sample.

### 2.7.4 Transmission Electron Microscopy (TEM) for Morphology and Physical Size analysis

Transmission electron microscopy (TEM) is a microscopy technique used to examine fine detail of the sample surface and determine the size of the particle.

### 2.7.5 Thermogravimetry (TGA) for Thermal analysis

Thermogravimetry analysis (TGA) is a type of testing performed on samples that determines changes in weight in relation to change in temperature.

# CHAPTER THREE

# METHODOLOGY

## 3.1 Material

In this study, the raw material used is Manganese (IV) oxide in powder form (ACROS Organics; purity: 80-85%). The chemical formula is $MnO_2$. It has specific gravity of 5.026m/$s^2$ and melting point of 1539 ℃. $MnO_2$ is insoluble in water and inert to most acids except when heated. The density of $MnO_2$ is 5.026g/$cm^3$ and molecular weight is 86.94g/mol.

## 3.2 Apparatus

Below is the list of laboratory apparatus & laboratory equipment used during $MnO_2$ sample preparation.

- Beaker 250ml
- Stirring rod
- Aluminium foil
- Stainless Steel Spatula
- Magnetic stirrer bars
- Volumetric Flask
- Filtering funnel
- Filtering paper – diameter 12 cm
- Evaporating dish
- Porcelain Crucible
- Sample bottles with cover (20 ml)
- Oven OF-12GW JEIO TECH
- LAC Furnace
- Ultrasonic Cleaner CHROM TECH

### 3.3 $MnO_2$ samples preparation

The steps of sample preparation are summarized in the flow chart below.

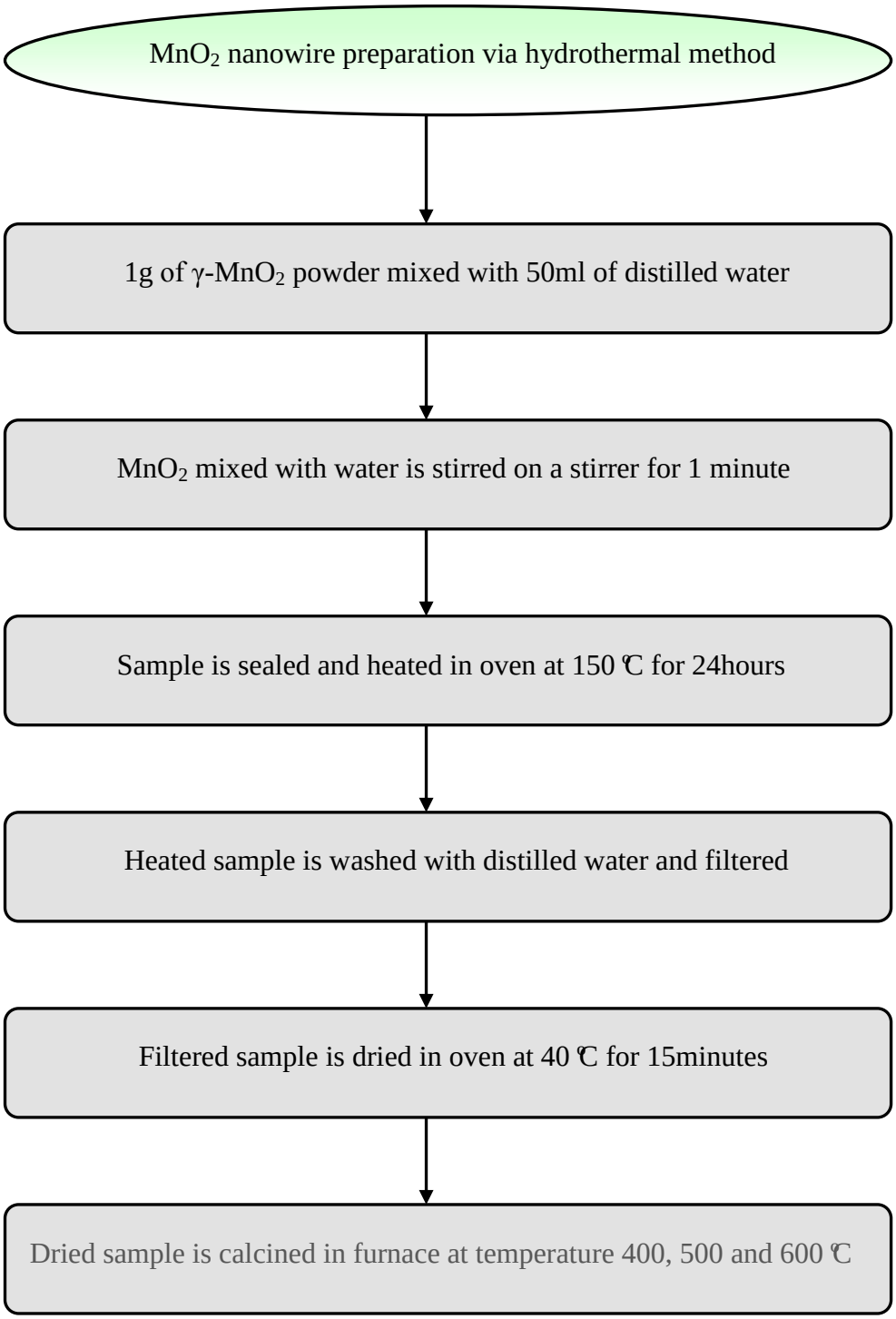


Figure 3.1: Flow chart of $MnO_2$ nanowire preparation via hydrothermal method

Figure 3.2 shows 1g of γ-$MnO_2$ powder mixed with 50ml of distilled water in a 250ml beaker for preparation of hydrothermal synthesis.

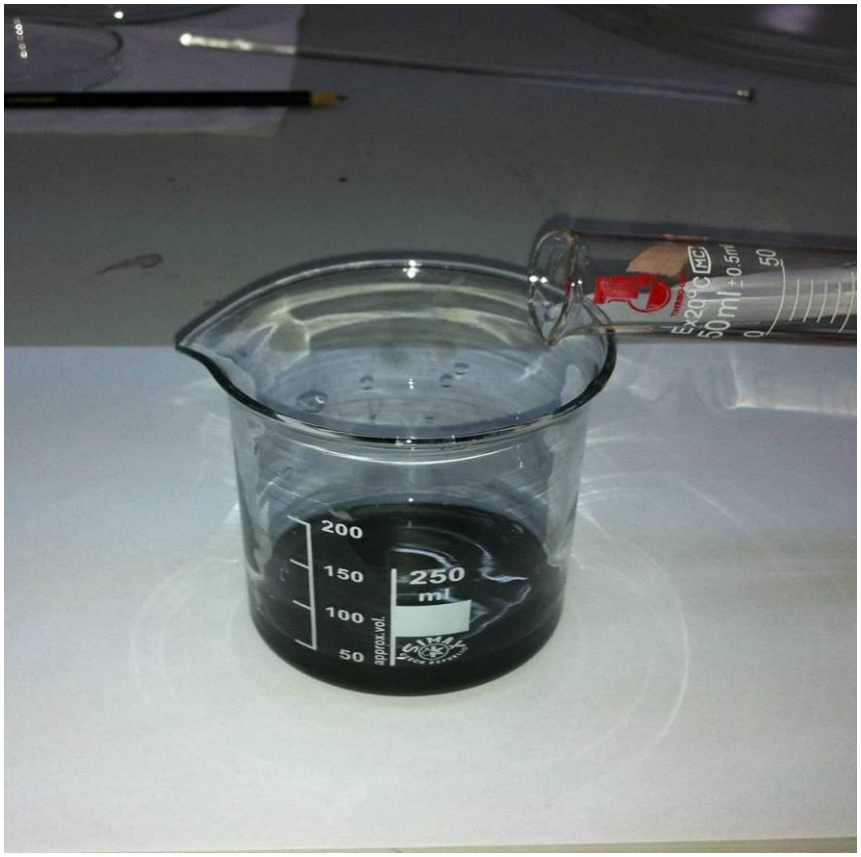


Figure 3.2: γ-$MnO_2$ mixed with distilled water

Figure 3.3 shows $MnO_2$ was stirred for 1 minute with the assistant of an octagon magnetic stirrer bar inside the beaker.


Figure 3.3: $MnO_2$ stirred on a stirrer

Figure 3.4 shows the beaker is sealed with Aluminium foil and heated in Oven JEIO TECH type OF-12GW at 150 ℃ for 24hrs. After heating, the system was allowed to cool to room temperature.


Figure 3.4: Beaker of $MnO_2$ sealed with Al foil is heated in oven at 150 ℃ for 24hrs

Figure 3.5 shows the resulting product washed with distilled water and filtered using filtering paper. Then, it was dried at 40 ℃ for 15 minutes in the oven again.

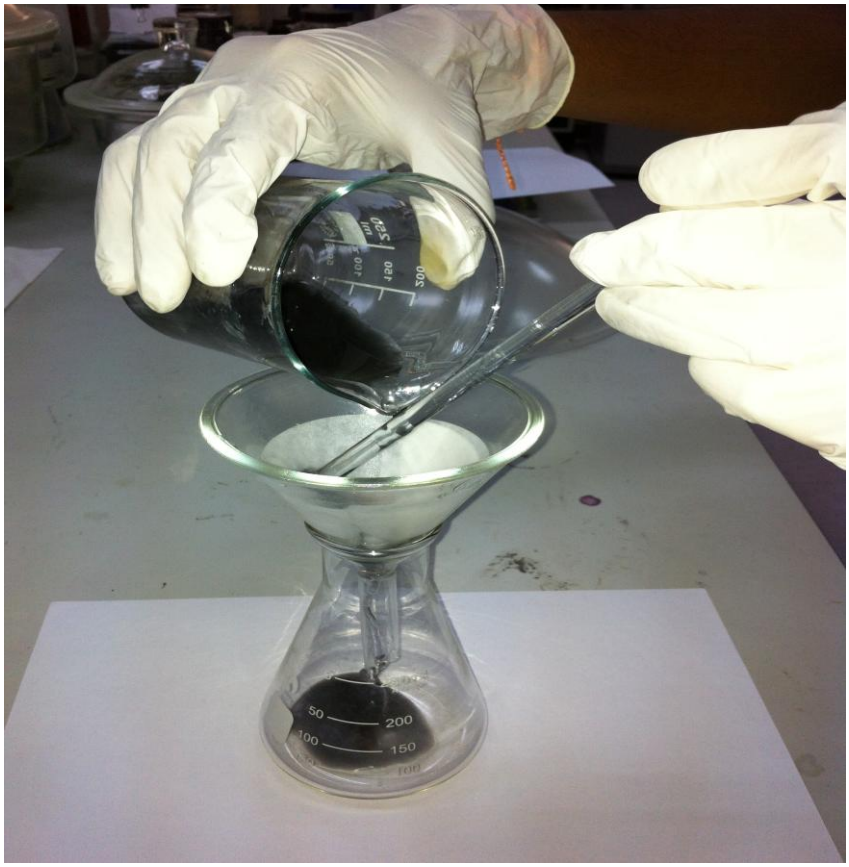


Figure 3.5: Heated $MnO_2$ washed with distilled water and filtered

Figure 3.6 shows the dried $MnO_2$ is placed in a porcelain crucible and calcined in the LAC Furnace at different temperature 400, 500 and 600 ℃ for 90 minutes.


Figure 3.6 Dried $MnO_2$ placed in a porcelain crucible and calcined

Finally Field Emission Scanning Electron Microscopy (FESEM), Electron Diffraction X-Ray (EDX), Transmission Electron Microscopy (TEM), X-Ray Diffraction (XRD) and Thermogravimetric Analyzer (TGA) were used to characterized the properties of all samples.

## 3.4 $MnO_2$ samples characterization - Equipment and Techniques

### 3.4.1 Equipment

Table 3.1 shows the list of equipments used for characterization of $MnO_2$.

Table 3.1: Equipments used for $MnO_2$ analysis

| Equipment | Model | Function |
|---|---|---|
| XRD | PANanalytical EMPYREAN | To study crystallographic structure |
| FESEM | ZEISS AURIGA | To study surface structure |
| EDX | ZEISS AURIGA | To identify elemental composition |
| TEM | LEO LIBRA 120kV | To study morphology and physical size |
| TGA | METTLER TOLEDO TGA/SDTA 851[e] | To study thermal stability |

### 3.4.2 Structural Analysis

X-ray Diffractometer (XRD) is used to study the structural properties (crystalline) of manganese oxide nanowires. It is a powerful method by which X-Rays of a known wavelength are passed through a sample to be identified in order to identify the crystal structure. The X-rays used are of the Copper-kα with wavelength 1.5406Å (0.15406nm) and values of 45 kV and 30 mA are used as the generator setting. Sample in powder form was placed on the stainless steel pallet and compacted before placing in the chamber and the scan is taken between 2 theta of 10 °- 80 °. These angles have been selected as this is where the important reflections lie for $MnO_2$ and other relevant impurities. Crystallographic structural changes due to different heating temperature were observed. The crystalline characteristic of samples was successfully done using the PANalytical Empyrean X-ray Diffractometer available in the Geology Laboratory, Faculty of Science, University of Malaya as shown in Figure 3.7.


Figure 3.7: X-Ray Diffractometer (XRD), PANanalytical Empyrean

The crystallite size can be calculated using Scherrer's Equation (3.1) below:

$$t = 0.9\,\lambda/(\beta_1 \cos\theta) \qquad (3.1)$$

Where $\theta$ : angle corresponding to the diffraction peak

$\lambda$ : X-Ray wavelength = 0.15406nm

t : Scherrer thickness to determine the crystallite size

$\beta_1$ : Full width at half maximum intensity (FWHM) of the diffraction peak in radians

$$\beta_1 = 2\theta_2 - 2\theta_1$$

Peak position for Full width at half maximum is shown in Figure 3.8.

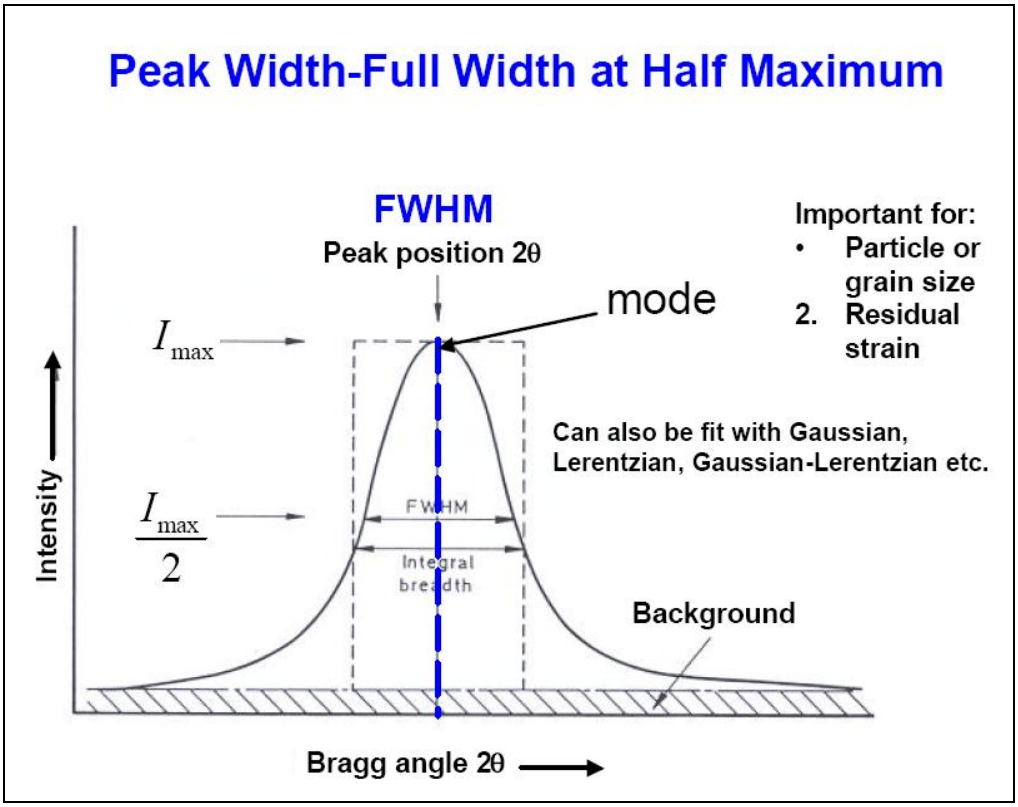


Figure 3.8: Intensity as a function for 2Theta for the Scherrer Equation (Wang, 2000)

### 3.4.3 Surface Analysis

Field Emission Scanning Electron Microscope (FESEM) is used for the surface analysis for manganese oxide nanowires. It is used to visualize very small topographic details on the surface due to its clearer, less electrostatically distorted images produced with spatial resolution down to 1 1/2 nm which is 3 to 6 times better than SEM. It works based on focused ion beam system. The surface characteristics of samples were examined using FESEM, ZEISS AURIGA available in FESEM-EDX Laboratory, Engineering Faculty, University of Malaya as shown in Figure 3.9. The powder samples of $MnO_2$ as received, as synthesized and as calcined at 400, 500 and 600 ℃ were placed on black tape pasted on metal base and placed inside the chamber for the surface viewing. Magnification 10KX, 40KX and 80KX were used for the image viewing.

### 3.4.4 Elemental Composition Analysis

Energy Dispersive X-ray Spectroscopy (EDX) is used for the elemental analysis of manganese oxide nanowires. EDX analysis is a technique used for identifying the elemental composition present in the nanowires. The EDX analysis system works as an integrated feature of a field emission scanning electron microscope (FESEM), and can not operate on its own without the latter. A high energy beam of charged particles is focused into the sample and by measuring the difference in energy between the two shells, elemental composition of the specimen is revealed. The elemental analysis of manganese oxide nanowires was successfully done using FESEM-EDX, ZEISS AURIGA available in FESEM-EDX Laboratory, Engineering Faculty, University of Malaya as shown in Figure 3.9.


Figure 3.9: Field Emission Scanning Electron Microscope (FESEM) & Energy Dispersive X-Ray Spectroscopy (EDX), ZEISS AURIGA.

### 3.4.5 Morphology and Physical Size Analysis

Transmission Electron Microscopy (TEM) is used for the examination on the surface and size of manganese oxide nanowires. It is capable of imaging at a significantly higher resolution than light microscopes. Manganese oxide nanowires dispersions were prepared by adding ethanol to manganese oxide powder treated at different temperature until fully dissolved. The dispersion were sonicated in distilled water using ultra sonic bath for 3 hours duration. Later, a drop of the manganese oxide nanowires dispersion was placed on a carbon-coated copper grid, which was allowed to dry for at least three days before being used for observation. The TEM investigation was performed at 120kV. The analysis of morphology and physical shape analysis was successfully done using Transmission Electron Microscopy, LEO LIBRA 120kV

available in Microscopy Electron Laboratory, Medical Faculty, University of Malaya as shown in Figure 3.10.

Figure 3.10: Transmission Electron Microscopy, LEO LIBRA 120kV

### 3.4.6 Thermal Analysis

Thermogravimetry (TGA) is used to determine the weight changes as a function of temperature to investigate the possible chemical reactions that occur between materials with atmosphere. This is accomplished by heating up the powder to 1000 ℃ at a heating rate of 10 ℃/min with an $N_2$ flow of 50mL/min. The sample amount used is about 20mg. Thermal gravimetric analysis is the act of heating a sample to a high enough temperature so that one of the components decomposes into a gas, which dissociates into the air. It is a process that utilizes heat and stoichiometry ratios to

determine the percent by mass ratio of a solute. Analysis is carried out by raising the temperature of the sample gradually and plotting the graphs of weight against temperature. The thermal analysis of manganese oxide nanowires was successfully done using Thermogravimetry, Mettler Toledo TGA/SDTA 851$^{e}$ in Polymer Laboratory, Engineering Faculty, University of Malaya as in Figure 3.11.


Figure 3.11: Thermogravimetry, Mettler Toledo TGA/SDTA 851$^{e}$

# CHAPTER FOUR

# RESULTS AND DISCUSSION

## 4.1 Structural Analysis

The crystalline structure of $MnO_2$ samples for as-received, as synthesized and after calcined at different temperature 400, 500 and 600 ℃ were thoroughly studied using the X-ray diffractometer (XRD). Figures 4.1 - 4.5 show the XRD patterns for all samples and Table 4.1 summarizes the results of crystallite size.

Figure 4.1 shows the diffraction peaks for as-received sample appeared at angle of $2\theta$ = 28.50 º, 37.50 º, 56.52 º and 59.22 º for (110), (101), (211) and (220) planes, respectively. It exhibits a characteristic XRD pattern of electrochemically prepared hexagonal γ-$MnO_2$ structure (Yuan, 2003). The lattice parameters for the hexagonal γ-$MnO_2$ are a = b = 0.965 nm and c = 0.443nm

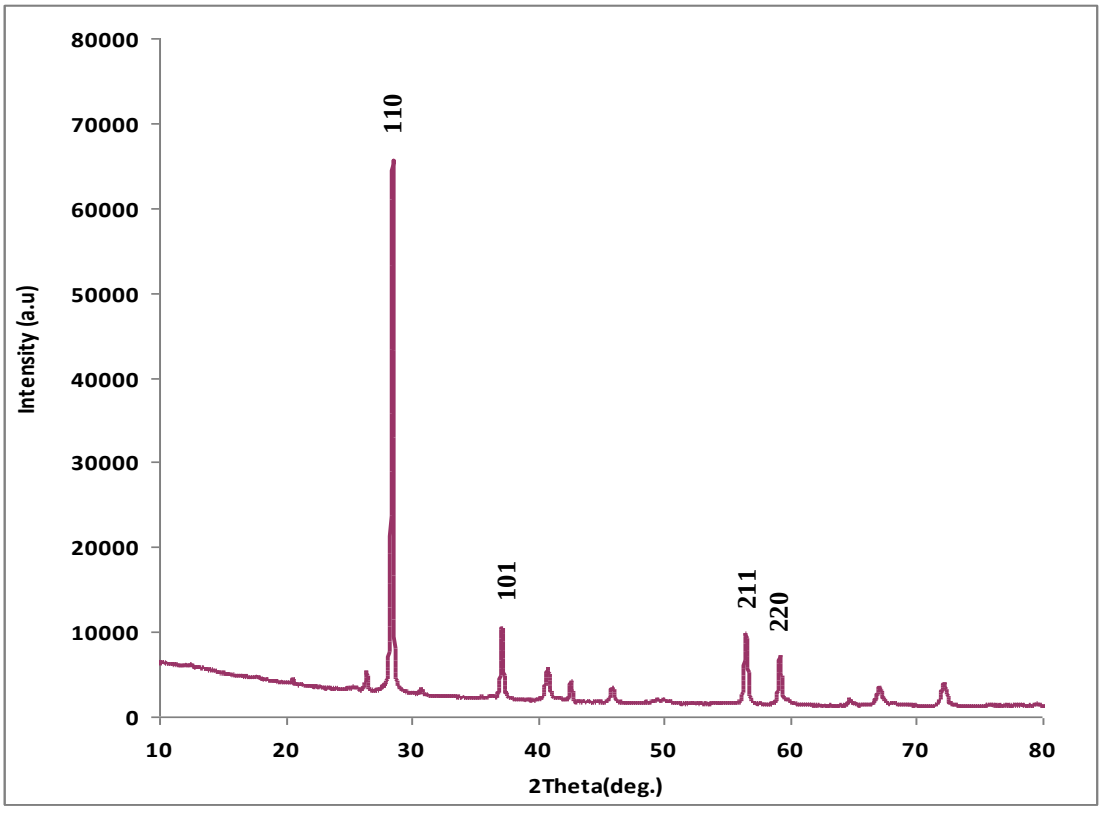


Figure 4.1: X-ray diffraction pattern of as-received $MnO_2$

Figure 4.2 shows the diffraction peaks for as-synthesized $MnO_2$ appeared at angle of 2θ = 28.50 º, 37.20 º, 56.52 ºand 59.22 ºfor (110), (101), (211) and (220) planes, respectively. Through this XRD pattern, it is noticed that the positions of the diffraction peaks for the γ-$MnO_2$ nanowires are almost unchanged. However, the intensities of the diffraction peaks decreases, accompanied by the broadening of the peaks. This reveals that the crystalline phase of the synthesized sample is similar with the as-received sample with the exception that the crystallite size is being reduced. Therefore, hydrothermal treatment has no effect on the crystalline phase of the material except for the size reduction of the crystals.

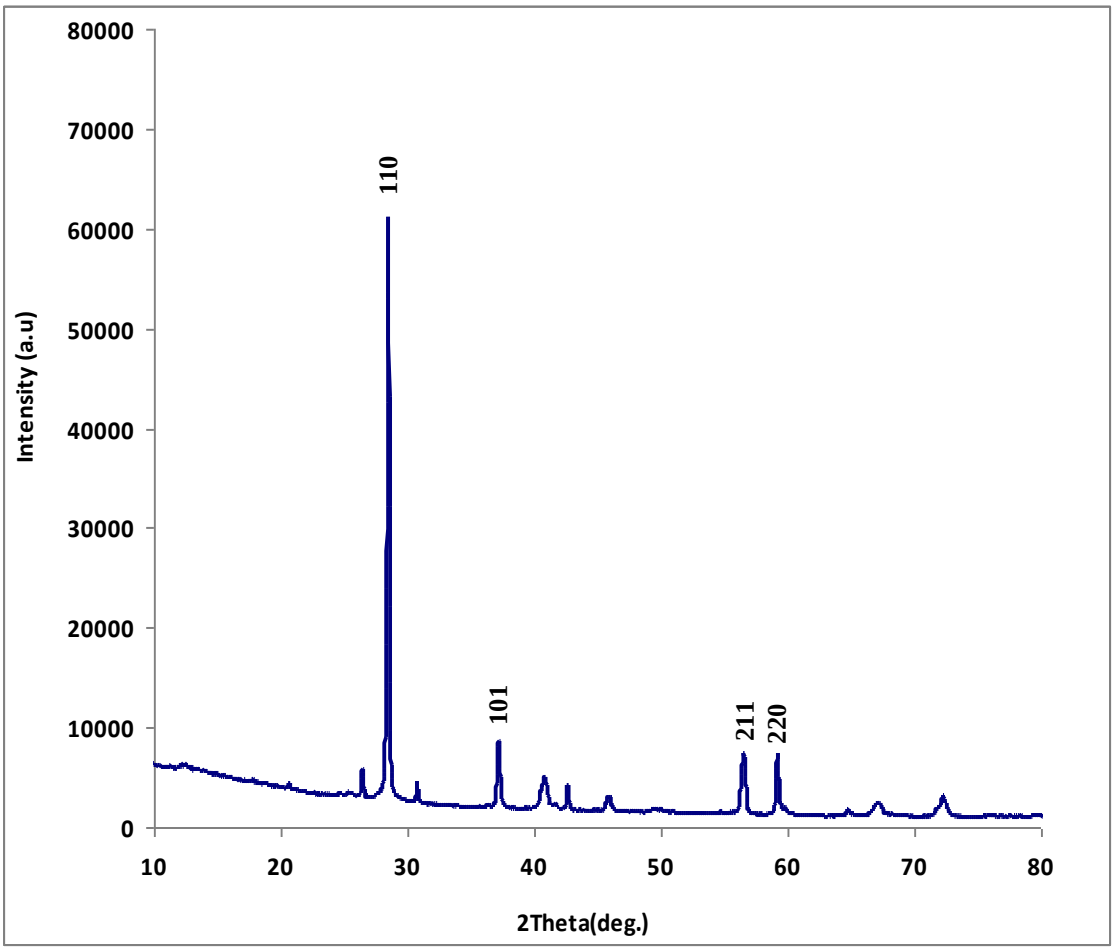


Figure 4.2: X-ray diffraction pattern of as-synthesized $MnO_2$

Figure 4.3 shows the diffraction for sample of $MnO_2$ after calcination at 400 ℃ at angle of 2θ = 28.50 º, 37.20 º, 56.52 ºand 59.22 ºfor (110), (101), (211) and (220) planes, respectively. The XRD pattern shows the positions of the diffraction peaks remain unchanged but the intensities of the diffraction peaks has further reduced accompanied by the further broadening of the peaks. The crystalline phase of this calcined sample remains unchanged but the size of the crystals getting much smaller. This indicates that heating the sample to temperature of 400 ℃ may further reduce the crystallite size without any phase transition occurred.

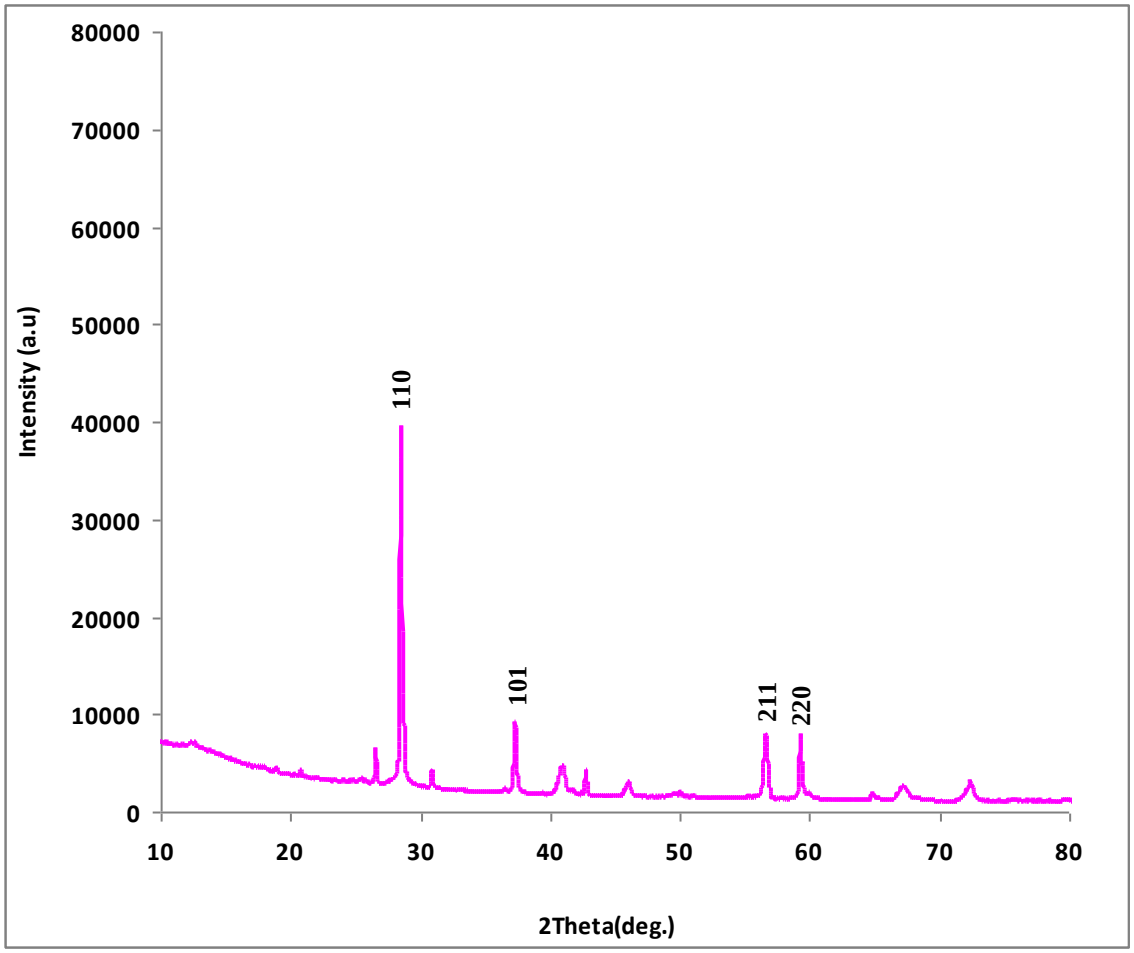


Figure 4.3: X-ray diffraction pattern of $MnO_2$ after calcination at 400 ℃

Figure 4.4 shows the XRD pattern for $MnO_2$ nanowires after calcination at 500 ℃. There are new peaks appeared at angle of 2θ = 23.19 º, 63.07 º and 65.97 º for (111), (002) and (301) planes, respectively. Peaks which appeared in sample of $MnO_2$ after calcination at 400 ℃ has slightly shifted to the right. However, the planes remain the same. This indicates phase transformation has occurred from γ-$MnO_2$ to β-$MnO_2$ at calcination temperature of 500 ℃. The crystal structure changed after calcined at 500 ℃ in the rutile crystal structure (this polymorph is called β-$MnO_2$), with three-coordinate oxide and octahedral metal centres. Like the previous XRD pattern, the intensities of the diffraction peaks are reduced but broaden in width. The lattice parameters for the β-$Mn0_2$ are a = b = 0.4399nm and c = 0.2874nm (JCPDS 24-0735). Significant broadening of the diffraction peaks is due to the reduction of the crystallite size.

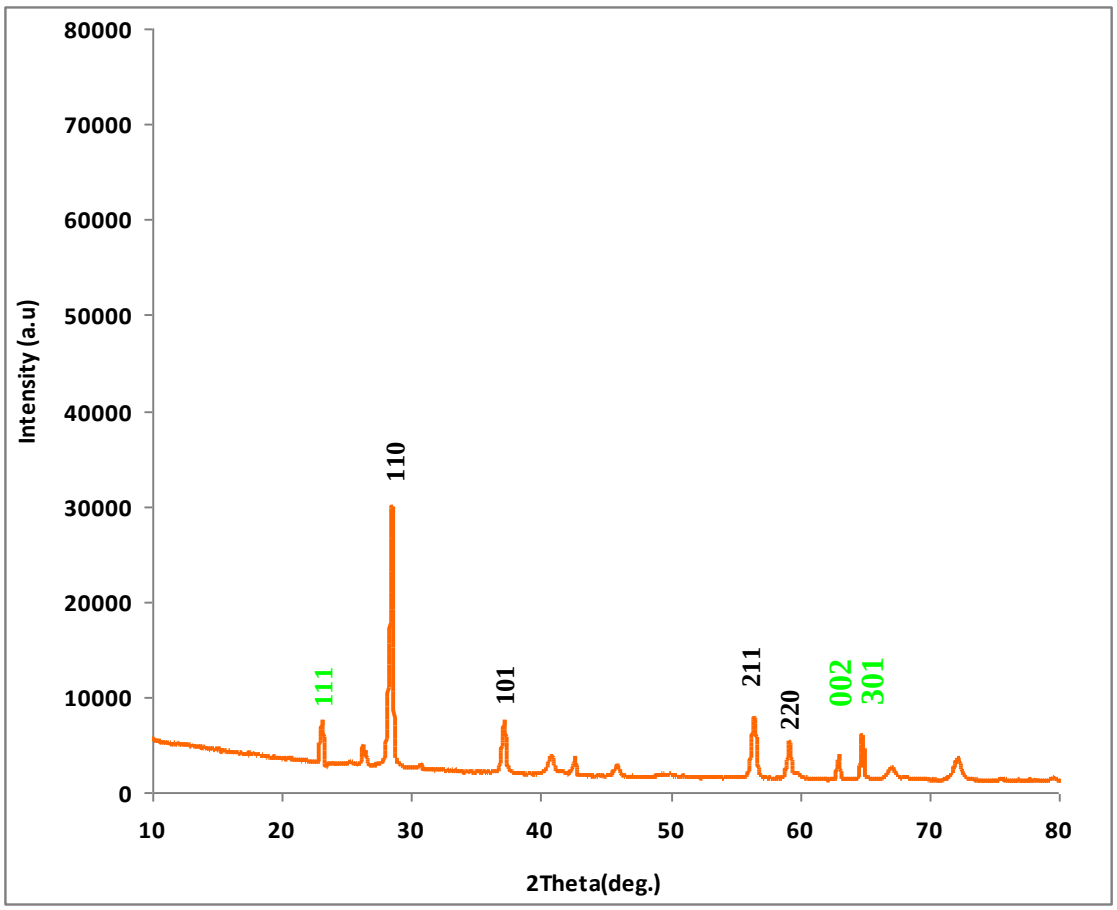


Figure 4.4: X-ray diffraction pattern of $MnO_2$ after calcination at 500 ℃

Figure 4.5 shows the XRD pattern for $MnO_2$ nanowires after calcination at 600 ℃. Many new peaks are noticed at angle of 2θ = 26.57, 32.83 º and 55.06 º (220), (400) and (440) planes, respectively. The new peak signifies changes in the crystalline phase at calcination temperature of 600 ℃. The lattice parameters for the α-$Mn_20_3$ are a = b = 0.9784.nm and c = 0.2863nm. According to JCPDS, the XRD pattern of nanowires calcined at 600C confirm the presence of pure phases of α-$Mn_2O_3$ (JCPDS 41-1442). Most of the peaks seen reduced and broaden.

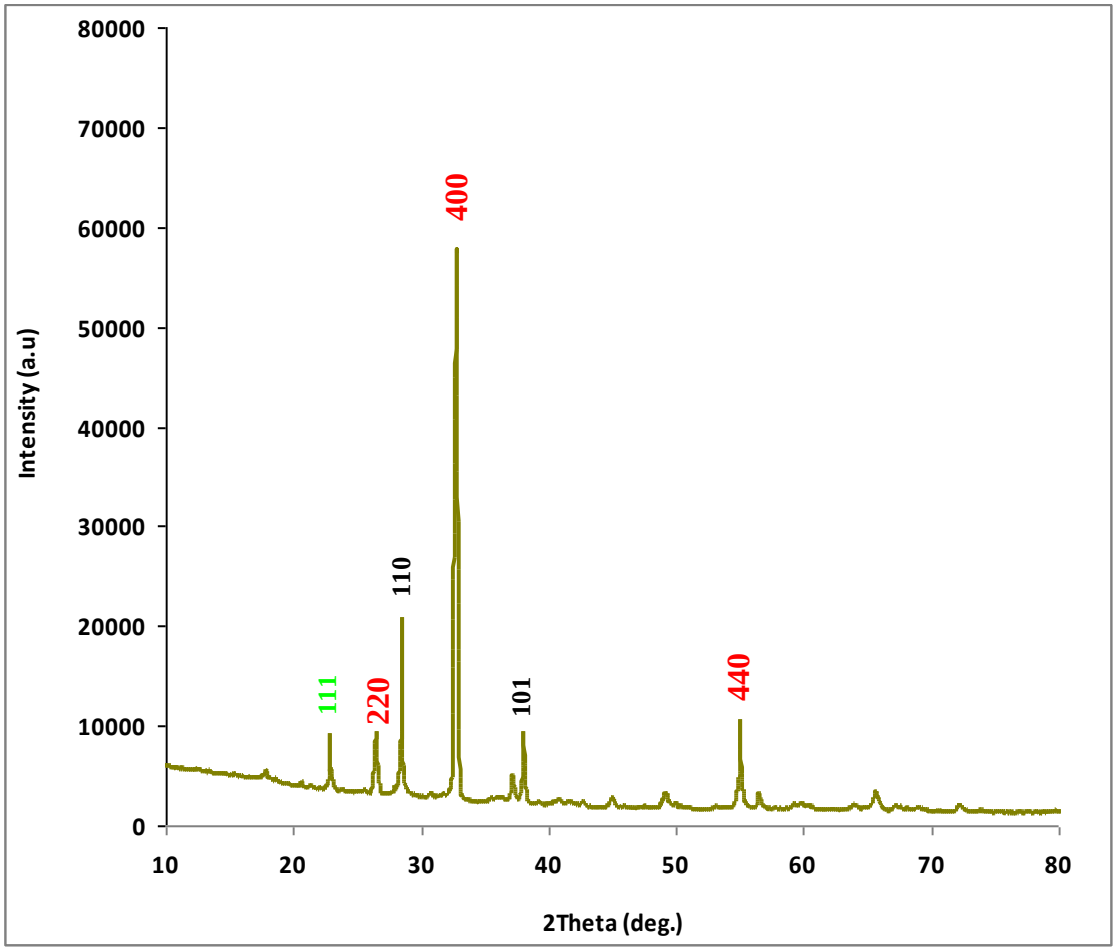


Figure 4.5: X-ray diffraction pattern of $MnO_2$ after calcination at 600 ℃

The phase transition of γ-$MnO_2$ due to calcination at different temperature is described in Figure 4.6 below:

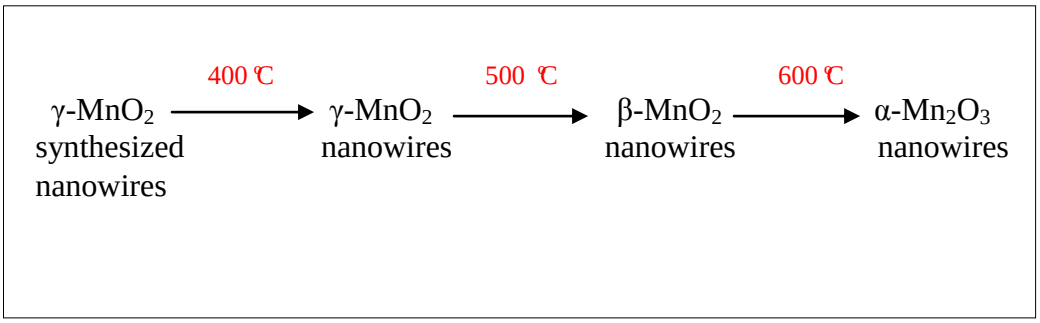


Figure 4.6: Phase transition for $MnO_2$ nanowires

Raw material of γ-$MnO_2$ is calcined at elevated temperature (400-500 ℃ and 600 ℃) to obtain β-$MnO_2$ and α-$Mn_2O_3$. The XRD patterns of the calcined nanowires then confirm the presence of pure phases of β-$Mn0_2$ and α-$Mn_20_3$. Samples calcined at 500 ℃ are mainly feature of Mn(IV), while the mean oxidation state decreases gradually towards higher calcination temperature to Mn(III) at 600 ℃ corresponding to α-$Mn_20_3$ (Najafpour, 2012). It shows an increase in crystallinity with respect to the increase of the calcination temperature.

Table 4.1: The crystallite size of all samples

| Sample | t (nm) |
|---|---|
| As-received $MnO_2$ | 102.44 |
| As-synthesized $MnO_2$ | 78.04 |
| Calcined $MnO_2$ at 400 ℃ | 74.48 |
| Calcined $MnO_2$ at 500 ℃ | 51.20 |
| Calcined $MnO_2$ at 600 ℃ | 41.39 |

Table 4.1 shows the crystallite size of $MnO_2$ samples for as received, as synthesized and after calcination at 400, 500 and 600 ℃. The crystallite size is calculated using Scherrer's Equation based on the XRD micrographs obtained for each sample.

From the table above, it is observed that the crystallite size is getting smaller as the calcination temperature increases. Calcination of the sample at higher temperature results in producing nanowires with smaller diameter.

## 4.2 Surface Analysis

The surface characteristic of $MnO_2$ samples for as-received, as synthesized, after calcination at different temperature 400, 500 and 600 ℃ were examined using Field Emission Scanning Electron Microscope (FE-SEM). Figures 4.7 – 4.11 show the FE-SEM images for all samples and Table 4.2 summarizes the results.

Figure 4.7a-b shows the FESEM image of as-received γ-$MnO_2$ at different magnification. The image clearly shows only irregular-shaped of granular particles which are mainly aggregates of small particles of micro and nanometer scales. The diameter of γ-$MnO_2$ pure varies from 100-200 nm with about 1000 nm in length.

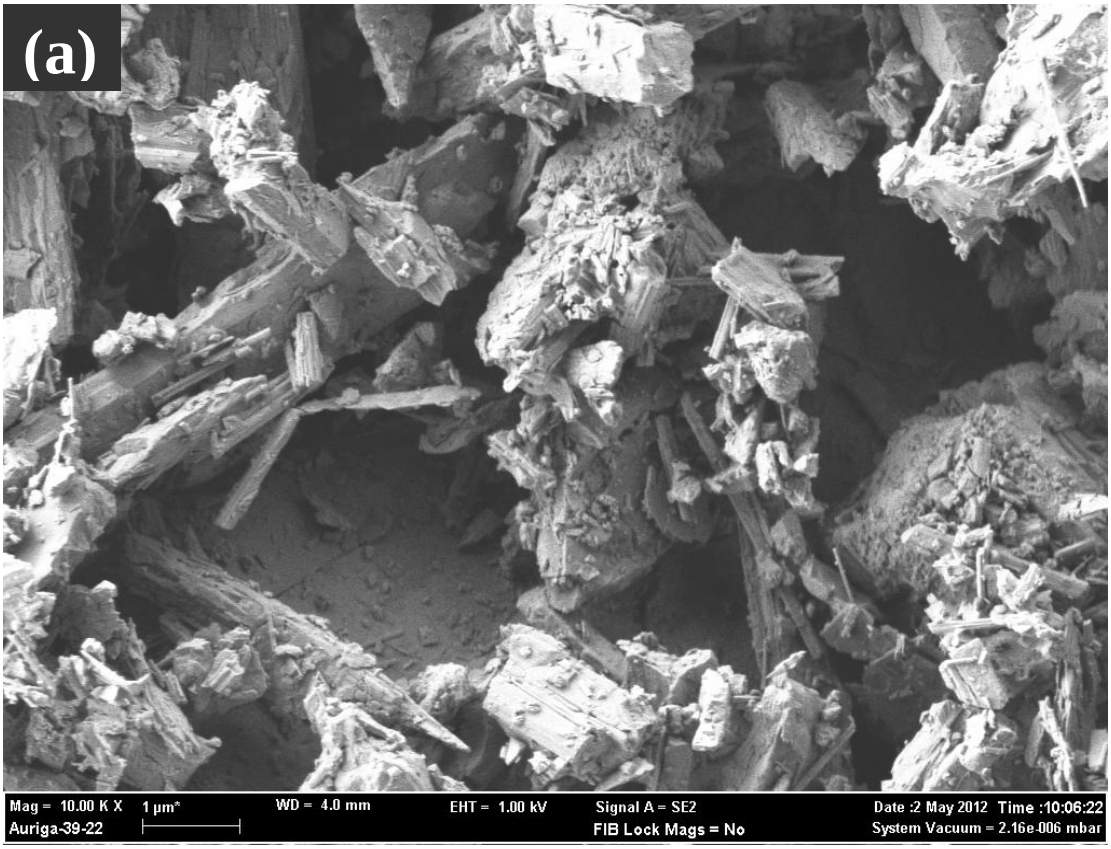


Figure 4.7a: FE-SEM image for as received γ-$MnO_2$ at magnification 10KX

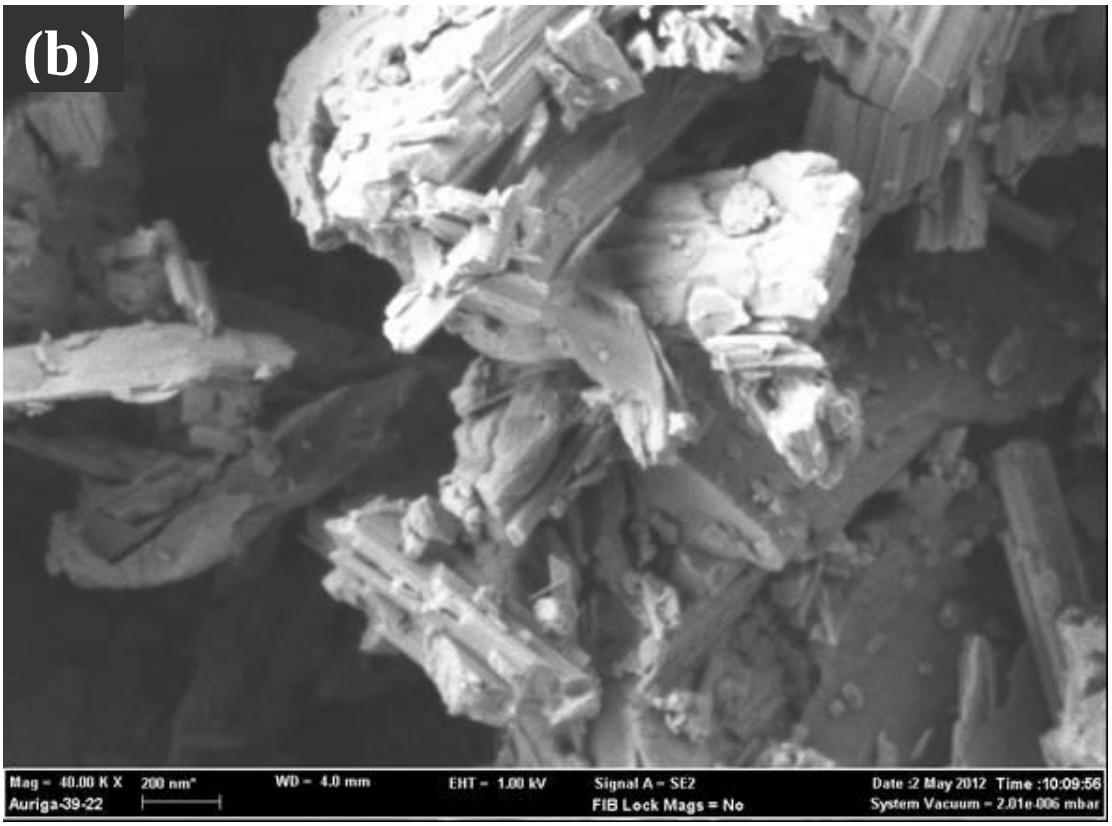


Figure 4.7b: FE-SEM image for as received γ-$MnO_2$ at magnification 40KX

Figure 4.8a-b shows the as-synthesized γ-$MnO_2$ with the presence of large quantity of nanowires besides a small quantity of nanoparticle aggregates. The diameter of γ-$MnO_2$ nanowires varies from 70-80 nm with about 300 nm in length. This result is supported by the diameter size obtained for γ-$MnO_2$ as-synthesized using TEM as tabulated in Table 4.4.

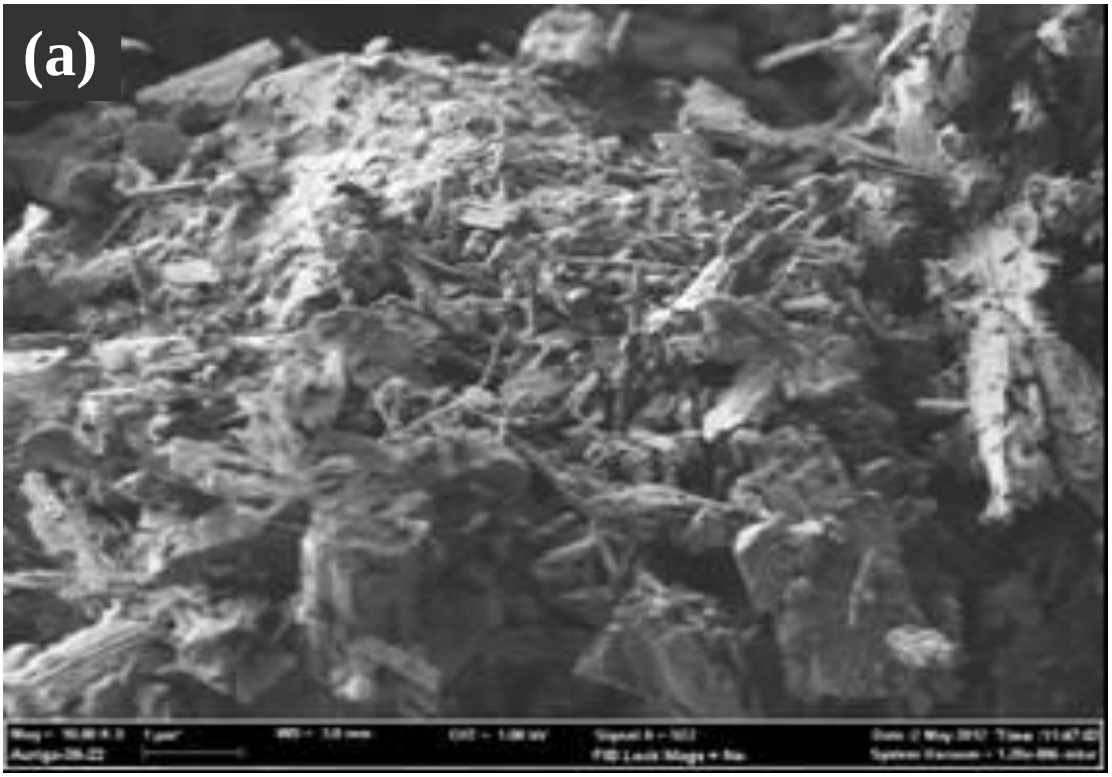


Figure 4.8a: FE-SEM image for γ-$MnO_2$ as-synthesized at magnification 10KX

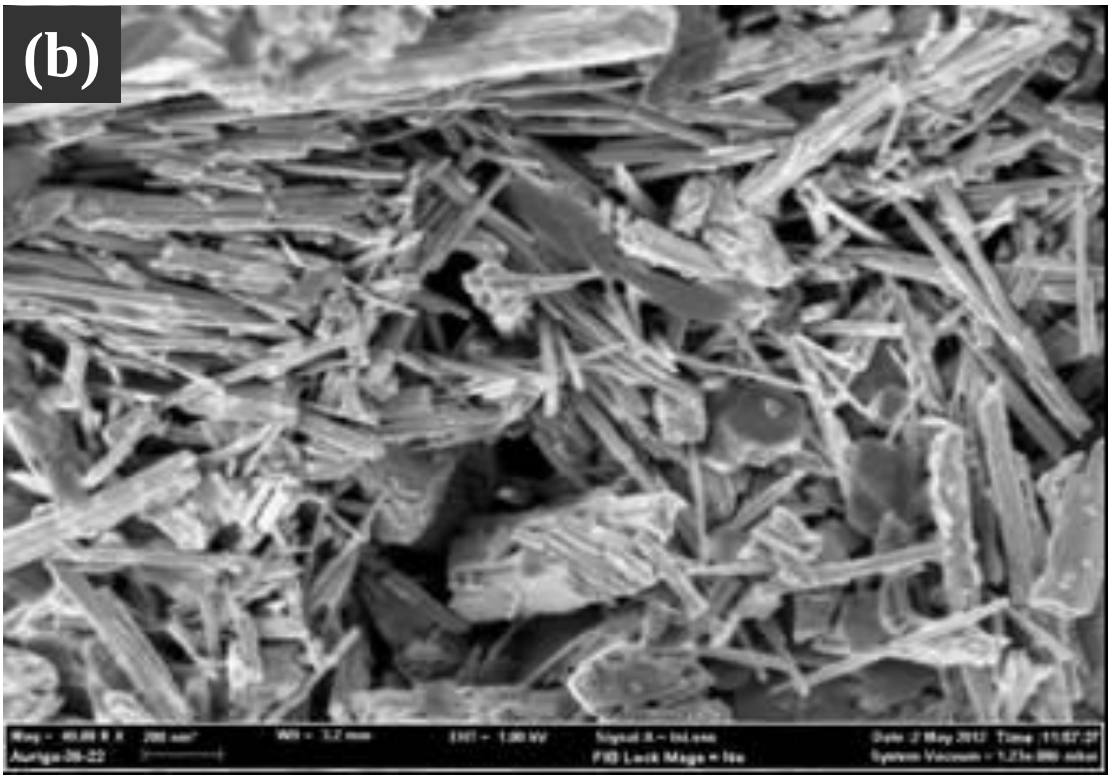


Figure 4.8b: FE-SEM image for γ-$MnO_2$ as-synthesized at magnification 40KX

Figure 4.9a-b shows the FE-SEM image of $MnO_2$ calcined at 400℃. It is observed that more nanowires are presence. However the structure seems to be more compact and tight than the as-synthesized $MnO_2$ which is much looser and more individual wires. The diameter for calcined $MnO_2$ at 400℃ varies from 70-90 nm with length about 300-400nm. The length of the nanowires increases as the calcination temperature increases.


Figure 4.9a: FE-SEM image for calcined $MnO_2$ at 400℃ at magnification 10KX

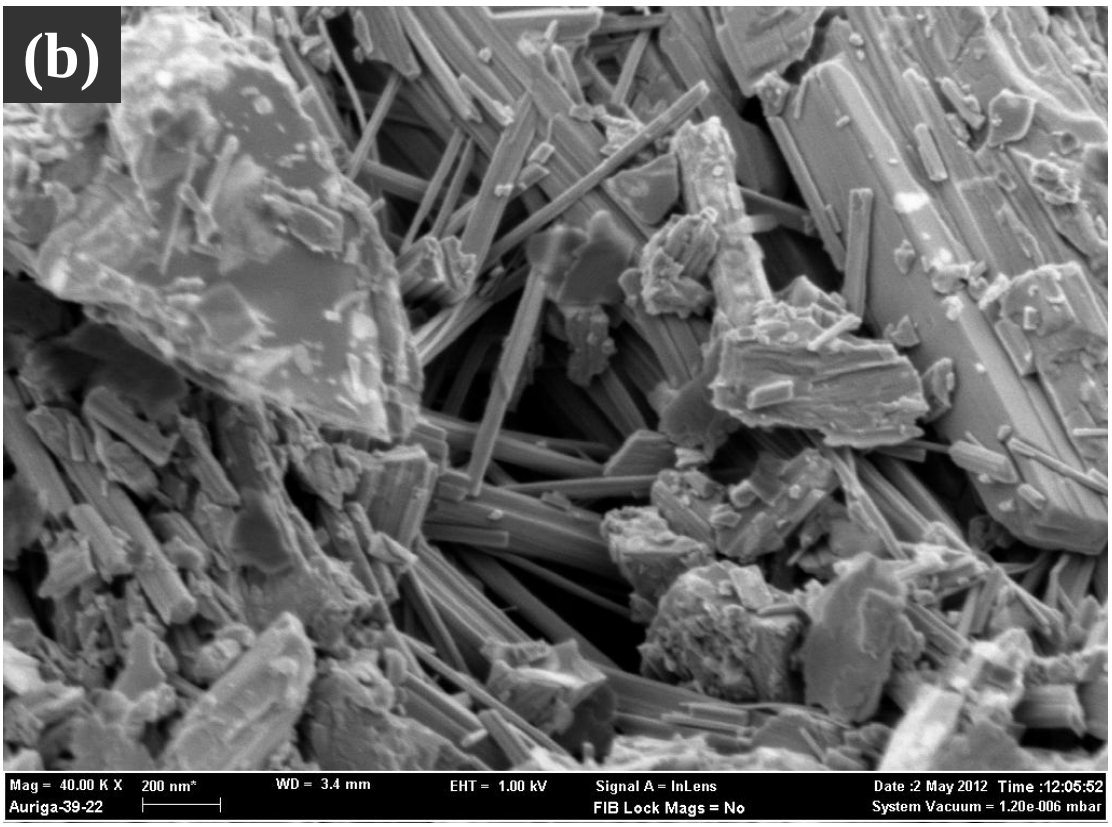


Figure 4.9b: FE-SEM image for calcined $MnO_2$ at 400 ℃ at magnification 40KX

Figure 4.10a-b shows the calcined $MnO_2$ at 500 ℃. It is observed that more nanowires are presence in a closer manner compared to calcined $MnO_2$ at 400 ℃. The diameter for calcined $MnO_2$ at 500 ℃ varies from 60-50 nm with length about 500-800 nm. The length of the nanowires is increases as the calcination temperature increases. This shows the nanowires produced at this phase is longer and slimmer wires.

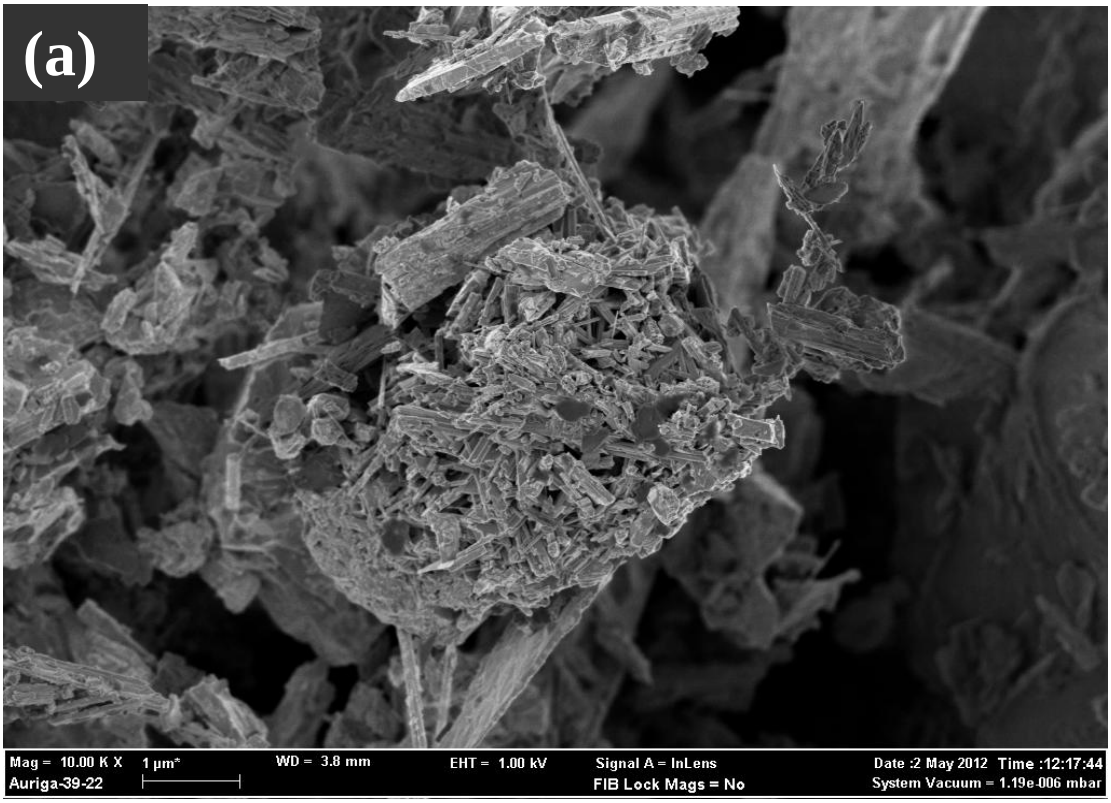


Figure 4.10a: FE-SEM image for calcined $MnO_2$ at 500 ℃ at magnification 10KX


Figure 4.10b: FE-SEM image for calcined $MnO_2$ at 500 ℃ at magnification 40KX

Figure 4.11a-b shows the calcined $MnO_2$ at 600 ℃. The α-$MnO_2$ nanowires presents in a well aligned cluster form and looks tighten together. Yield of nanowires increases with the increase of calcination temperature. This is in good agreement with the XRD results in Figure 4.5. The diameter for calcined $MnO_2$ at 600 ℃ varies from 30-40 nm with length about 1000 nm. The nanowires has projected even longer and slimmer due to the diameter gets smaller while the length gets longer. The morphology of nanowires can be preserved after certain high temperature of calcinations (Yuan, 2003).

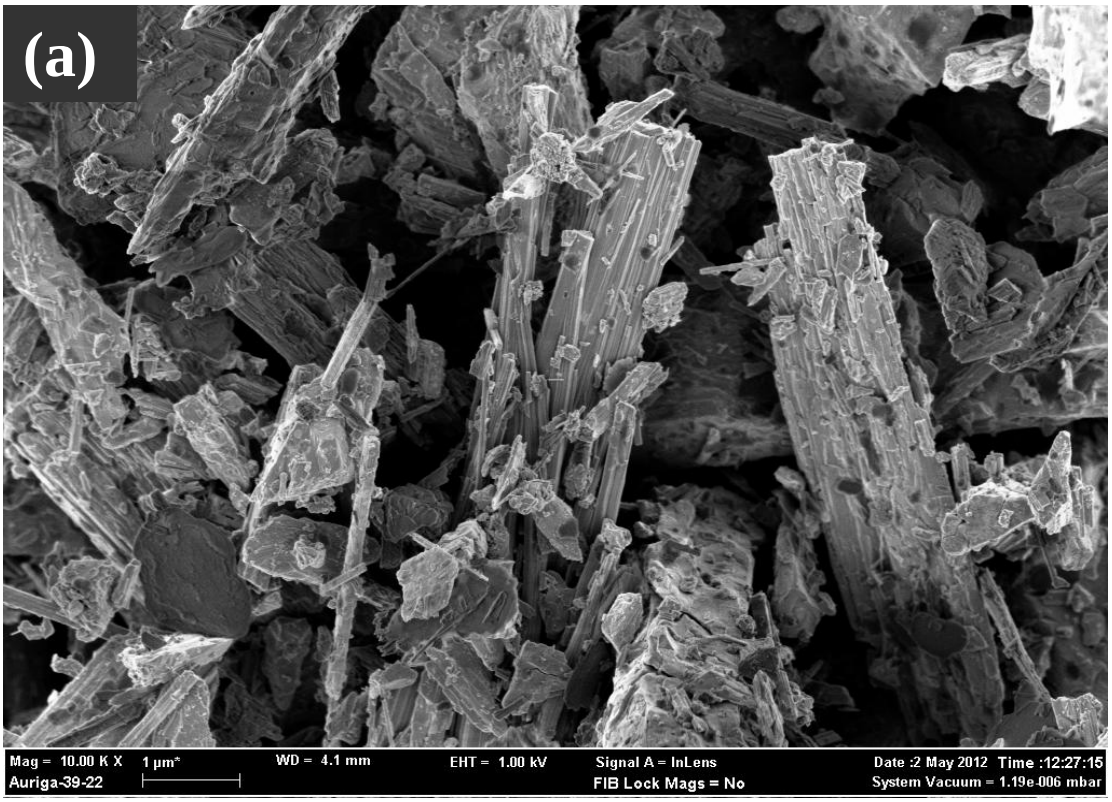


Figure 4.11a: FE-SEM image for calcined $MnO_2$ at 600 ℃ at magnification 10KX

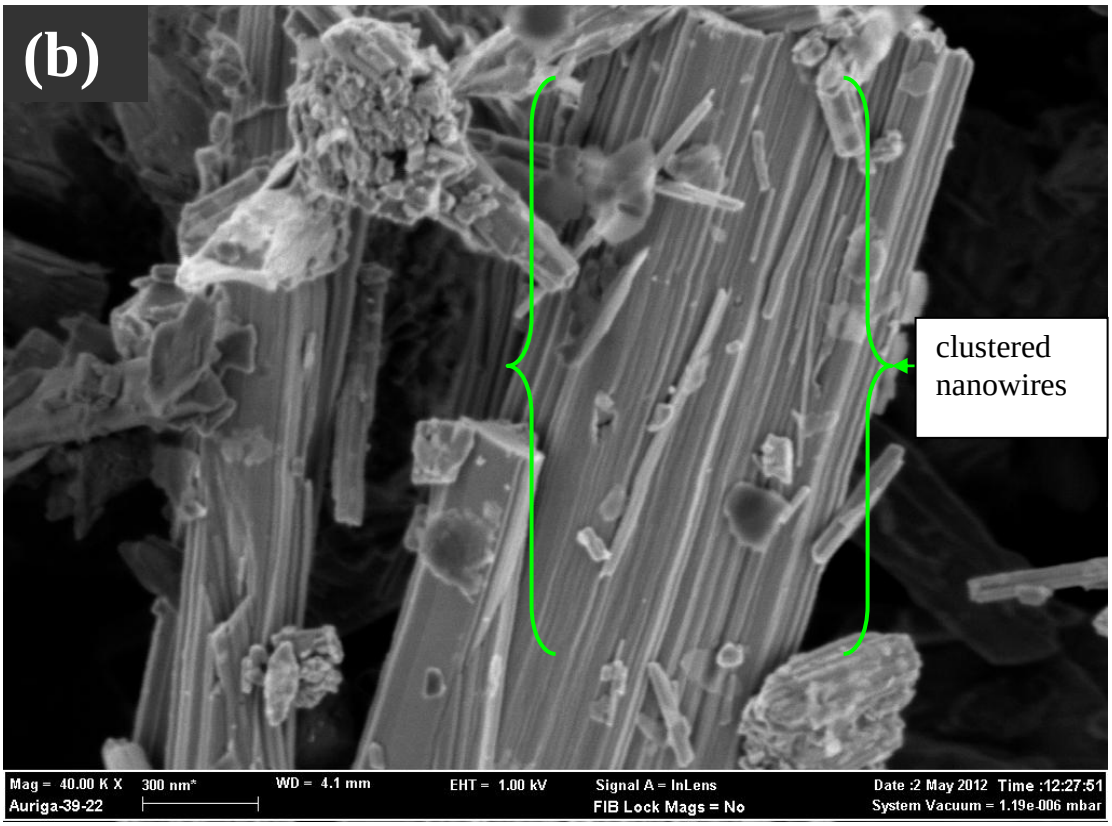


Figure 4.11b: FE-SEM image for calcined $MnO_2$ at 600 ℃ at magnification 40KX

Table 4.2: Diameter and length of all samples

| Sample | Diameter (nm) | Length (nm) |
|---|---|---|
| As-received $MnO_2$ | 100 -150 | 1000 |
| As-synthesized $MnO_2$ | 75 – 80 | 300 |
| Calcined $MnO_2$ at 400 ℃ | 70 -75 | 400 |
| Calcined $MnO_2$ at 500 ℃ | 50 – 60 | 500 |
| Calcined $MnO_2$ at 600 ℃ | 30 - 50 | 1000 |

Table 4.2 summarizes the diameter and length size in nm obtained from FE-SEM. The diameter gets smaller but the length gets longer as the calcination temperature increases.

## 4.3 Elemental Analysis

The elemental analysis of all $MnO_2$ samples has been performed using the Energy Dispersive X-ray (EDX). The EDX revealed the presence of Mn, O, Al and Si elements in the compound as shown in Figure 4.12a-e.

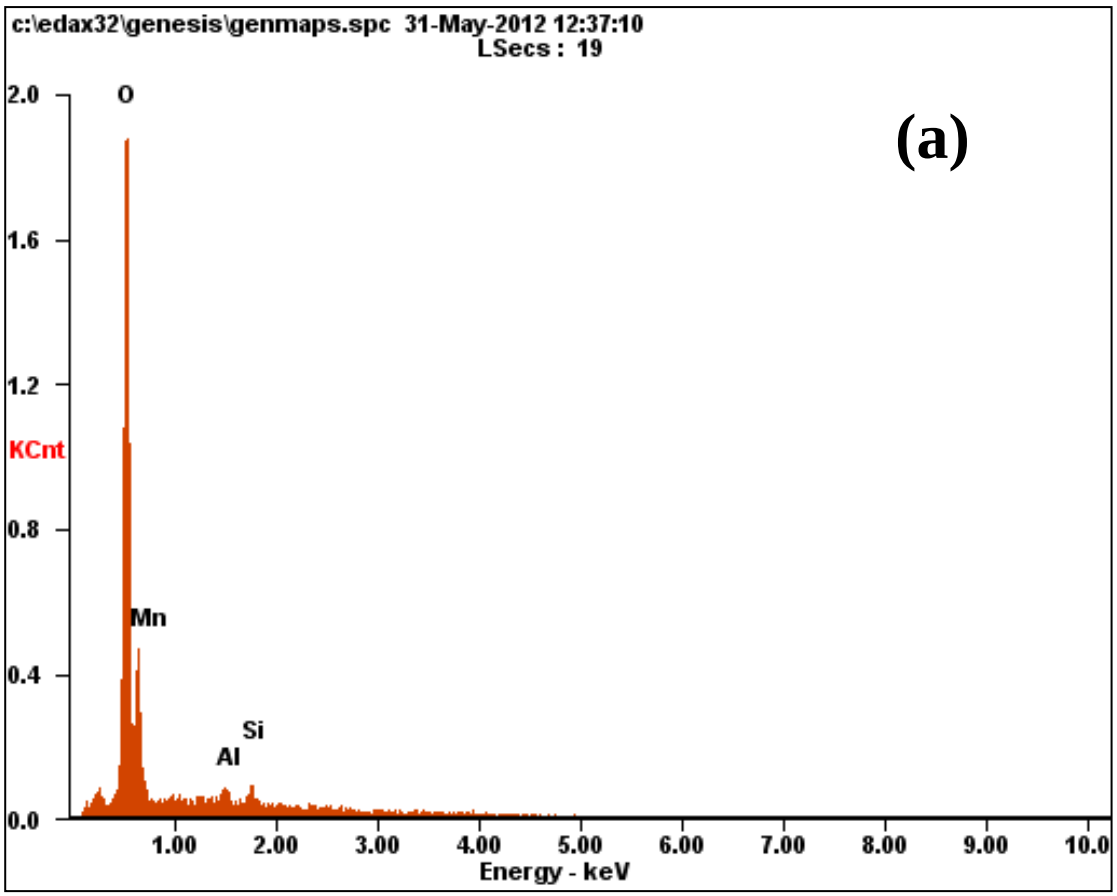

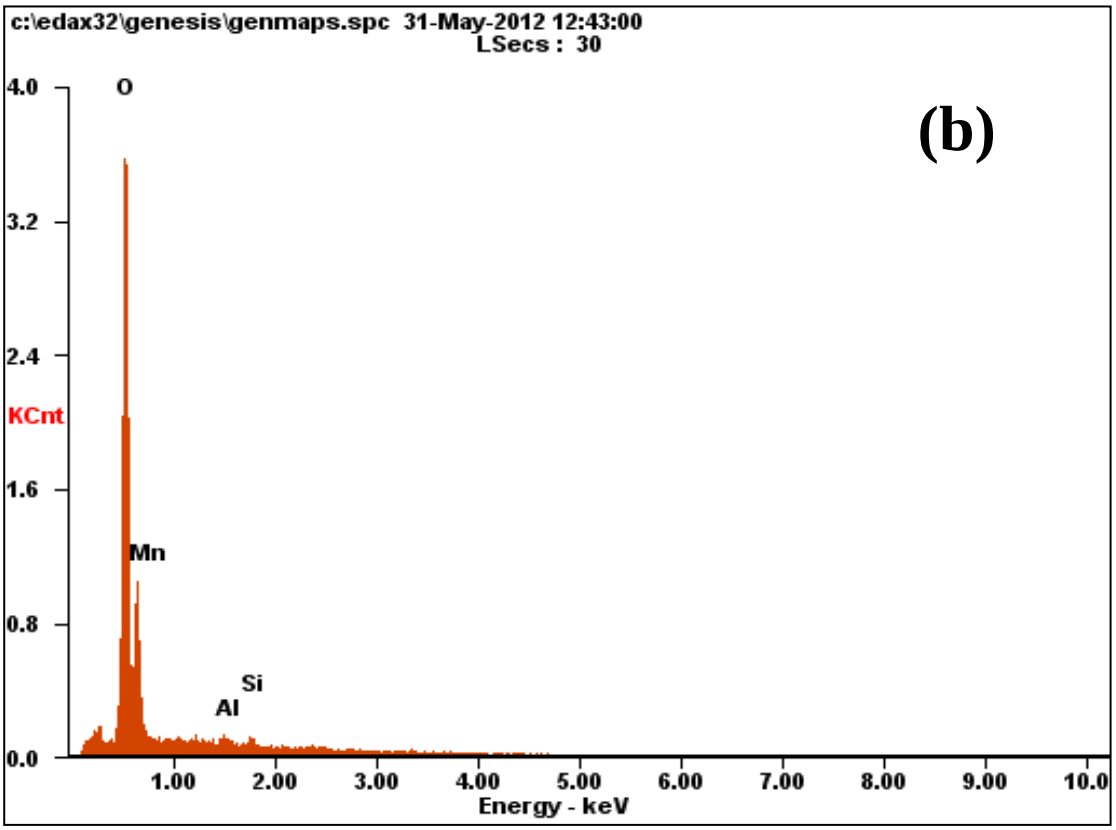
c:\edax32\genesis\genmaps.spc 31-May-2012 12:43:00
LSecs : 30
(b)
O
Mn
Si
Al
KCnt
4.0
3.2
2.4
1.6
0.8
0.0
1.00
2.00
3.00
4.00
5.00
6.00
7.00
8.00
9.00
10.0
Energy - keV

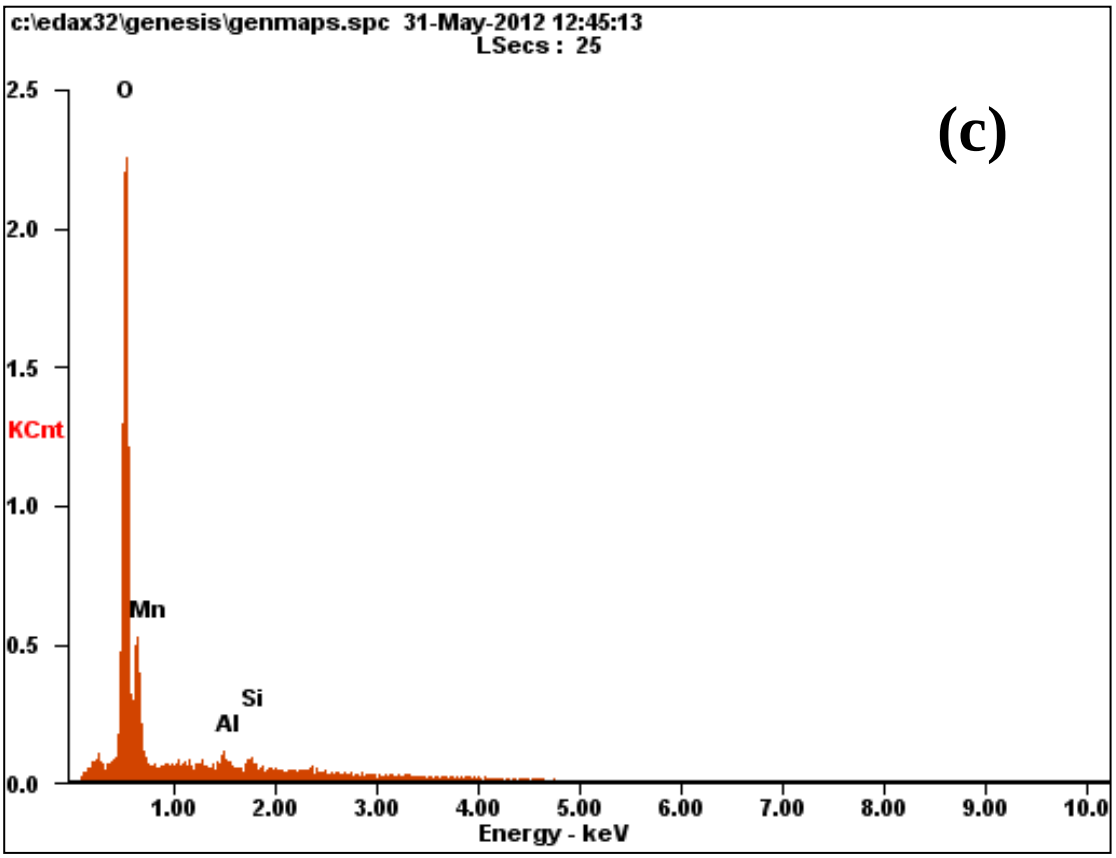
c:\edax32\genesis\genmaps.spc 31-May-2012 12:45:13
LSecs : 25
(c)
O
Mn
Si
Al
KCnt
2.5
2.0
1.5
1.0
0.5
0.0
1.00
2.00
3.00
4.00
5.00
6.00
7.00
8.00
9.00
10.0
Energy - keV

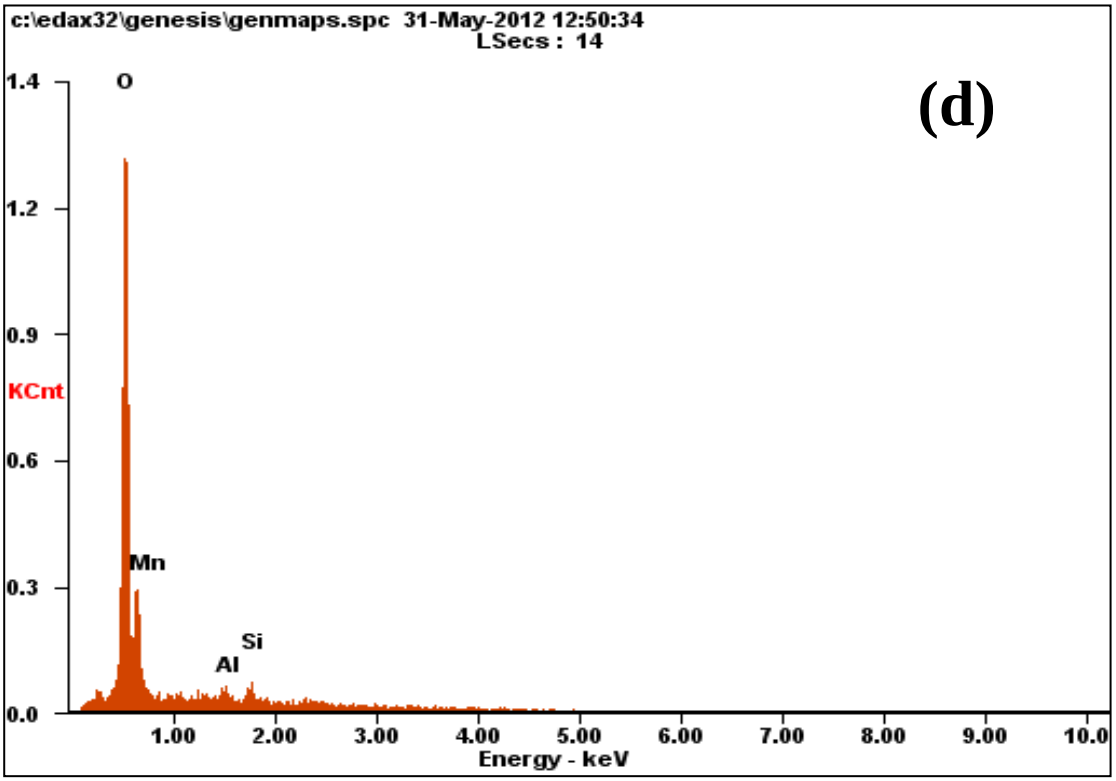


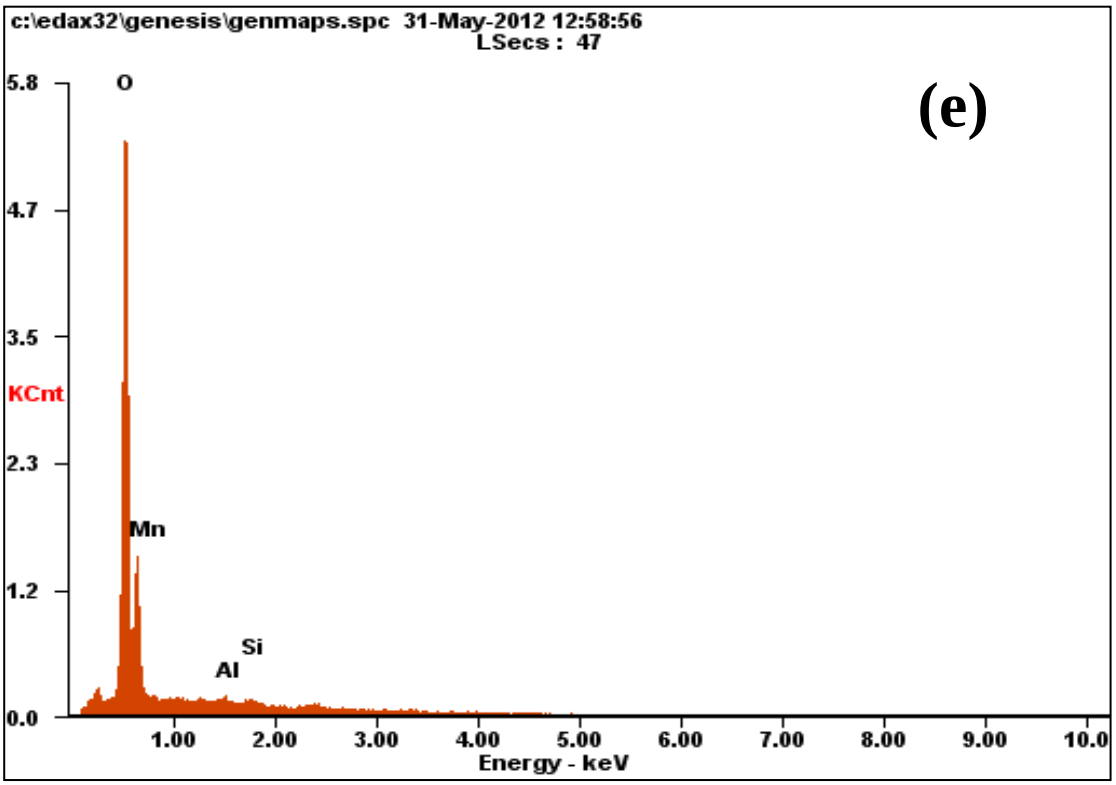


Figure 4.12: EDX spectra of $MnO_2$ (a) as-received; (b) as-synthesized; (c) calcined at 400 ℃; (d) calcined at 500 ℃; (e) calcined at 600 ℃

Table 4.3: Elemental composition of all samples

| Sample | Element | Wt (%) | At (%) |
|---|---|---|---|
| As-received $MnO_2$ | O | 28.69 | 57.26 |
| | Mn | 69.06 | 40.14 |
| | Al | 0.97 | 1.15 |
| | Si | 1.27 | 1.45 |
| As-synthesized $MnO_2$ | O | 30.84 | 58.76 |
| | Mn | 63.94 | 35.48 |
| | Al | 2.19 | 2.48 |
| | Si | 3.03 | 3.29 |
| Calcined $MnO_2$ at 400 ℃ | O | 27.20 | 55.21 |
| | Mn | 69.76 | 41.23 |
| | Al | 1.25 | 1.50 |
| | Si | 1.79 | 2.07 |
| Calcined $MnO_2$ at 500 ℃ | O | 31.89 | 61.14 |
| | Mn | 53.48 | 27.22 |
| | Al | 3.67 | 3.80 |
| | Si | 7.87 | 7.84 |
| Calcined $MnO_2$ at 600 ℃ | O | 29.51 | 58.47 |
| | Mn | 68.98 | 39.80 |
| | Al | 0.71 | 0.84 |
| | Si | 0.79 | 0.90 |

The weight and atomic percentage of the elements are tabulated in Table 4.3. It is found that manganese element has the highest weight percentage followed by oxygen for all the $MnO_2$ samples. However it is vise versa when comes to atomic percentage. The highest atomic percentage is recorded for oxygen followed by manganese. Oxygen has higher atomic numbers compared to manganese in the compound. Aluminium and Silicon are natural impurities presents in manganese dioxide with very small amount which can be neglected. From EDX analysis, it is confirmed that Mn and O is the dominant elements presence in the compound. It is worth to notice that the elemental composition is preserved after high temperature calcination.

### 4.4 Morphology and Physical Size Analysis

Morphology of all $MnO_2$ samples has been examined using Transmission Electron Microscopy (TEM). The diameter of $MnO_2$ nanowires were analyzed from the TEM images.

Figure 4.13 shows the TEM image of as-received γ-$MnO_2$ with the diameter of about 254 nm. One single nanostructure was selected and tilted along its axis, and was found to have a circular cross-section perpendicular to its axis. The image shows typical plate or lamellar particles for $MnO_2$.

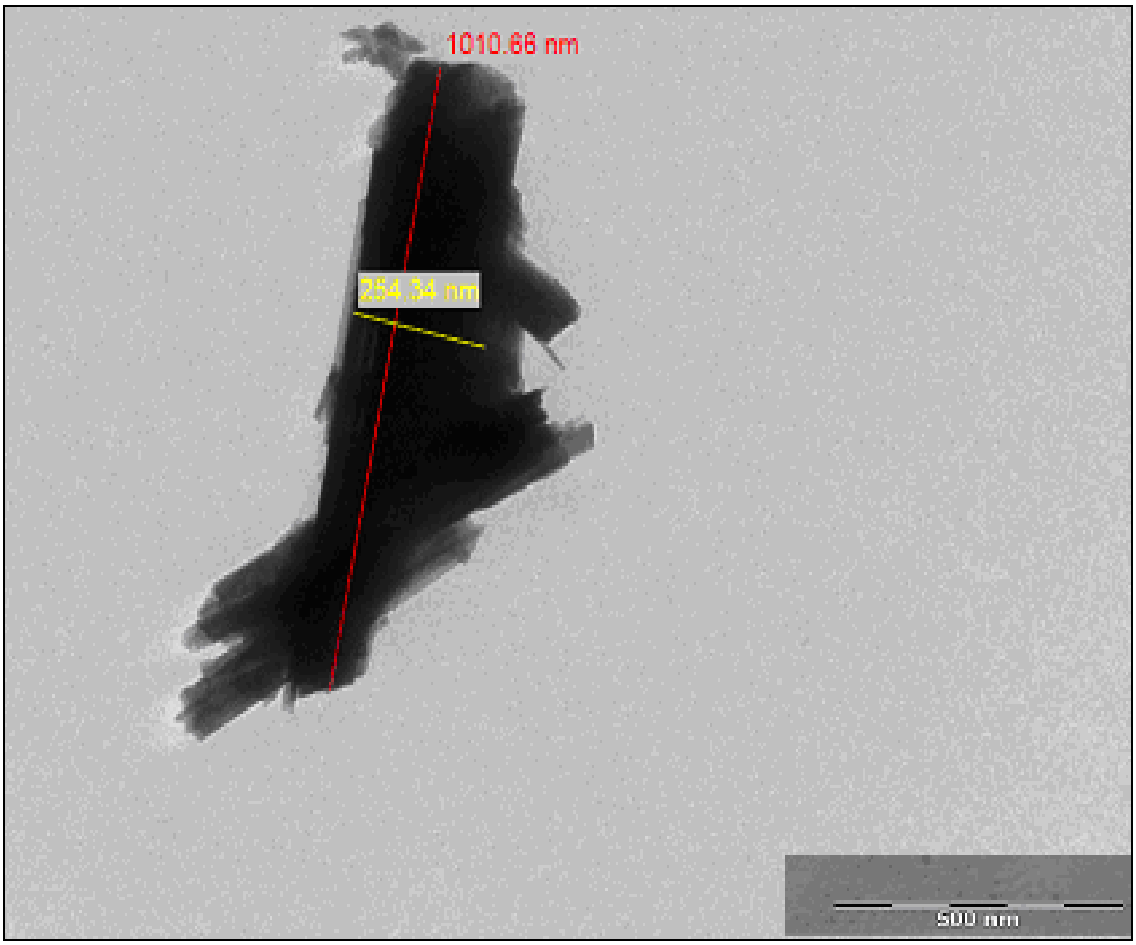


Figure 4.13: TEM image of as-received γ-$MnO_2$

Figure 4.14 shows the as-synthesized $MnO_2$ with the clear diameter about 77 nm and 300 nm in length. A few nanowires can be seen clearly after heating the as-received manganese oxide at 150 ℃ for 24 hours, if compared to pure material γ-$MnO_2$.

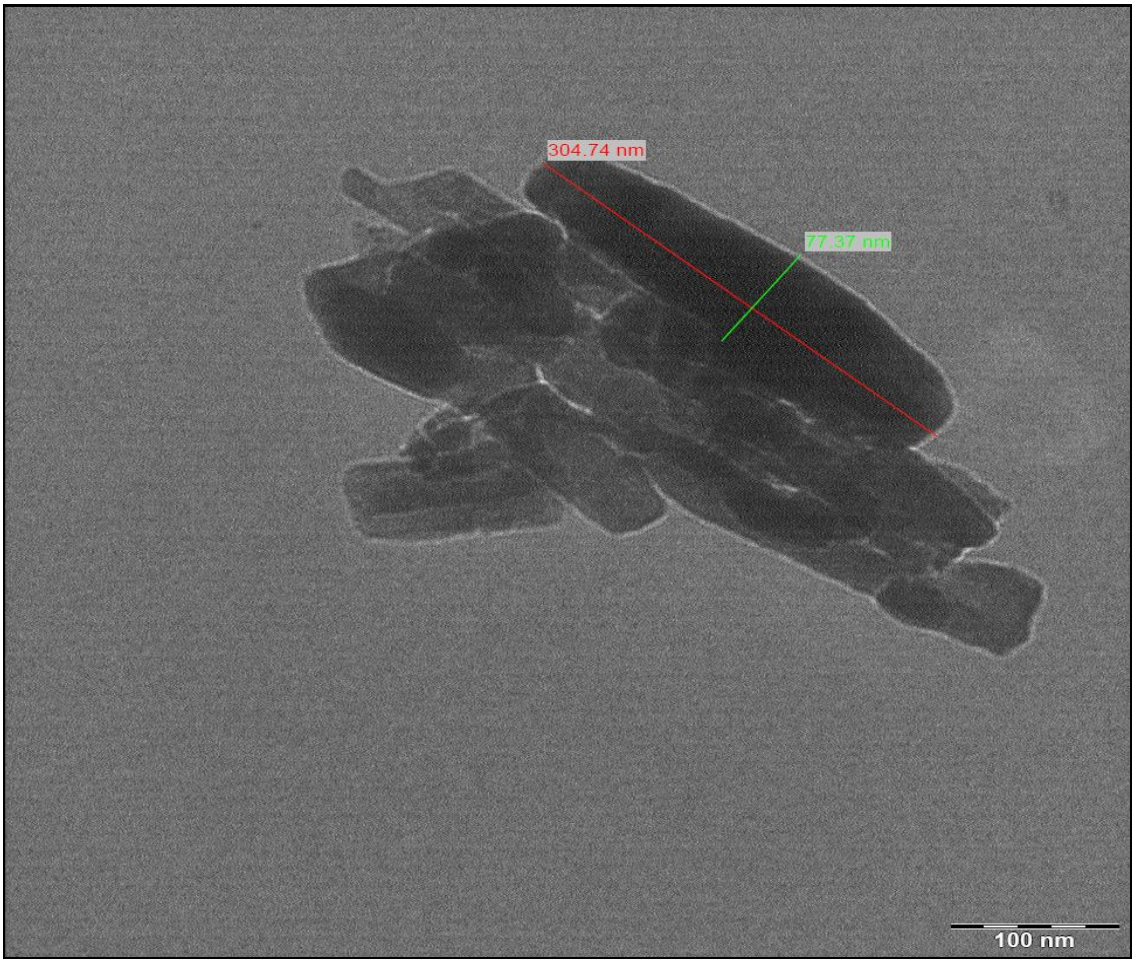


Figure 4.14: TEM image of as-synthesized $MnO_2$

Figure 4.15 shows the calcined $MnO_2$ nanowires at 400 ℃ with the clear diameter about 70-100 nm and 300-400 nm in length.

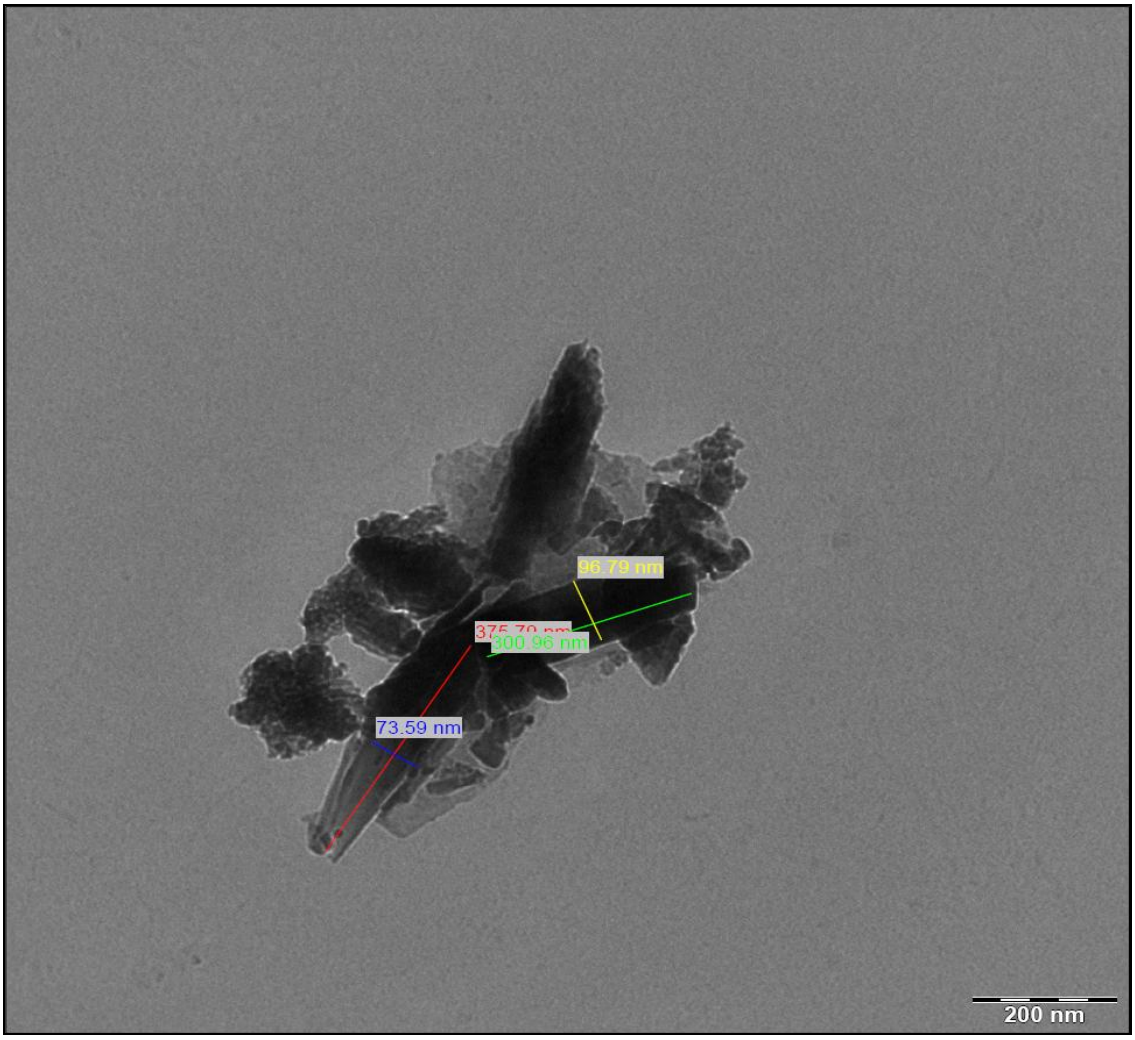


Figure 4.15: TEM image of calcined $MnO_2$ at 400 ℃

Figure 4.16 shows the calcined β-$MnO_2$ nanowires with the clear diameter about 60-70nm and 500-800nm in length.

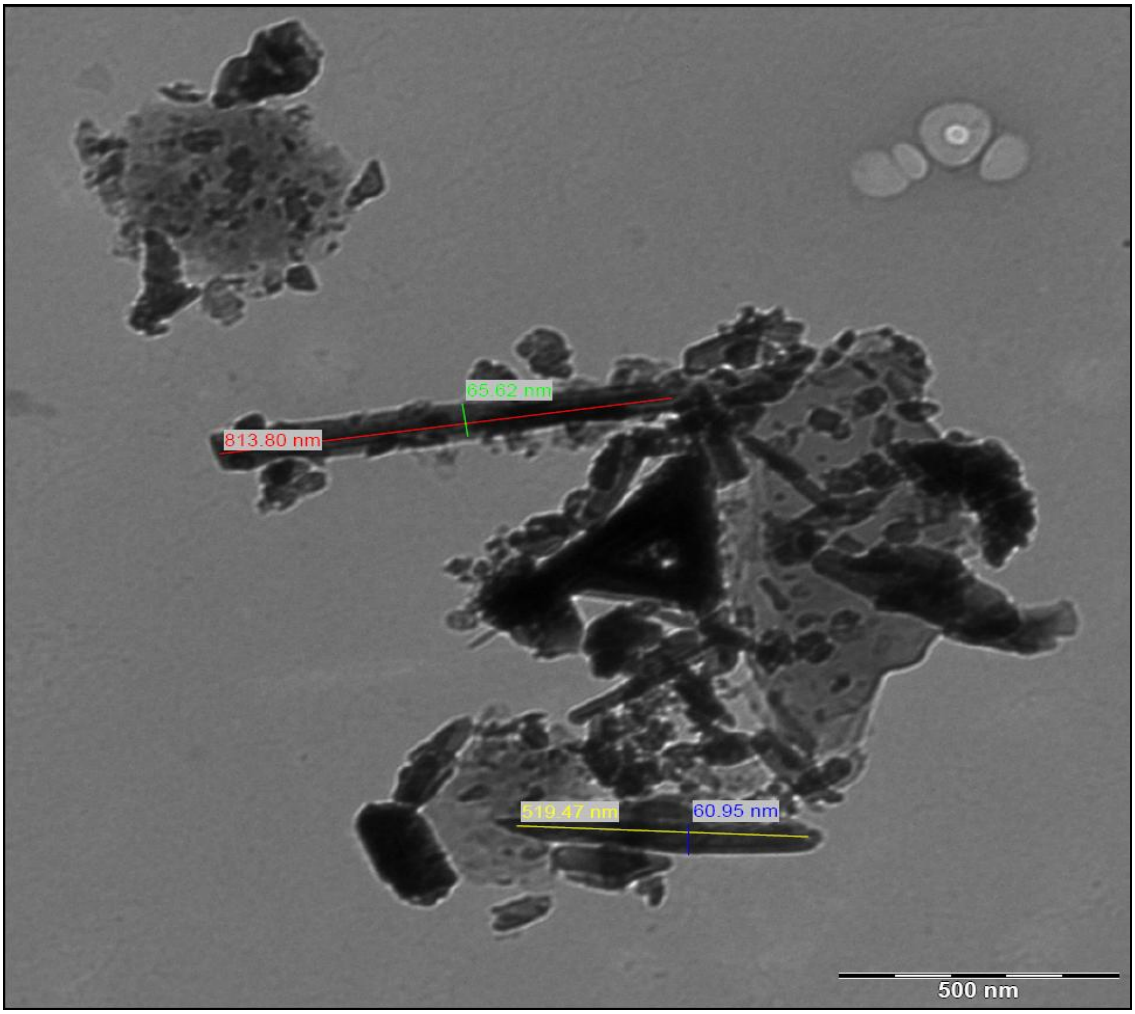


Figure 4.16: TEM image of calcined $MnO_2$ at 500 ℃

Figure 4.17 shows the calcined α-$Mn_2O_3$ nanowires with the clear diameter about 30-40 nm and 1000 nm in length. The nanowire is very long which tend to bend.

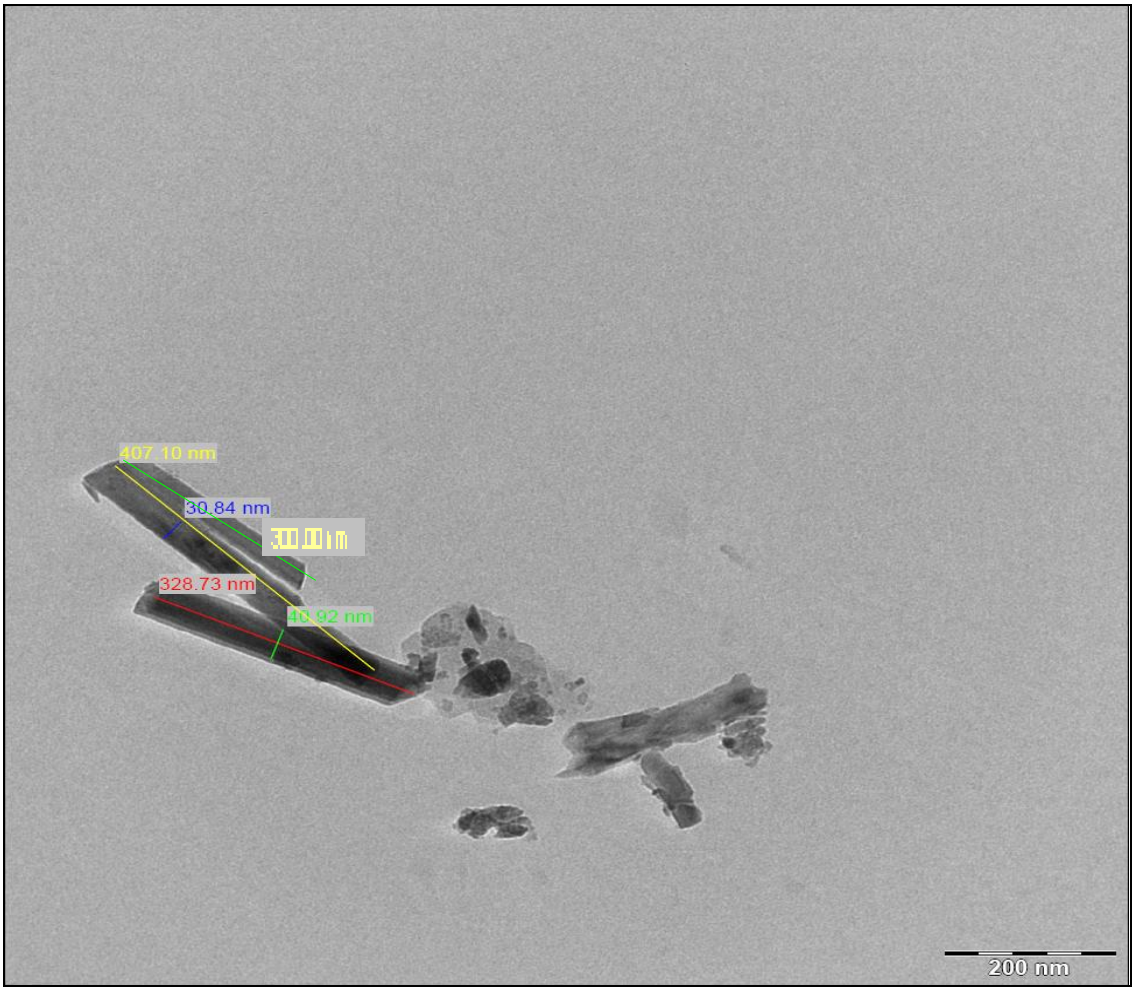


Figure 4.17: TEM image of calcined $MnO_2$ at 600 ℃

Table 4.4: Size distribution of all samples

| Samples | Diameter (nm) | Length (nm) |
|---|---|---|
| As-received $MnO_2$ | 254.34 | 1010.66 |
| As-synthesized $MnO_2$ | 77.37 | 304.74 |
| Calcined $MnO_2$ at 400 ℃ | 73.59 | 375.79 |
| Calcined $MnO_2$ at 500 ℃ | 65.62 | 813.80 |
| Calcined $MnO_2$ at 600 ℃ | 30.84 | 1035.83 |

Table 4.4 above shows the average diameter and length of the samples. It clearly shows that the higher the calcination temperatures, the lower the diameters are as the nanowires become slimmer and protrude longer.

## 4.5 Thermal Analysis

The thermal properties of as-received $MnO_2$ samples for as synthesized, after calcination at different temperature 400, 500 and 600 ℃ has been investigated using the Thermogravimetry (TGA).

The TGA curves in Figure 4.18 - 4.22 shows three weight loss stages occurred for all samples. The first weight loss stage occurred from 30 ℃-600 ℃, shows a small and less weight reduction. This is resulted from the removal of physically adsorbed water, $H_2O$ presence in the sample (Yuan, 2003). The second weight loss stage occurred from 600 ℃-730 ℃ which shows a significant and major weight reduction as sharp drop occurred at this stage in the TGA curves. This is due to the Mn oxidation during the phase transition from β-$MnO_2$ to α-$Mn_2O_3$. Finally, the third weight loss stage occurred from 720 ℃-950 ℃ which shows slight and gradual weight reduction. This corresponds

to the continues of Mn oxidation from α-$Mn_2O_3$ until the stable alpha-phase, α-$Mn_3O_4$ which is obtained at 950 ℃.

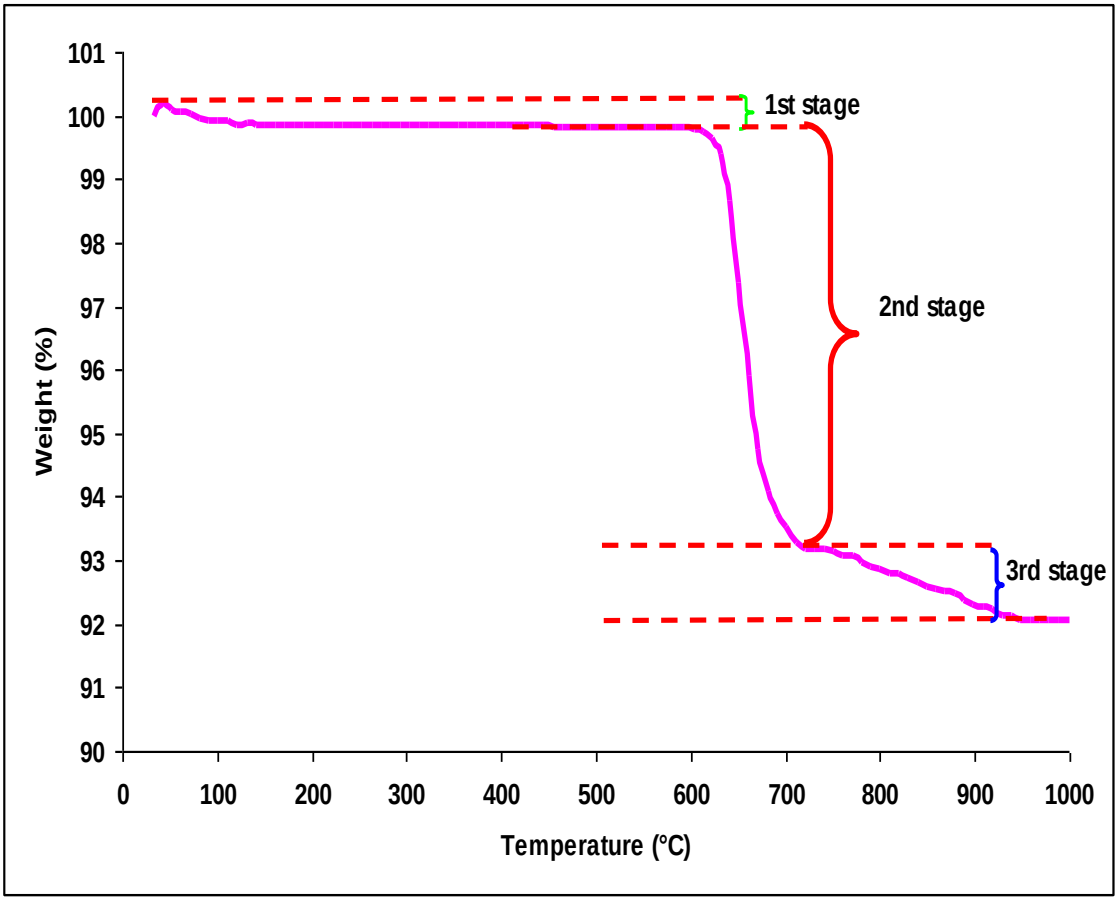


Figure 4.18: TGA curve for as-received $MnO_2$

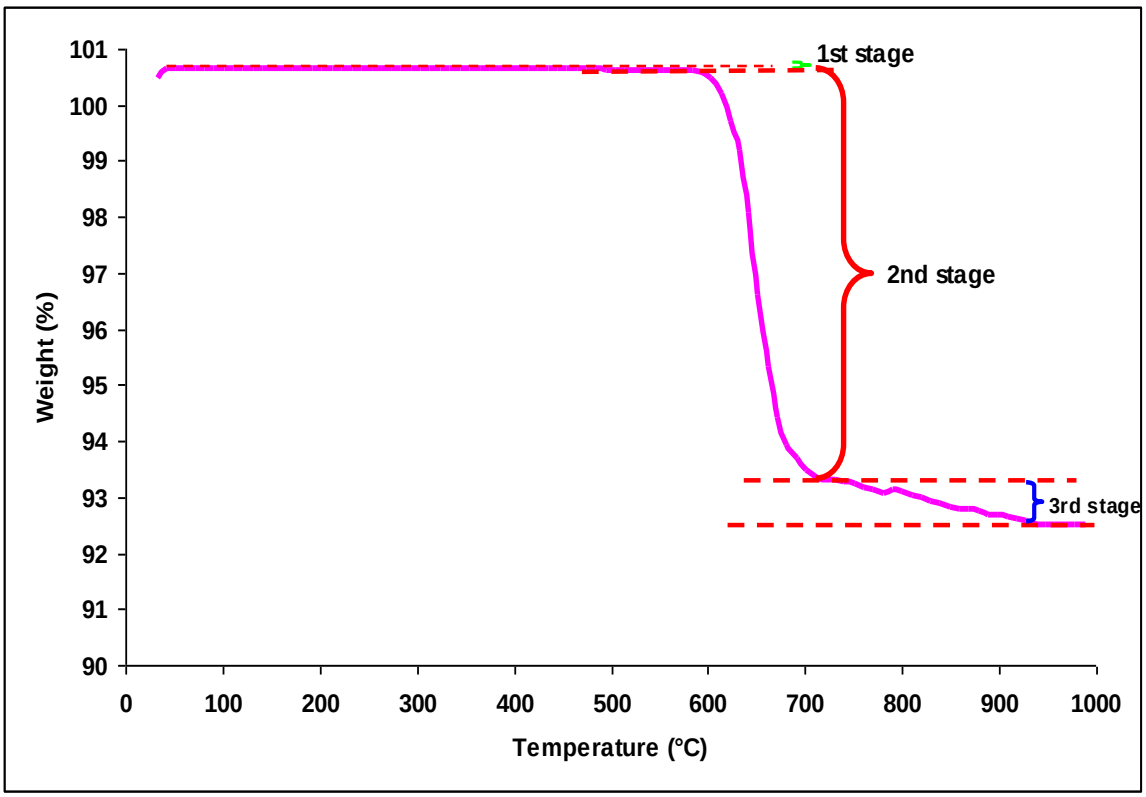


Figure 4.19: TGA curve for as-synthesized $MnO_2$

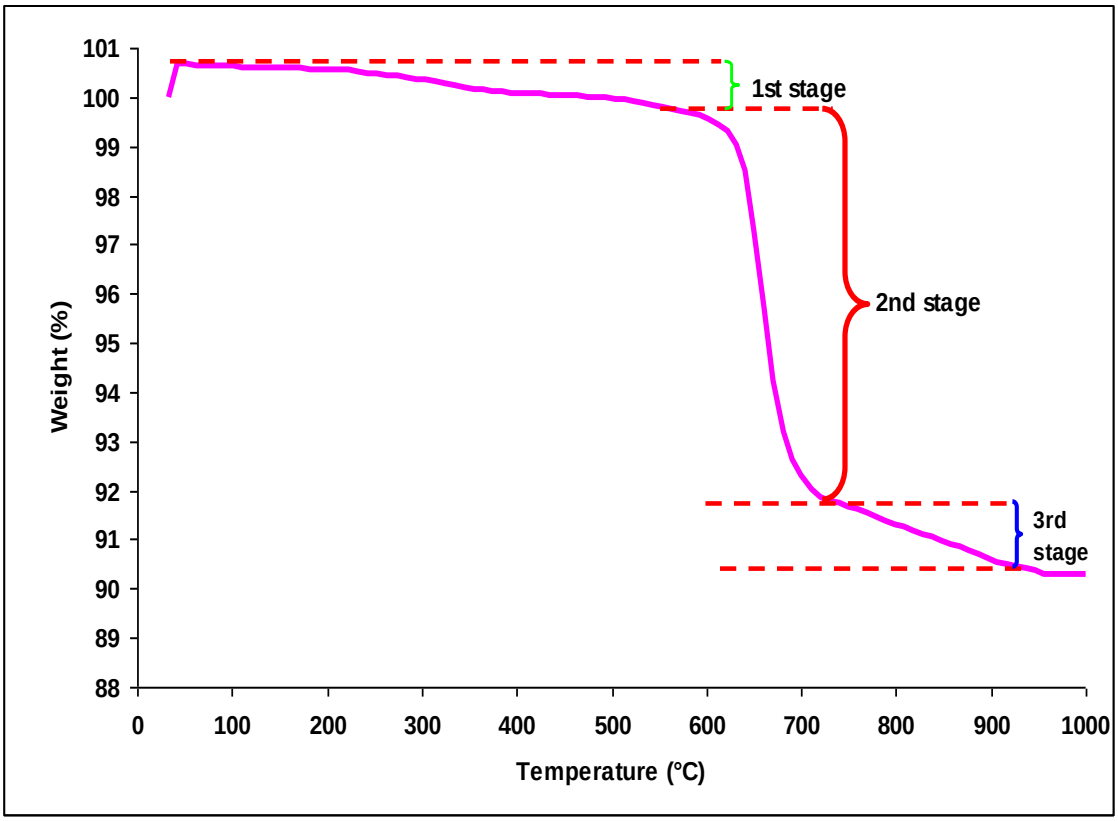


Figure 4.20: TGA curve for calcined $MnO_2$ at 400 ℃

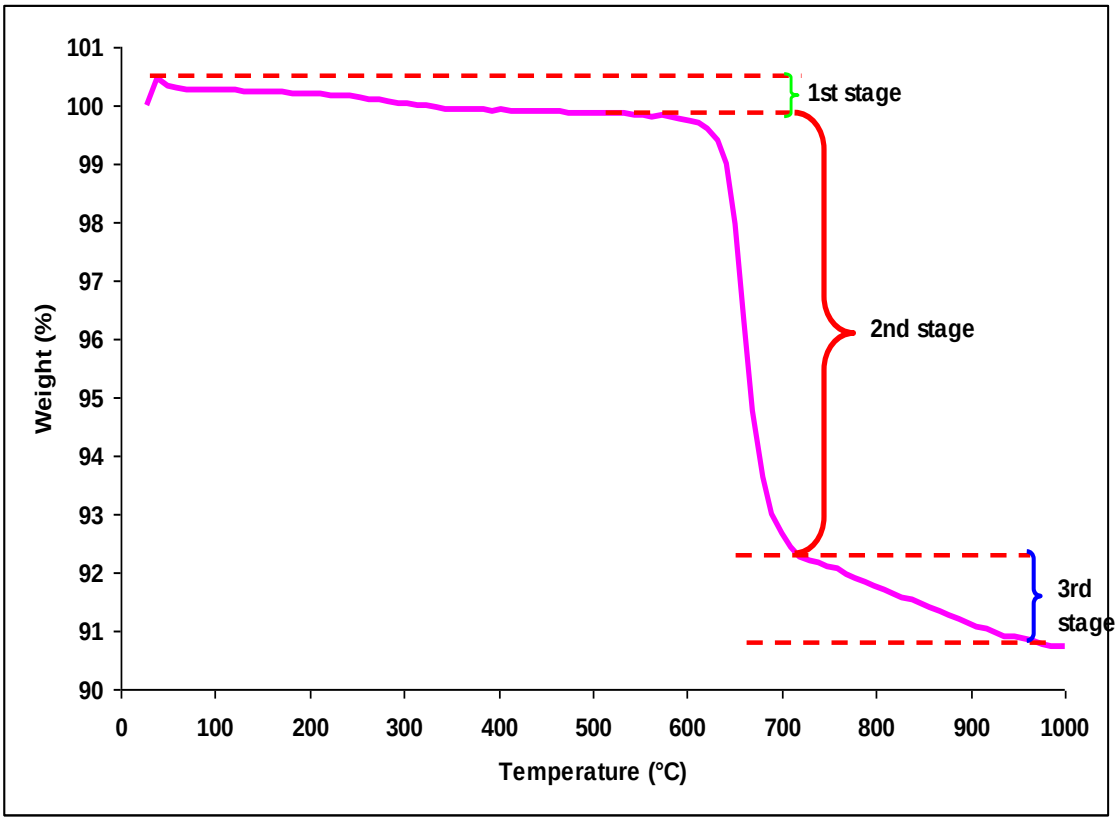


Figure 4.21: TGA curve for calcined $MnO_2$ at 500 ℃

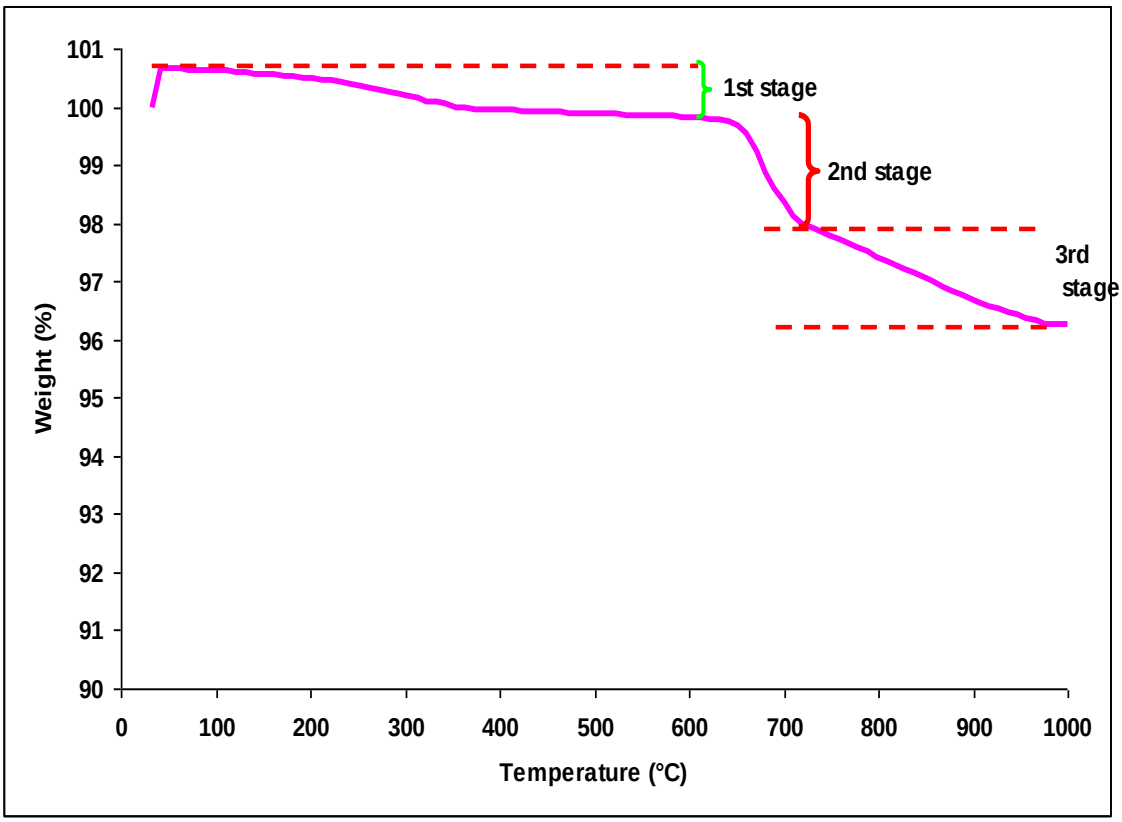


Figure 4.22: TGA curve for calcined $MnO_2$ at 600 ℃

Table 4.5: Specific temperatures and weight loss percentage of all samples

| Sample | Initial Weight Loss Temp (℃) | Weight Loss (%) | Decomp. Temp (℃) | Weight Loss (%) | Final Weight Loss Temp (℃) | Weight Loss (%) | Total Weight Loss (%) |
|---|---|---|---|---|---|---|---|
| $MnO_2$ as received | 42 | 0.545 | 613 | 6.466 | 721 | 0.913 | 7.924 |
| $MnO_2$ as synthesized | 52 | 0.001 | 604 | 7.316 | 721 | 0.805 | 8.122 |
| $MnO_2$ after calcination at 400 ℃ | 42 | 1.138 | 603 | 7.676 | 730 | 1.549 | 10.363 |
| $MnO_2$ after calcination at 500 ℃ | 38 | 0.739 | 602 | 7.477 | 720 | 1.531 | 9.747 |
| $MnO_2$ after calcination at 600 ℃ | 42 | 0.858 | 632 | 1.819 | 720 | 1.709 | 4.386 |

Table 4.5 summarized the initial, intermediate and final weight loss temperature and total weight loss percentage for $MnO_2$ as-received, as synthesized and after calcination at temperature 400, 500 and 600 ℃. The total weight loss percentage in the TGA curve for as synthesized $MnO_2$ is higher compared to as received $MnO_2$. This is due to the liberation of absorbed and interlayer water molecule bonding between $Mn_{4+}$ and $O_{2-}$ (Ma, 2007) is higher for as synthesized $MnO_2$. For calcined $MnO_2$ at 400 ℃, the total weight loss is even higher due to oxidation takes place which releases oxygen during the phase transformation to β-$MnO_2$ and α-$Mn_2O_3$ at the decomposition temperature. Decreasing weight loss after that shows the increase of thermal stability of $MnO_2$ with respect to the increase of the calcination temperature.

# CHAPTER FIVE

# CONCLUSION AND RECOMMENDATION

## 5.1 Conclusion

In this study, manganese oxide nanowires have been successfully synthesized through a simple hydrothermal method by using the commercial γ-$MnO_2$ crystals and water as solution. The benefits of hydrothermal method are that it is quite facile in preparation without the use of any surfactants or catalyst. It can be performed in higher temperature and gives good reproducibility. It is a cost saving method as not necessary to use the very expensive coordination compounds as raw material. This simple synthetic method has the potential to be developed as a general method for the preparation of other 1-D nanoscaled materials. The produced nanowires own great significant novel properties induced by their dimensionality.

The influence of calcination temperatures ranging from 400-600℃ on manganese oxide nanowires have been revealed in this study. The increase of calcination temperature has shown some important effects on $MnO_2$ nanowires. The crystal phase of manganese oxide nanowires was confirmed by XRD. Significant phase transformation involving redox reduction has occurred for calcination temperature at 500-600℃ from β-$MnO_2$ to α-$Mn_2O_3$. Well aligned cluster form surface resulting from FE-SEM for calcined $MnO_2$ at 600℃ proves the yield of nanowires increases with the increasing of calcination temperature. Elemental analysis by EDX confirms the presence of Mn and O as the dominant elements in all the samples. The elemental composition is preserved after high temperature calcination which makes it very stable material for application in catalysts, batteries, capasitors and others. TEM confirms the diameter size of nanowires produced is 30-40nm after calcined at 600℃. TEM results corresponds with XRD and FE-SEM results as the diameter size of nanowires produced gets smaller and smaller, with the increase of calcination temperature. Smaller diameter

nanowires are expected to grow by further increasing the calcination temperature. TEM shows the manganese oxide nanowires presented here are not amorphous but nanocrystalline. TGA analysis reveals the presence of structural water and release of oxygen during the heating process and it becomes thermally stable after 600 ℃.

## 5.2 Recommendation:

There are some recommendations I would like to suggest for future study:

- After the samples were prepared, it is better to run the analysis as soon as possible due to aging might affect the properties of the sample.
- The samples shall be stored in a drying cabinet to avoid moisturization due to $MnO_2$ powders tends to absorb water from the air after a couple of days.
- The calcination temperature could have been increased to obtain a more convincing results and to facilitate better comparison.
- It will be very convenient if XRD and TEM machine is available in Engineering Faculty rather than waiting for long time after booking to use those machines in other faculties.
- Impedance Spectroscopy (IS) and Ultraviolet-visible Spectrophotometer (UV-VIS) are suggested for further study to investigate the electrical and optical properties of the manganese (IV) oxide nanowires respectively.

## REFERENCES


Alkaline Miniature Manganese Dioxide Handbook and Application Manual. *Version: AlkMin1.3*. Retrieved 19 March 2012, from http://data.energizer.com

Alyamani, A., & Lemine, O. M. (2011). FE-SEM Characterization of Some Nanomaterial. National Nanotechnology Research Centre, KACST, Riyadh, Saudi Arabia.

Ammundsen, B., Paulsen, J. (2001). Novel Litium-Ion Cathode Materials Based on Layered Manganese Oxides. *Advance Materials, 13*, 943-956.

Ardizzone, S., Bianchi, C.L., Tirelli, D. (1997). Surface reactivity of $\alpha$-$Mn_2O_3$ powders in aqueous suspensions. *Journal of Electroanalytical Chemistry, 425,* 19-23.

Chandra, R., Taneja, P., Ayuub, P. (1999). A simple method to synthesis single-crystalline manganese dioxide nanowires. *Nanostructural Materials, 4,* 505-512.

Chu, L.Q. (1998). Advances in FE-SEM and It's Physical Basis. *Journal Of Chinese Electron Microscopy Society* (Central Iron and Steel Research Institute, Beijing 100081)

Coustier, F., Xu, J.J., Manhart, L.H., Passerijni, S., Owens, B.B., Smyrl, W.H. (1997). Various function extracted from nanomaterials. *Material Research Society Symposium Proceeding, 548,* 113-119.

Dias, D., Monteiro, R., Carvalho, P.A., Ferro, A.C., Lohwasser, W. (2006). TEM and XRD Investigation of $MnO_2$ Microstructure and its influence on ESR of Ta Capasitors. *Materials Science Forum Vols, 514-516,* 26-273.

Devaraj, S., & Munichandraiah, N. (2007). Electrochemical Supercapacitor Studies of Nanostructured $MnO_2$ Synthesized by Microemulsion Method and the Effect of Annealing. *Journal of The Electrochemical Society, 154*, 80-88.

Dresselhaus, M.S., Lin, Y.M., Rabin, O., Black, M.R. (2003). Determination of Carrier Density in Te-doped Bi Nanowires. *Applied Physics letters 83,* 3567-3569.

Eftekhari, A., Moztarzadeh, F., & Kazemzad, M. (2005). Template-free preparation of bunches of ligned manganese oxide nanowires. *Journal Of Physics, 38,* 628–631.

Huang, M., Pan, G.T., Chen, L.C., Yang, C.K.T., & Chang, W.S. (2009) Effects of Synthesis Conditions on the Crystalline Phases and Photocatalytic Activities of Silver Vanadates via Hydrothermal Method. *Journal Online Proceedings Library,* 1171.

Khan, M. H., & Kurny, A.S.W. (2012). Characterization of Spent Household Zinc-Carbon Dry Cell Batteries in the Process of Recovery of Value Metals. *Journal of Minerals & Materials Characterization & Engineering, 11,* 641-651.

Laherto, A. (2010). An analysis of the educational significance of nanoscience and nanotechnology in scientific and technological literacy. *Science Education International,21*, 160-175.

Li, L., Chu,Y., Liu, Y., Don, L. (2007). Synthesis and shape evolution of novel cuniform-like $MnO_2$ in aqueous solution. *Journals of Materials Letters, 61,* 1609–1613.

Li, W., Liu, Q., Su, Y., Sun, J., Zou, R. (2012). $MnO_2$ ultralong nanowires with better electrical conductivity and enhanced supercapacitor performances. *Journal Material Chemistry***,** *22,* 14864-14867.

Linden, D., Reddy, T.R. (2002). Handbook Of Batteries 3rd Edition. McGraw-Hill.

Luo, H., Wei, M., Wei, K. (2008). Formation of single-crystal $\gamma$-$MnO_2$ nanowires at room temperature. *Journal of Crystal Growth, 310*, 2738 – 2741.

Ma, S.B., Ahn, K.Y., Lee, E.S., Oh, K.H., Kim, K.B. (2007). Synthesis and characterization of manganese dioxide spontaneously coated on carbon nanotubes. *Journal of Carbon 45,* 375-382.

Murata, K., Izuchi, S., Yoshihisa, Y. (2005). Nanostructured amorphous manganese dioxcide cryogel as a high rate lithium intercalation host. *Electrochim.Act., 45,* 1501-1508.

Najafpour, M.M., Rahimi, F., Aro,E.M., Lee, C.H., & Allakhverdiev, I.S. (2012). Nano-sized manganese oxides as biomimetic catalysts for water oxidation in artificial photosynthesis: a review of *Journal of The Royal Society*, 35-47.

Nam, H.S., Yoon, J.K,. Ko, J.M., Kim, J.D. (2010). Electrochemicalcapacitors of flower-like and nanowire structured $MnO_2$ by a sonochemical method**.** *Materials Chemistry and Physics, 123* , 331–336.

Pang, S.C., Chin, S.F. & Ling, C.Y. (2012). Controlled Synthesis of Manganese Dioxide Nanostructures via a Facile Hydrothermal Route. *Journal of Nanomaterials Article ID 607870,* pages 7.

Park, M.S., Yoon, W.Y. (2003). Characteristics of a Li/$MnO_2$ battery using a lithium powder anode at high-rate discharge. *Journal of Power Sources 114,* 237–243.

Passerini, S., Ressler, J.J., Le,D.B., Owens,B.B., Smyrl, W.H.(1988). Amazing Electrochim in nanotechnology. *Journal of New Material in Nanotechnology, 2,* 209.

Potter, R. & Rossman, G, (1979). Mineralogy of Manganese Dendrites and Coatings. *American Journal of Science, 35,* 243.

Rao, C.N.R., Muller,A., Cheetham,A.K. (2004). The Chemistry of Nanomaterials, Synthesis, Properties and Applications. Wiley-VCH.

Ren, Y., Liu, Q., Wang, J., Wang, H., Xue, D. (2009). Large scale of synthesis of single-crystal alpha manganese sesquioxide nanowires via solid-state reaction. *Journals of Materials Letter, 63,* 661-663.

Subramaniam,V., Zhu, H., Vaitai, R., Ajayan, P.M., & Wei, B. (2005). Hydrothermal synthesis and pseudocapacitance properties of $MnO_2$ nanostructures. *Journal of Physical Chemistry B, 109,* 20207-20214.

Thackeray,M.M.(1997). *Prog.Solid State Chem.* 25

Wang, H., & Zhou, J. (2000). Data smoothing and distortion of X-ray diffraction peaks. II. Application. *Journal of Applied Crystallography, 33,* 1136-1142.

Wei, M.D., Konishi, Y., Zhou, H., Sugihara, H., & Arakawa, H. (2005). Synthesis of single-crystal manganese dioxide nanowires by a soft chemical process. *Journal Nanotechnology, 16,* 245-249.

West, A.R. (1999). *Basic solid state chemistry,* John Wiley & Sons.

Xia, Y., Yang, P., Sun Y. (2003). One-Dimensional Nanostructures: Synthesis, Characterization and Applications. *Advance Materials, 15*.

Yang Y., Xiao, L., Zhao, Y., & Wang, F. (2008). Hydrothermal Synthesis and Electrochemical Characterization of a-MnO2 Nanorods as Cathode Material for Lithium Batteries *International. Journal of. Electrochemical. Science, 3*, 67 – 74.

Yuan, Z.Y., Zhang, Z., Du, G., Ren, T.Z., & Su, B.L. (2003). A simple method to synthesise single-crystalline manganese oxide nanowires. *Journal Chemical Physics Letter, 378,* 349-353.

Zhang, X., Yang, W., Yang, J., David G. E (2008). Synthesis and characterization of α-$MnO_2$ nanowires: Self-assembly and phase transformation to β-$MnO_2$ microcrystals. *Journal of Crystal Growth, 310,* 716–722.

**Internet References:**

http://en.wikipedia.org/wiki/Manganese_dioxide; retrieved on 15/01/2012.

http://simple.wikipedia.org/wiki/File:Pyrolusite-229779.jpg; retrieved on 26/01/2012.

http://en.wikipedia.org/wiki/File:Zincbattery.png; retrieved on 08/02/2012.

# *Microanalysis Report*

***Prepared for:*** ***Subashini A/P Supramaniam***

***Prepared by:*** ***Your Name Here*** ***5/31/2012***

**B1- AS RECEIVED MNO2**

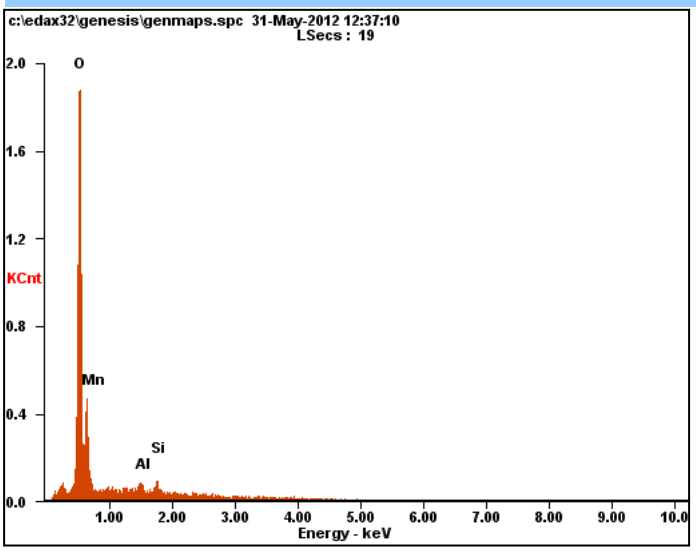


| *Element* | *Wt%* | *At%* |
|---|---|---|
| ***OK*** | 28.69 | 57.26 |
| ***MnL*** | 69.06 | 40.14 |
| ***AlK*** | 00.97 | 01.15 |
| ***SiK*** | 01.27 | 01.45 |
| ***Matrix*** | Correction | ZAF |

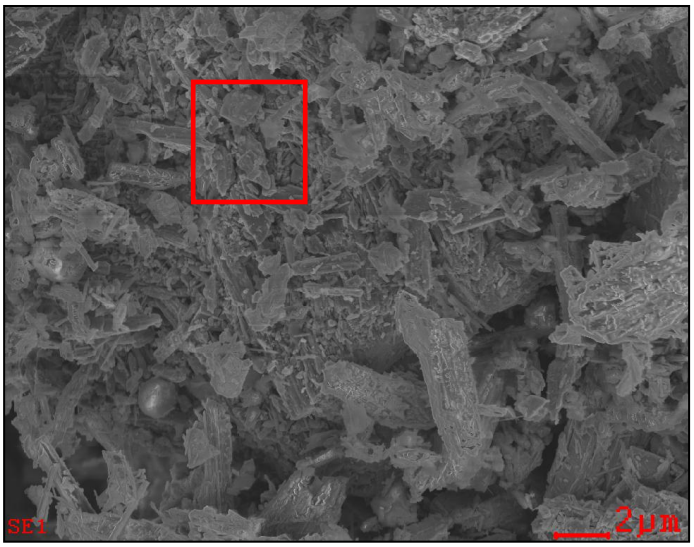

# *Microanalysis Report*

***Prepared for:*** ***Subashini A/P Supramaniam***

***Prepared by:*** ***Your Name Here*** ***5/31/2012***

**B2-AS SYNTHESIZED MNO2**

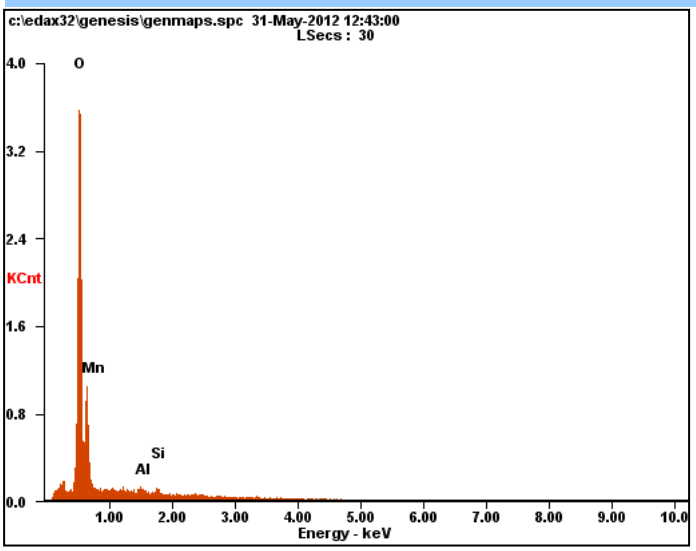


| *Element* | *Wt%* | *At%* |
|---|---|---|
| ***OK*** | 30.84 | 58.76 |
| ***MnL*** | 63.94 | 35.48 |
| ***AlK*** | 02.19 | 02.48 |
| ***SiK*** | 03.03 | 03.29 |
| ***Matrix*** | Correction | ZAF |

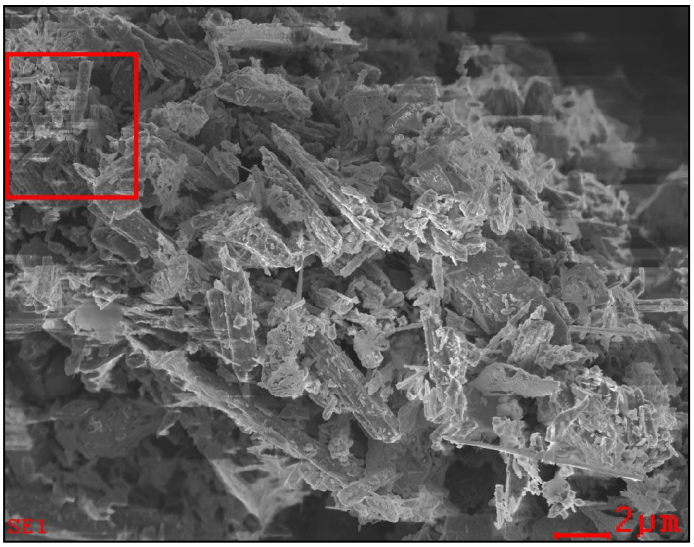

# *Microanalysis Report*

***Prepared for:*** ***Subashini A/P Supramaniam***

***Prepared by:*** ***Your Name Here*** ***5/31/2012***

**B3-CALCINED MNO2 AT 400C**

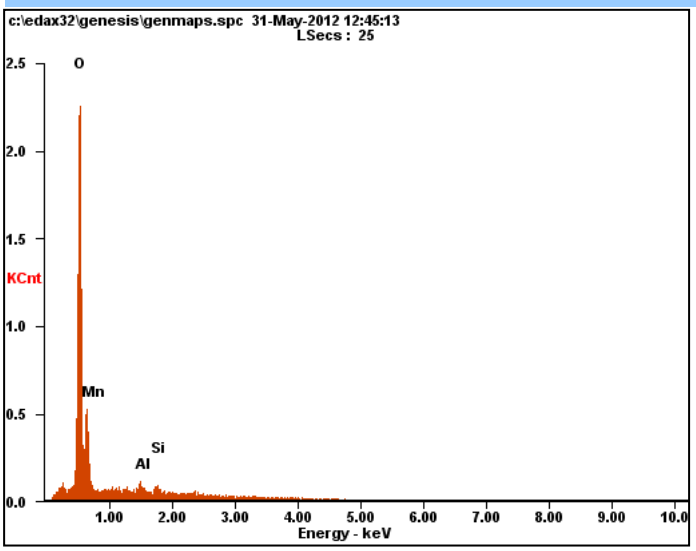


| *Element* | *Wt%* | *At%* |
|---|---|---|
| ***OK*** | 27.20 | 55.21 |
| ***MnL*** | 69.76 | 41.23 |
| ***AlK*** | 01.25 | 01.50 |
| ***SiK*** | 01.79 | 02.07 |
| ***Matrix*** | Correction | ZAF |

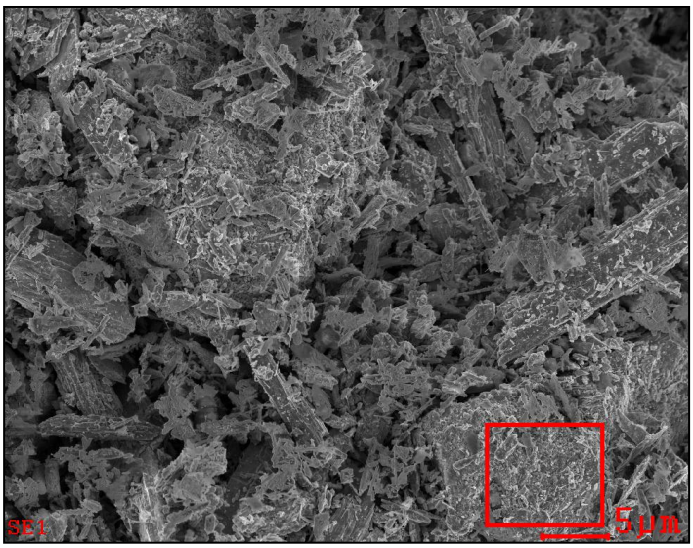

# *Microanalysis Report*

***Prepared for:*** ***Subashini A/P Supramaniam***

***Prepared by:*** ***Your Name Here*** ***5/31/2012***

**B4-CALCINED MNO2 AT 500C**

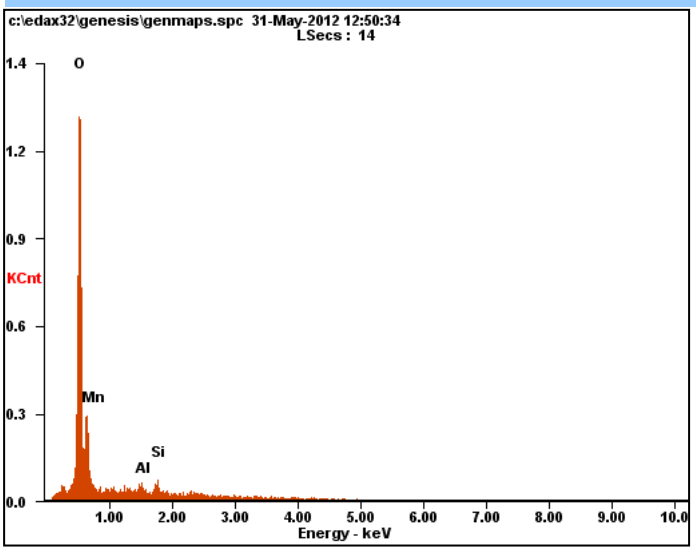


| *Element* | *Wt%* | *At%* |
|---|---|---|
| ***OK*** | 31.89 | 61.14 |
| ***MnL*** | 53.48 | 27.22 |
| ***AlK*** | 03.67 | 03.80 |
| ***SiK*** | 07.87 | 07.84 |
| ***Matrix*** | Correction | ZAF |

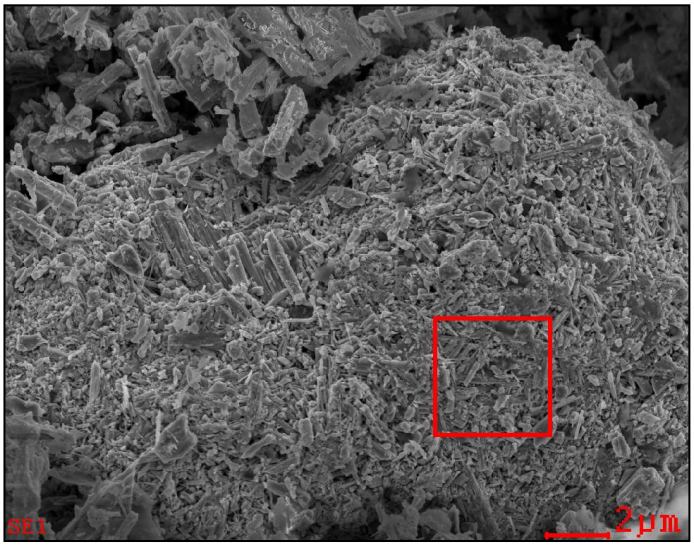

# *Microanalysis Report*

***Prepared for:*** ***Subashini A/P Supramaniam***

***Prepared by:*** ***Your Name Here*** ***5/31/2012***

**B5-CALCINED MNO2 AT 600C**

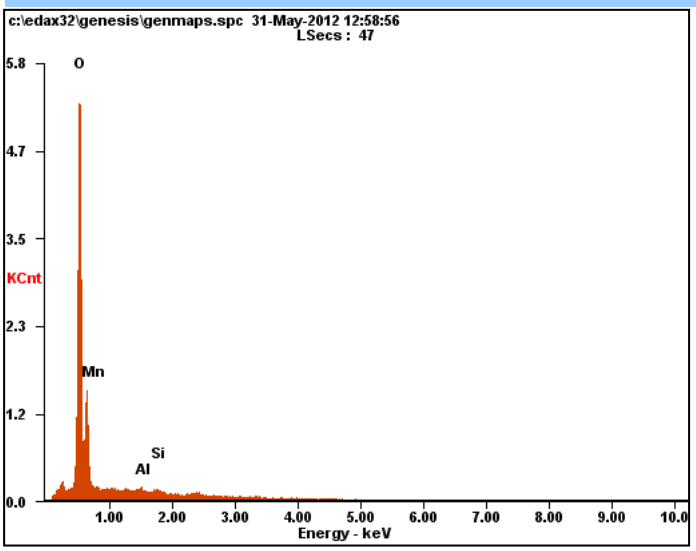


| *Element* | *Wt%* | *At%* |
|---|---|---|
| ***OK*** | 29.51 | 58.47 |
| ***MnL*** | 68.98 | 39.80 |
| ***AlK*** | 00.71 | 00.84 |
| ***SiK*** | 00.79 | 00.90 |
| ***Matrix*** | Correction | ZAF |

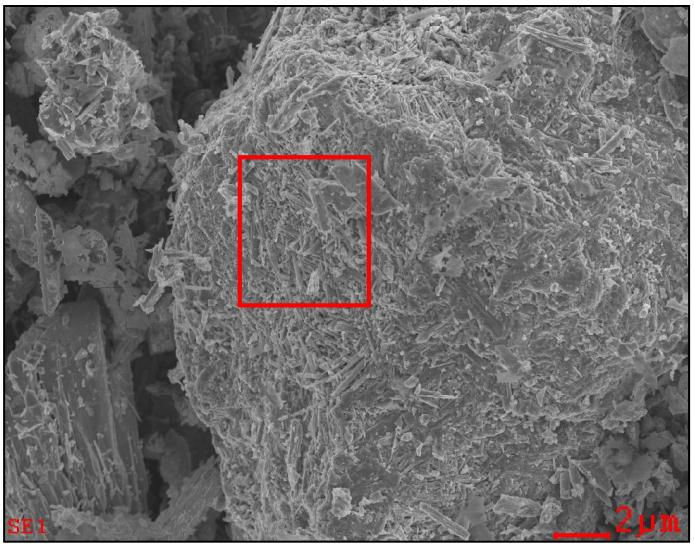

# *Microanalysis Report*

***Prepared for:*** ***Subashini A/P Supramaniam***

***Prepared by:*** ***Your Name Here*** ***5/31/2012***